http://researchcommons.waikato.ac.nz/

Research Commons at the University of Waikato

Copyright Statement:

The digital copy of this thesis is protected by the Copyright Act 1994 (New Zealand).

The thesis may be consulted by you, provided you comply with the provisions of the Act and the following conditions of use:

- Any use you make of these documents or images must be for research or private study purposes only, and you may not make them available to any other person.
- Authors control the copyright of their thesis. You will recognise the author's right to be identified as the author of the thesis, and due acknowledgement will be made to the author where appropriate.
- You will obtain the author's permission before publishing any material from the thesis.

Limited Changes in Microbial Respiration along a Geothermal Gradient

A thesis

submitted in partial fulfilment

of the requirements for the degree

of

Master of Science (Research) in Environmental Sciences

at

The University of Waikato

by

Allycia van de Laar

THE UNIVERSITY OF
WAIKATO
Te Whare Wānanga o Waikato

2021

Abstract

Soil carbon is the largest terrestrial stock of carbon (C) globally. This C stock has the potential to be negatively impacted by global warming through the acceleration of microbial respiration via positive feedback loops. Microbial respiration is a temperature dependent process that releases carbon dioxide (CO_2). Thermal adaptation of microbial respiration may partially offset positive feedback loops, alleviating accelerated responses. The first aim of this thesis was to determine the temperature response of microbial respiration (of labile C and soil organic matter (SOM)) in soil and evaluate the potential for thermal adaptation using a geothermal gradient as a proxy for soil warming. Here, the geothermal gradient, located in Rotorua, New Zealand, spanned average soil temperatures of 18-36 ^oC, encompassing a range of temperatures experienced in temperate and tropical ecosystems. Soil from along this gradient was sampled and incubated in a laboratory temperature block at 40 different temperatures (~1.8-53 ^oC) for five hours. For the experiments, 40 control (soil + distilled water) and 40 treatment (soil + glucose solution) tubes were used to separate the SOM and labile C respiration temperature responses. CO_2 concentrations were measured on an Infrared Gas Analyser (IRGA) after five hours. The second aim of the thesis was to determine the temperature response of priming along the geothermal gradient. Soil priming occurs when added labile C substrates in soil promote the acceleration or deceleration of SOM decomposition. This aim was also completed using the temperature block and IRGA for CO_2 measurements, but instead using a $\delta\ ^{13}C$ labelled glucose solution to separate the temperature response of priming. These samples were also run on an Off Axis Integrated Cavity Output Spectroscopy (OA-ICOS) instrument to measure the isotopic fraction. A mixing model allowed the separation of SOM, glucose and priming temperature responses.

This thesis used a temperature model called Macromolecular rate theory (MMRT) to characterise the temperature responses in terms of temperature optimum (T_{opt}) and temperature inflection point (T_{inf}). Changes in these parameters gave insight into potential responses to warming temperatures.

The results of this thesis found evidence for modest thermal adaptation occurring for the T_{opt} of labile C respiration and the T_{inf} of SOM respiration in response to soil warming. However, these changes were small with changes no larger than 0.198 ^oC per ^oC change in environmental temperature ($^oC\ ^oC^{-1}$) and 0.263 $^oC\ ^oC^{-1}$, respectively. There was no evidence that the T_{inf} of labile C respiration and the T_{opt} of SOM respiration changed with

increasing environmental temperature. The priming results suggested that the temperature response of priming remains constant at different environmental temperatures but differs largely with soil properties. The degree of priming decreased with increasing incubation temperatures (particularly above 40 ^{o}C).

Overall, the results suggested that thermal adaptation may occur in response to global warming, however, this adaptation is likely minor. This means that feedback loops may be alleviated in response to climate change. However, the modesty of the observed changes may indicate that thermal adaptation may not occur or may not be enough to offset feedback loops. Additionally, the negative relationship of priming with increasing temperature may dampen feedback loops with climate change. Overall, further work is required to fully understand the implications of soil warming on microbial responses.

Acknowledgments

This thesis has been a wonderful journey that I will treasure for many years to come. There is a long list of people I would like to acknowledge for helping with the completion of my thesis, but I will list just a few here. Firstly, I would like to thank my supervisor, Professor Louis Schipper, for his support and encouragement throughout this past year. I am grateful and honoured for the opportunity to have worked with Louis on this project. Louis has been an amazing supervisor and he has taught me invaluable skills that have greatly prepared me for my science career. I would like to thank Louis for all the hard work he put into helping me complete this thesis. I look forward to continue working with you in the future.

I would like to acknowledge Charlotte Alster and Kristyn Numa for their extensive help with many aspects of my thesis. Without Kristyn, I would not have learned the methods and techniques required to complete my research. Thank you, Kristyn, for your patience and for putting up with me bugging you regularly with questions, it was a joy working with you. I would like to thank Charlotte, who was a huge help with my experiments, thesis writing, and fieldwork. I have enjoyed getting to know you and having the opportunity to work with you. Your kind heart and willingness to help made a huge difference to my thesis and I am grateful for it.

A big thank you to Holly Harvey-Wishart who helped me hugely in the laboratory and getting set up for the field. Thank you for always greeting me with a smile and being willing to help. I would also like to thank Dr. Jordan Goodrich and Dr. Aaron Wall for their significant help with computer coding and GIS mapping. Also, thank you to Vic Arcus for help with the MMRT equations and Jasmine Robinson for helping me with my methods.

I am grateful to have received funding for this project from the Marsden Fund of New Zealand (MFP-UOW1904), as well as, receiving the University of Waikato Masters Research Scholarship. I would also like to thank Kerry Smith at the Arikikapakapa golf course in Rotorua for sharing his knowledge and allowing me access to my field site.

I would like to thank everyone at the WaiBER research group for their kindness and support. I would like to thank Alice Wheatley-Wilson in particular for being my

companion throughout this experience, thank you for the late evening conservations and all the laughs. Thank you for keeping me sane over the past year!

Last but not least, I would like to thank my family, friends, and partner for supporting me throughout my masters. Thank you for listening to me ramble about my research and for making me smile when I forgot to. I love you guys heaps and I could not have completed this thesis without you all.

Table of Contents

List of Figures

List of Tables

Chapter 1
Introduction

1.1 Relevant Background

Soil carbon is the largest terrestrial stock of carbon (C) globally (Scharlemann *et al.*, 2014). The cycling of soil C is important for all terrestrial biological organisms as it contains nutrients for growth and metabolism. In the soil, there are different types of soil C pools that determine how the C interacts with biotic (living) and abiotic (non-living) factors (Davidson & Janssens, 2006). In simple two pools models, these pools are called labile (readily available) and stable (less available) soil C (Kirschbaum, 2004). Soil C stocks are partly dependent on soil microbial respiration, a metabolic process that converts organic C into CO_2, water and energy. Microbial respiration is a temperature dependent process, with rates generally having a positive relationship with temperature (Xu & Shang, 2016). Climate change and rising global temperatures have the potential to negatively impact our soil C stocks through the acceleration of microbial respiration (Davidson & Janssens, 2006). These effects on soil C are not fully understood and so further work is required to understand the implications (German *et al.*, 2011).

To understand the effect climate change will have on microbial respiration and soil C, the concept of temperature sensitivity needs to be understood (Davidson & Janssens, 2006). Temperature sensitivity is a metric of the degree of change (e.g. in respiration rate) with increasing temperature (Robinson *et al.*, 2017). The temperature sensitivity of soil organic matter decomposition (respiration) in soil can be intrinsic (expressed the direct effect of temperature) or apparent (the observed response under environmental constraints e.g. flooding, chemical/physical protection) (Davidson & Janssens, 2006; Dash *et al.*, 2019). These temperature sensitivities can be measured as relative (relative ratios of rate changes) and absolute terms (absolute rate change at a given temperature) (Sierra, 2012). Many models have been developed to understand these different temperature sensitives. The Arrhenius and Macromolecular rate theory (MMRT) are two of these models focussed on in this thesis.

Arrhenius and MMRT are temperature models that are used to model the temperature responses of microbial respiration and other biological processes (Fang & Moncrieff, 2001; Schipper *et al.*, 2014). The Arrhenius model is a well-established model of the

temperature response of chemical reactions. Whereas, MMRT incorporates the principles of enzyme behaviour, particularly large changes in heat capacity (C_p) during catalysis, to describe microbial rate responses with changing temperature (Hobbs *et al.*, 2013). The MMRT model predicts that respiration rates will increase with temperature until the temperature optimum (T_{opt}) where the maximum rate is measured. Beyond this T_{opt} the enzymes in the reaction decline as their performance declines and ultimately they become denatured (Hobbs *et al.*, 2013). The point where the change in respiration rate is at its greatest is called the temperature inflection point (T_{inf}) (Schipper *et al.*, 2014). The T_{opt} and T_{inf} of microbial respiration can be used to help describe the effect of temperature on microbial respiration rates under different conditions. These parameters have already been used to understand the effects of varying C content, soil moisture and different soil types on microbial respiration rates (Schipper *et al.*, 2014; Robinson *et al.*, 2017; Robinson *et al.*, 2020; Numa *et al.*, 2021). These temperature models can help further our understanding of microbial responses to changes in temperature, which can help predict potential responses to climate change.

Climate change will have some direct impacts on soil microbial communities and their respiration rates through increased temperature, however, the magnitude of this impact is dependent on whether the microorganisms undergo thermal adaptation. The occurrence of thermal adaptation in soil microorganisms is not fully resolved in the literature (e.g. Carey *et al.* (2016), Alster (2019)). Thermal adaptation can be simplified as the adjustment of an organism's metabolic rates (e.g. respiration) to sustained temperature increases or decreases (Bradford *et al.*, 2008). The principles of thermal adaptation can be investigated using many approaches including, artificial soil warming, geothermal gradients and elevational gradients (Luo *et al.*, 2001; Xu *et al.*, 2013; Walker *et al.*, 2018). These temperature gradients can act as proxies for soil warming with future climate change (Boscutti *et al.*, 2018). These gradients are valuable for deepening our understanding of temperature interactions with microorganisms and soil C.

Soil priming is another key factor to consider when investigating the consequences of climate change and specifically, its interactions with soil C stocks. The soil priming effect is the increased or decreased response of soil microbial respiration to the addition of an exogenous C compound (Kuzyakov *et al.*, 2000). Soil priming effects are not well understood and so more research is required in this area. Soil priming effects can result in a large increase in microbial respiration, so it is important to consider the effect when exploring climate change impacts.

A geothermal gradient located in Rotorua, New Zealand, was used in this research as a proxy for soil warming with climate change. The temperature gradient in the soil spanned on average from ~18-36 ^{o}C and so represented a wide range of soil systems from temperate to tropical ecosystems. Consequently, changes in temperature along the gradient may provide insight into how soils across a wide range of mean annual temperatures will respond to seemingly small temperature increases with global warming. Soil from this geothermal gradient was incubated at a range of temperatures to determine if the T_{opt} and T_{inf} of microbial respiration changed along this geothermal gradient. These parameters were measured for both added labile substrate (glucose) and the organic matter in the soil at collection. Differences in these parameters can give insight into whether thermal adaptation has occurred with time and whether, and to what extent, thermal adaptation may occur in response to climate change. The temperature dependence of soil priming was also measured on these geothermal soils to see if the temperature response of priming changed along a geothermal gradient.

1.2 Aims and objectives

The first aim of this study was to investigate the temperature dependence of soil microbial respiration along the length of a geothermal soil gradient. To complete this aim, the soil microbial respiration rates from the consumption of labile C (using glucose) and soil organic matter (SOM; more stable C) were measured at a range of temperatures. The results were modelled using MMRT to determine the T_{opt} and T_{inf} from soil collected from different locations along the geothermal gradient.

The second aim was to investigate the extent of soil priming along this geothermal gradient. The priming response of the soil was measured at a range of incubation temperatures and also modelled using MMRT to determine the T_{opt} and T_{inf} from soil collected from different locations along the geothermal gradient.

This thesis had three main objectives:

1. To determine if the T_{opt} and T_{inf} of SOM- and glucose-induced microbial respiration along a geothermal soil gradient varied with environmental temperature.

2. To determine if the results of objective 1 were also applicable to other labile compounds using yeast extract as a model substrate.

3. To determine the temperature dependence of priming along the geothermal gradient using ^{13}C labelled glucose and characterise it in terms of T_{opt} and T_{inf}.

1.3 Thesis outline

Chapter 2 is a literature review that reviews the current literature and knowledge around the concepts of soil carbon cycling, microbial respiration, temperature sensitivity and temperature models, thermal adaptation, and soil priming. This section will review and evaluate the current knowledge to give insight into the need for future studies.

Chapter 3 provides a full description of the geothermal field site used in this study describing the site's location, history and geological properties. This chapter also describes the methods used to characterise the site in terms of temperature and nutrients.

Chapter 4 describes the full methodology used for the temperature dependence and priming studies. The details of field collection, preliminary studies and data analysis are also discussed.

Chapter 5 is written in the form of a journal paper including a brief description of the site (chapter 3) and methods (chapter 4), and then adding in results and discussion.

Chapter 6 encompasses conclusions made from this thesis work and a discussion of future opportunities.

Chapter 2

Literature Review

2.1 Global Carbon Cycle

Carbon (C) is an element that makes up the base of all living things. C can cycle between organic and inorganic states through growth, decay and decomposition (Janzen, 2004). The global C cycle flows through four main pools that are connected through various pathways, such as, respiration, photosynthesis and fossil fuel burning (**Figure 2.1**). These main pools consist of the biota (mostly vegetation), the atmosphere, soil and the ocean (Janzen, 2004), that can act as sources or sinks of C. Soil is the largest terrestrial C pool, containing more C than the atmosphere and biosphere combined (Jobbágy & Jackson, 2000; Scharlemann *et al.*, 2014). Soil C cycling and its interaction with the atmosphere is of most interest to this thesis and will be the focus of subsequent sections.

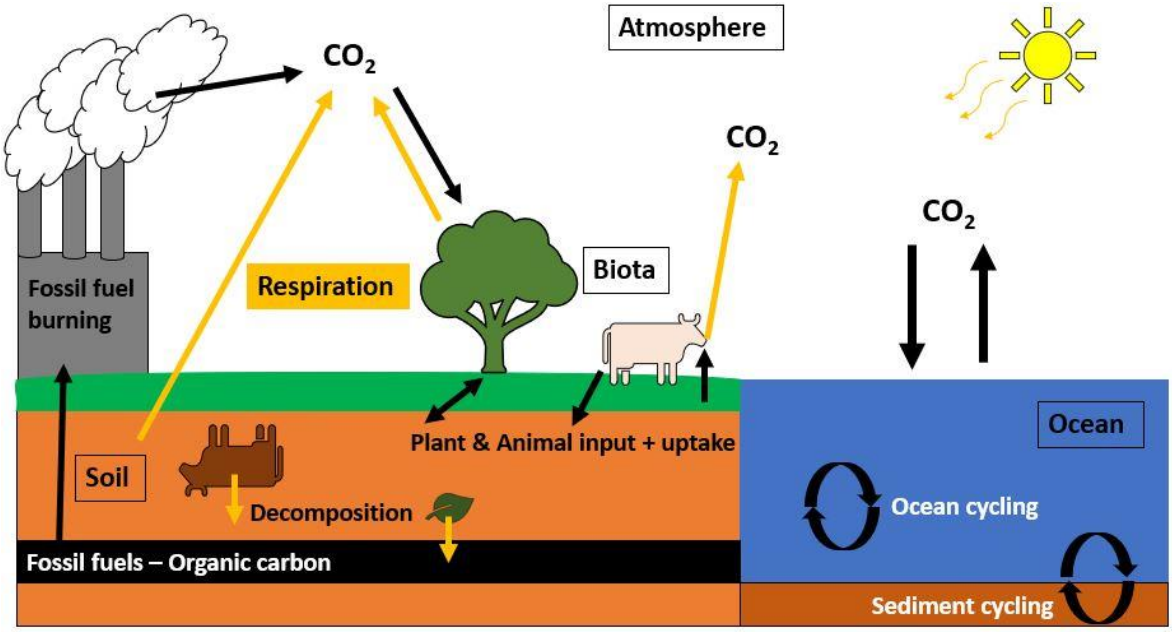

Figure 2.1 The global carbon (C) cycle showing the four main pools of C cycling. The orange arrows represent relevant respiration pathways of carbon dioxide (CO_2). The black arrows represent C flows and cycling.

2.1.1 Climate Change

Greenhouse gases are gas molecules that absorb and release energy in the infrared range of light. The absorption of infrared radiation by these molecules and the subsequent emission back towards the earth leads to atmospheric warming. This warming effect is

referred to as global warming and is a naturally occurring process that is being exacerbated by human activities. Carbon dioxide (CO_2) is a common greenhouse gas produced by natural processes such as respiration, but also produced through anthropogenic fossil fuel burning and land-use change (IPCC, 2007). As the global population has continued to increase over the last decade, the impacts of human activities have increasingly distorted the global C cycle (Janzen, 2004). Increases in fossil fuel burning and land-use changes have led to a drastic increase in atmospheric CO_2 concentrations, from 330 ppm in December 1975 to 415 ppm in January 2021 (Lindsey (2021), **Figure 2.2**). This large excess of CO_2 in the atmosphere has resulted in an increase in the mean global temperature of around 0.85 ^oC since 1880 (IPCC, 2014). The global average temperature has experienced larger positive temperature anomalies since the 1940s which can be seen as the expression of climate change effects (**Figure 2.3**).

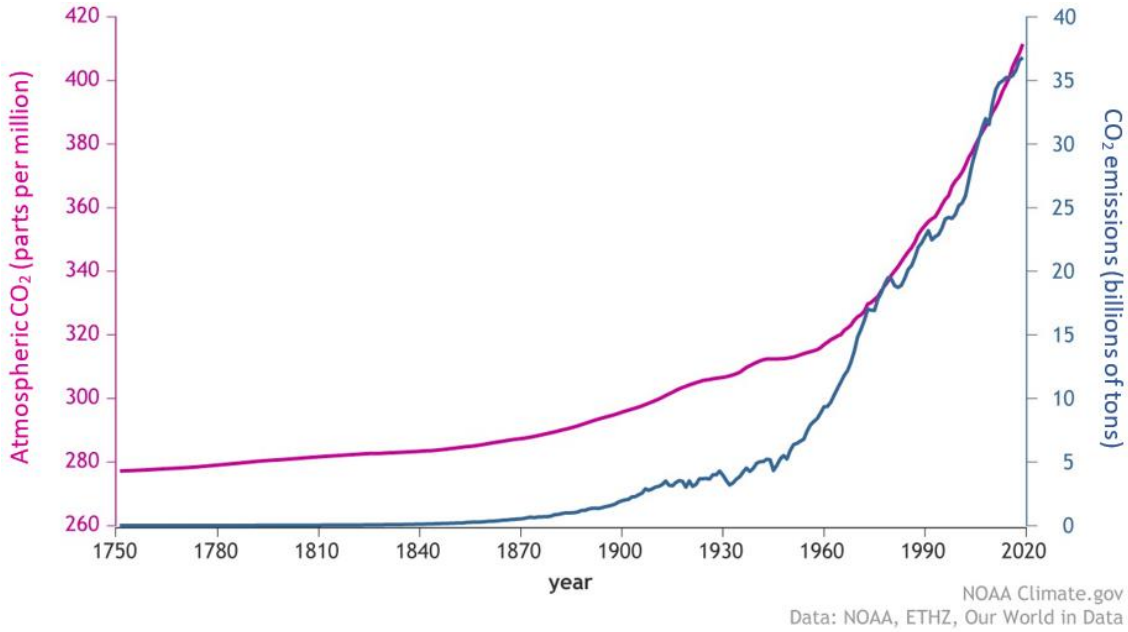

Figure 2.2 Relationship between the amount of CO_2 in the atmosphere (raspberry line) and the increasing human CO_2 emissions (blue line). Data begins at the start of the industrial revolution until the start of 2020. Graph taken from Lindsey (2021).

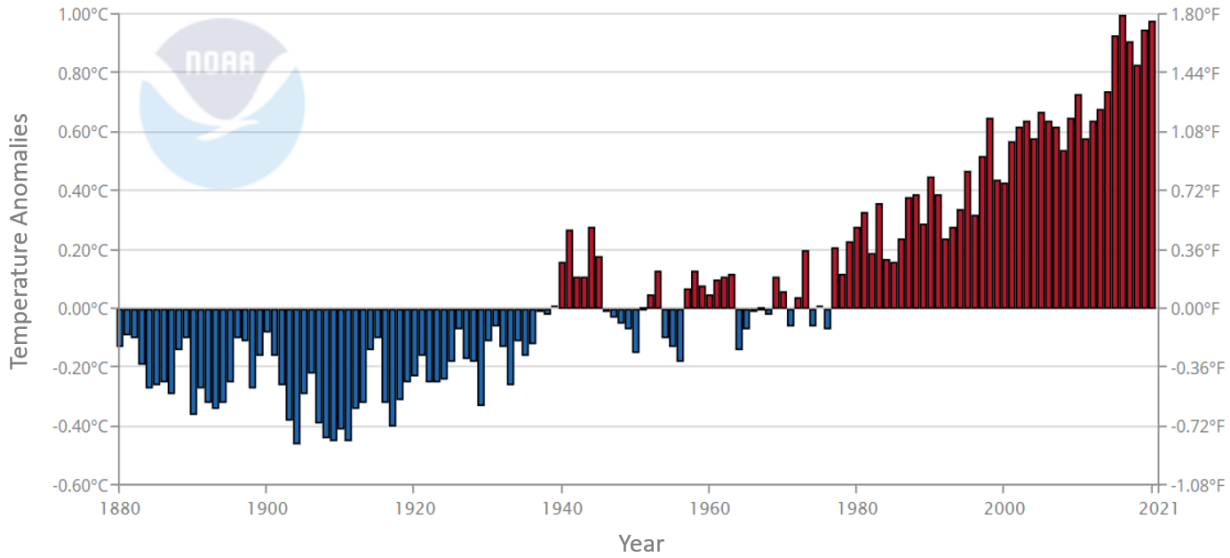

Figure 2.3 Global land and ocean January-December temperature anomalies in both degrees Celsius (left axis) and Fahrenheit (right axis). The anomalies are with respect to the 20th century average. Data taken from NOAA website. https://www.ncdc.noaa.gov/cag/global/time-series/globe/land_ocean/ytd/12/1880-2021.

Global warming causes many negative impacts, such as more frequent extreme weather events, melting polar ice caps and arctic permafrost, extreme droughts, ocean acidification, and coral reef bleaching. Increasing global temperatures also has implications for the stability of the Earth's soil C stock, although the effects are not fully understood (German *et al.*, 2011). There are potential positive and negative feedback loops in soil that may result from increasing global temperatures. A positive feedback occurs when warming accelerates the decomposition rate of C in soil, further releasing CO_2 to the atmosphere (Davidson & Janssens, 2006). Conversely, a negative feedback occurs if plant-derived inputs of C exceed the increase in decomposition rate, leading to greater storage than decay (Davidson & Janssens, 2006). A warming study by Zhang *et al.* (2017) found a significant decrease in soil organic matter (SOM) content with ~ 1.1 ^{o}C climate warming over a 5-year study, suggesting positive feedbacks in response to global warming. There are many other studies that also agree with these findings, for example, Jenkinson *et al.* (1991) and Woodwell *et al.* (1998). However, Field *et al.* (2007) identified that most modelling studies of the 21st century implied that net feedbacks would be negative. Although, the also study suggested that larger warming temperatures will favour positive feedbacks. Field *et al.* (2007) also suggested that at modest warming levels, net feedbacks are likely to be positive at high latitudes and negative at the tropics.

These contrasting conclusions are the reason more research needs to be completed in this area. With large uncertainty of the effect of climate change on our soil C stocks, it is important to conduct studies that can deepen our understanding of temperature and soil C interactions. This knowledge is important for understanding long-term C balances, future climate models and predictions, mitigation options and climate change policies (Tarnocai *et al.*, 2009; Scharlemann *et al.*, 2014).

2.2 Carbon Cycling in Soil

Soil C cycling can be accelerated or decelerated through human influences such as land-use change (Scharlemann *et al.*, 2014). Environmental conditions also influence the rate of soil C cycling. To determine the effects that climate change may have on our soil C stocks, it is important to understand how C is cycled in the soil and its interaction with the other C pools (**Figure 2.4**).

2.2.1 Inputs and losses

Soil C stocks are the function of plant inputs through photosynthesis (primary production; equation (2-1)) and outputs through heterotrophic decomposition (heterotrophic respiration) and autotrophic respiration (equation (2-2)) (Schlesinger, 1977; Janzen, 2004). The production of CO_2 from soils comes from the respiration of plant roots and microbial populations. These types of respiration are generally lumped together as 'soil respiration' (Davidson & Janssens, 2006). The cycling of C in soil can depend on, and is influenced, by many factors including, soil properties, land management practices and weather/climate (Davidson & Janssens, 2006).

$$6CO_{2(g)} + 6H_2O + Light\ Energy \rightarrow C_6H_{12}O_6 + 6O_2 \qquad (2\text{-}1)$$

$$C_6H_{12}O_6 + 6O_2 \rightarrow 6CO_{2(g)} + 6H_2O + Energy\ (ATP) \qquad (2\text{-}2)$$

Equation (2-1) shows the conversion of CO_2 and water (H_2O) to a simple sugar glucose ($C_6H_{12}O_6$) and oxygen (O_2). Photosynthesis is completed primarily by plants on the terrestrial landscape and requires light energy from the sun to proceed. Plants use this

process to acquired C for their growth and development. Plants release C and nutrients into the soil through root decomposition, leaf litter and root exudates (Xu & Shang, 2016).

Microbial respiration occurs when microorganisms break down C compounds and release CO_2. Equation (2-2) is in simple terms the reverse of photosynthesis, where a simple sugar (e.g. glucose) is broken down using oxygen (aerobic respiration) to form CO_2, water and energy for the plant cells (ATP). The CO_2 can then be released from the soil through diffusive processes to the atmosphere (Xu & Shang, 2016).

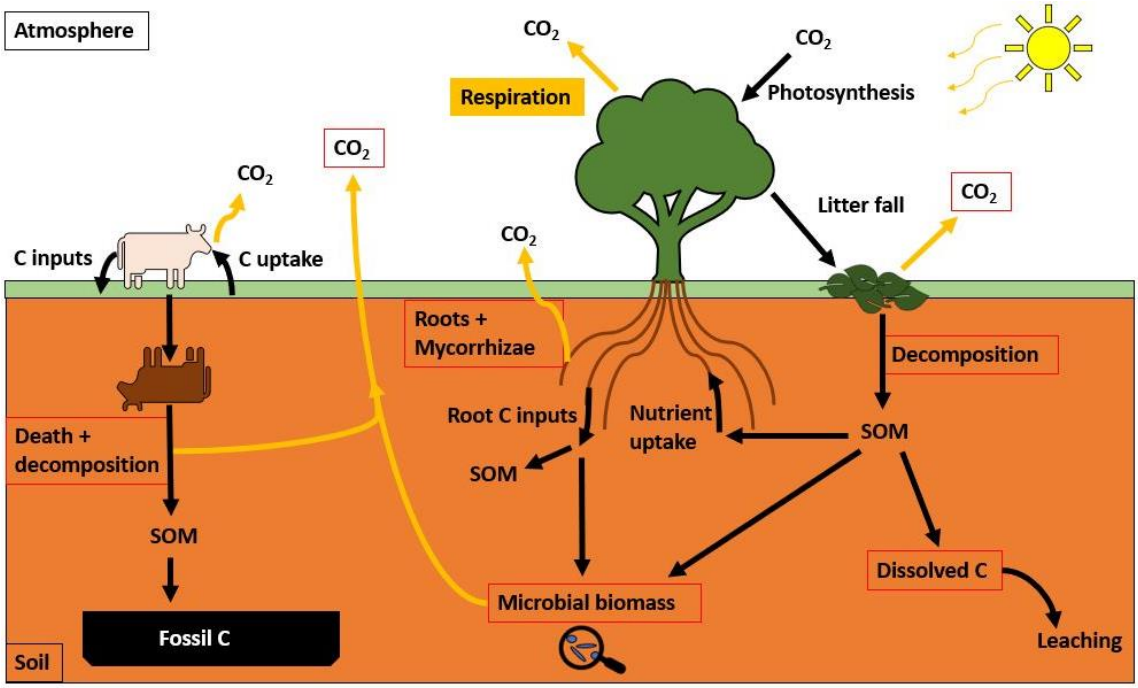

Figure 2.4 Soil C cycling and its interaction with biota and atmosphere. The orange arrows represent pathways of respiration (system outputs). The red boxes identify the processes and their outputs that involve microbial communities. SOM stands for soil organic matter which includes organic C.

2.2.2 Soil carbon pools

Soil C is not uniformly available in the soil and can consist of various forms and compounds. Soil C can be divided into a range of pools based on their relative properties. Each C pool has different properties, such as turnover and residence times, temperature sensitivity and overall availability (Davidson & Janssens, 2006). There are several conceptual models that are used to describe the C pools/SOM pools in soil; three of these are depicted below (**Figure 2.5**). These models separate C into three pools to describe their different properties. When investigating soil processes, two-pool models are often used for simplicity

(Kirschbaum, 2004). These two-pool models are typically split into labile and stable C pools. A simple two-pool model used in this thesis and will be further discussed in Chapter 4.

There are two terms used to describe the general availability of C compounds, labile and stable. Labile C is C that is readily available for energy use. Stable C, also known as 'recalcitrant C', is less available to living organisms (Kleber, 2010) and forms a larger proportion of total soil C (~95 %) (Knorr *et al.*, 2005; Davidson & Janssens, 2006; Kleber, 2010). Compared with labile C, stable C also exhibits higher temperature sensitivity (based on Q_{10}), according to many studies (Craine *et al.*, 2010; Tucker *et al.*, 2013). The type of substrate and pool size determines the amount of substrate available for microbial respiration.

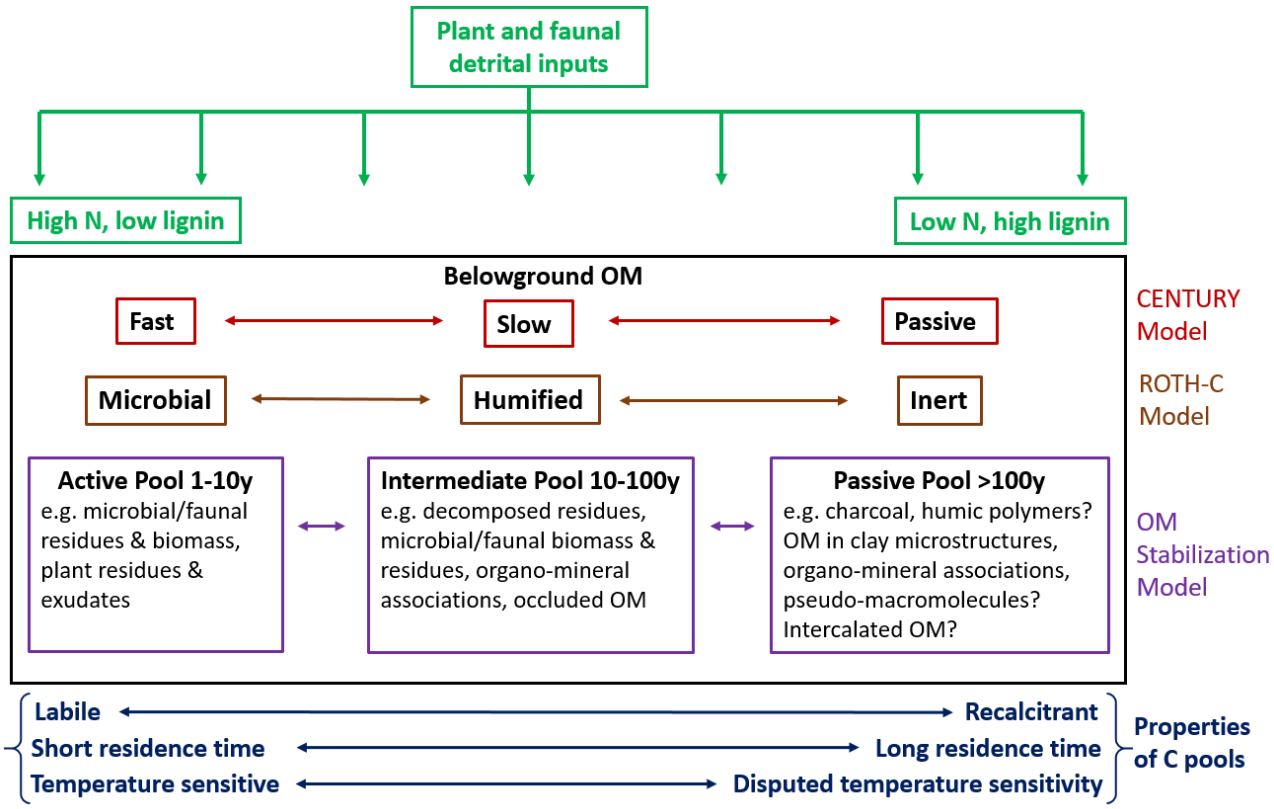

Figure 2.5 This diagram summarises the conceptual belowground C pools of three common models. The first two are the CENTURY and ROTH-C models, respectively. The organic matter (OM) Stabilization model is based on work completed by Sollins *et al.* (1996) and von Lützow *et al.* (2006). Detrital material enters the system and joins a C pool based on the OM properties. The "?" at the end of an example signifies the postulated pool segments that are not verified by direct measurements. The years indicate turnover times. Image adapted from Davidson and Janssens (2006), with ideas from von Lützow *et al.* (2008).

2.3 Controls on Microbial Respiration

Microbial populations respond rapidly to variations in environmental conditions (Mackelprang *et al.*, 2011). Typically, they respond through changes in reaction rates that results in changes in growth, reproduction and respiration. Soil microbes are the main decomposers in soil, consisting of a large variety of bacterial and fungal species (Hartley *et al.*, 2008; Xu & Shang, 2016). Soil microbes can undertake both aerobic and anaerobic processes to decompose organic matter and respire CO_2 (Xu & Shang, 2016). Competitive interactions or abilities, between and within, microbial populations can influence the microbial respiration rates from soil (Crowther & Bradford, 2013). However, the process of soil microbial respiration is primarily controlled by five main factors; substrate availability, soil moisture and oxygen availability, soil pH and temperature (Davidson & Janssens, 2006). These proximal controls affect the rate of respiration and hence, the amount of CO_2 produced from the soil. These factors are influenced by distal controls such as land management practices (e.g. irrigation, fertiliser inputs) and climatic factors such as rainfall (Davidson & Janssens, 2006).

2.3.1 Substrate availability

Substrate bioavailability, including the quality, quantity and recalcitrance, largely affects microbial respiration (Knorr *et al.*, 2005; Tucker *et al.*, 2013). Substrate is required for microorganisms to obtain energy and respire CO_2, without access to such compounds they cannot gain energy for processes such as growth and reproduction.

More complex substrates are less available and less favoured by microbes as they required more energy to break down. Therefore, labile substrates are favoured due to their greater accessibility and bioavailability. The availability of substrate is influenced by pH, moisture content, temperature, plant growth, land management practices and physical chemistry such as diffusion, adsorption, and desorption processes.

The size of C pools in the soil will also determine substrate availability to microorganisms and will determine if substrate depletion may occur (Tucker *et al.*, 2013). If there is no or little substrate available then it is difficult for microbes to gain access to the necessary compounds required for growth and reproduction, hence, they will respire less to save energy. Substrate depletion typically causes reduced rates of respiration and can negatively affect the growth of microbial organisms (Hartley *et al.*, 2008). The amount

of substrate available is a limiting factor for sustained respiration and is a dominant factor influencing the response of microbial respiration to warming (Hartley *et al.*, 2007).

Microbial populations have developed evolutionary tactics to help them gain access to external compounds in their environment, increasing substrate availability to them. Microbes can produce extracellular enzymes into the soil to degrade complex SOM compounds into easily assimilated molecules, giving them access to nutrients and energy previously unavailable (Allison & Vitousek, 2005). However, producing these enzymes is costly and so if labile substrate is abundant then the decomposition of more recalcitrant SOM will be inhibited and extracellular enzymes will not be produced. If substrate availability is low, then organisms may benefit from producing extracellular enzymes to find nutrients, however, the nutrients and energy required for enzyme synthesis may constrain their production (Allison & Vitousek, 2005).

The type of SOM also makes a difference to the availability. Bulk soil is separated into two functionally different fractions consisting of particulate organic matter (POM) and mineral-associated organic matter (MAOM) (Lugato *et al.*, 2021). The breakdown of POM leads to the formation of MAOM. Particulate organic matter consists of structural polymeric compounds primarily from plants (e.g. visible leaf material). The stability of POM is determined by its protection by soil aggregates. It is incredibly vulnerable to environmental changes compared to MAOM which is more protected. Mineral-associated organic matter is primarily made up of low molecular weight compounds (formed from plant inputs) that form associations with mineral surfaces (Lugato *et al.*, 2021). Overall, if the MAOM is destabilized it is a more useful source of labile C and nutrients for plants and microbiota (Lavallee *et al.*, 2020). Particulate organic matter is more readily available than MAOM but it can vary in its usefulness as quality varies. These two broad types of SOM function differently so it can be important to consider them separately (Lavallee *et al.*, 2020).

2.3.2 Soil moisture and oxygen

Soil moisture is an important proximal control on soil respiration (Lellei-Kovács *et al.*, 2011). Soil moisture affects microbial respiration both directly and indirectly (Xu & Shang, 2016). The moisture content (MC) of soil influences respiration by affecting the diffusion of soluble substrates and oxygen levels, both of which can limit microbial respiration (Davidson *et al.*, 2006).

Soil MC is influenced by several factors which Reynolds (1970) suggested is divided non-exclusively into two broad groups: static (slow changing factors) and dynamic (more rapidly changing). Some static factors include; the amount of soil homogeneity, SOM content, soil structure/texture/properties, infiltration rate and topographic factors (e.g. slope, elevation). Some dynamic factors include; precipitation/weather conditions, depth of the water table, and variability in vegetation type/cover/cover density and litter layer extent.

High soil moisture increases substrate availability and mobility, as well as, the mobility of microbes as water films create pathways for essential nutrients (Xu & Shang, 2016). However, too much moisture can cause negative effects on microbial performance through suppressing oxygen levels and the diffusivity of oxygen. This can create a stressful environment for aerobic organisms. Oxygen is the ideal terminal electron acceptor in microbial decomposition/respiration. For ATP synthesis (cell energy) and CO_2 formation, oxygen supply is a critical component (Xu & Shang, 2016). When the soil oxygen levels are low, some organisms can switch metabolic pathways from aerobic respiration to alternative anaerobic pathways, but these are generally slower and less energy-yielding (Xu & Shang, 2016).

In contrast, low soil moisture favours high oxygen levels in the soil pore spaces but decreases the diffusivity of soluble substrates required for microbial activity (Xu & Shang, 2016). Consequently, there is an optimum moisture content in soil at which aerobic respiration is stable (**Figure 2.6**).

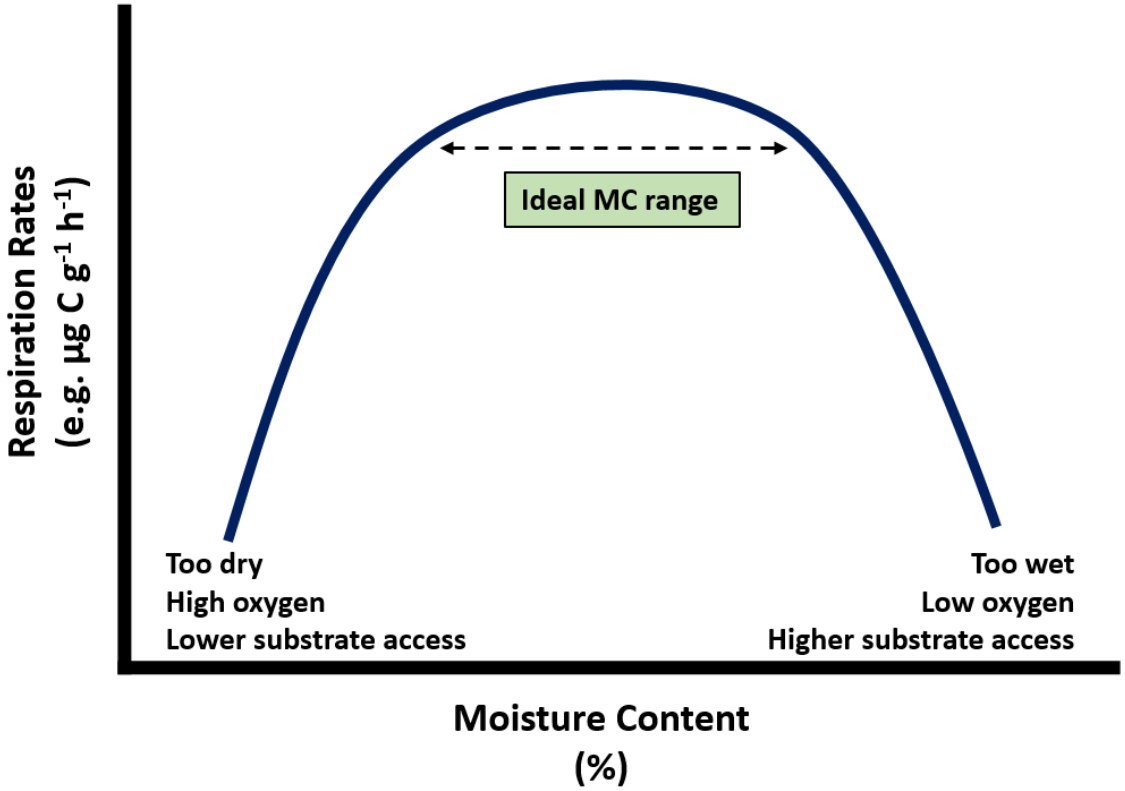

Figure 2.6 A schematic diagram of the relationship between moisture content (MC) percentages on the x-axis and respiration fluxes on the y-axis (µg C g^{-1} h^{-1}) in the soil, with reference to oxygen levels. This is a widely accepted concept for aerobic respiration, which is the focus of this thesis.

2.3.3 Soil pH

Soil pH can influence all the chemical, biological and physical properties of soil (Aciego Pietri & Brookes, 2008). Soil type and soil water balance largely influence pH through modifying a soil's buffering capacity to pH changes (Fabian *et al.*, 2014; Slessarev *et al.*, 2016; Hong *et al.*, 2019). However, soil pH is affected also by plants, soil leaching, nitrogen deposition, SOM content and changes in climate (Hong *et al.*, 2019). Different organisms have different tolerances to pH, for example, acidophilic bacteria are adapted to low pH environments (acidic), whereas most organisms require a neutral pH to survive. Soil pH affects microbial distributions in soil, which thereby influences organic matter decomposition and hence, soil respiration rates (Yang *et al.*, 2019). The availability of substrates for microbial processes is highly influenced by soil pH through processes such as cation exchange capacity (Meyer, 2013). This can affect the rate of microbial respiration both directly and indirectly by affecting the health and distribution of microorganisms (**Figure 2.7**). Nutrients such as aluminium can become toxic at low pH,

further limiting the ability of microorganisms to grow and respire in extreme pH environments.

A study by Sharp *et al.* (2014) showed that pH had a significant effect on microbial diversity. They showed that the diversity of species lowered as the pH dropped below 6 because fewer microbial species can tolerate the stress of a low pH environment. High concentrations of hydrogen ions (low pH) or hydroxide ions (high pH) can cause problems with a cell's internal solute concentrations. Substrates diffuse from an area of high concentration to an area of lower concentration. If the extracellular concentration of ions is high, the cell struggles to keep its intracellular pH neutral (required for the stabilisation of DNA & RNA). When this balance is disrupted and the cell can no longer maintain a survivable intracellular pH, the cell degrades and the membrane lyses. If a microorganism can survive these stressful conditions (e.g. < pH 4 or > pH 8), it has the potential to respire more CO_2 than under stable environmental pH values (e.g. pH 7). This is due to the increased energy required for cell maintenance to stay alive (Aciego Pietri & Brookes, 2008). This stress response relates to C use efficiency (CUE), where more available C will be partitioned to maintenance processes (e.g. efflux pumps, defence compounds), requiring more energy (ATP), proportionally greater C amounts must be diverted into respiration to gain this energy rather than cell growth (Jones *et al.*, 2019).

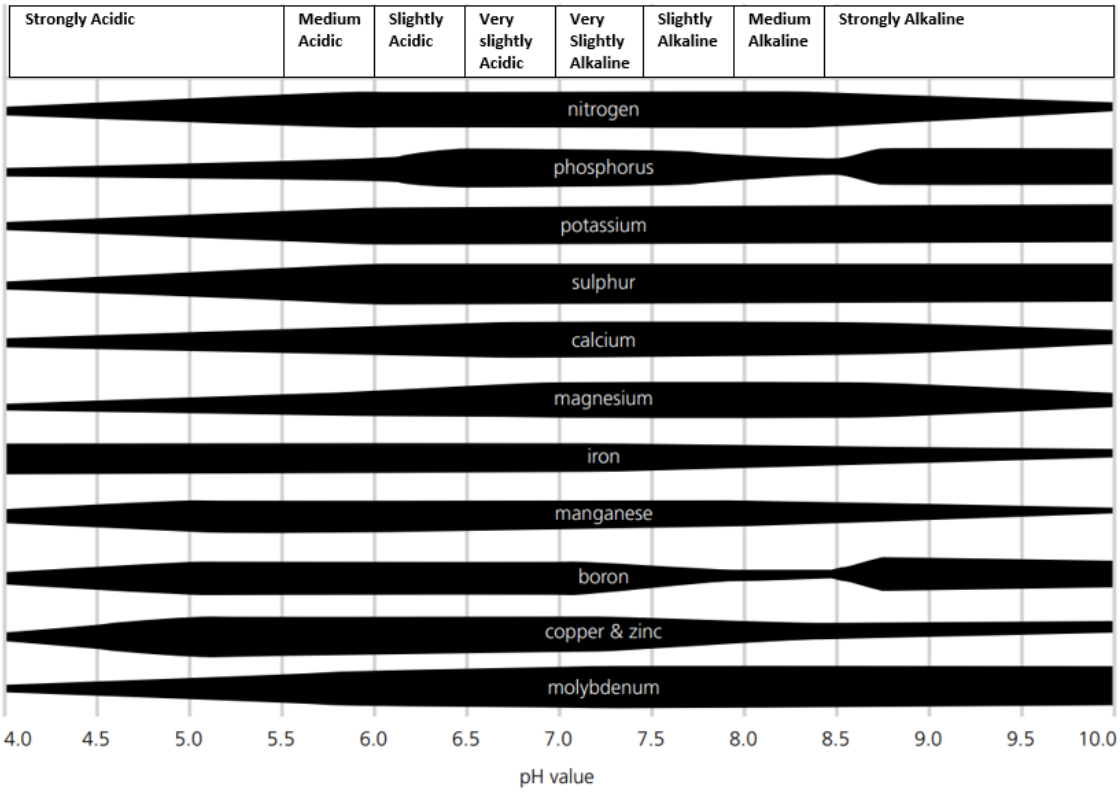

Figure 2.7 Nutrient availability across a range of pH values found in soils. Image updated from Meyer (2013).

2.3.4 Temperature

Temperature accelerates the rates of microbial respiration in a positive relationship (Bradford *et al.*, 2008), that has been shown in many field (e.g. Lloyd and Taylor (1994)) and laboratory studies (e.g. Hartley *et al.* (2007)). This increase in rate with temperature continues until a point called an optimum where the maximum reaction rate occurs. Beyond this point, reaction rates decline as organisms become negatively impacted. This initial relationship with reaction rates (e.g. respiration rate) and temperature tends to be exponential or nonlinear until the optimum is reached (Xu & Shang, 2016; Liang *et al.*, 2017; Robinson *et al.*, 2020). Temperature is also a strong driver of microbial diversity and distribution (Sharp *et al.*, 2014). Sharp et al. (2014) showed that temperature explained the majority of microbial diversity distribution when compared with pH.

Temperature is a major factor influencing microbial respiration, so much so, that it interacts with the other factors previously described, primarily soil MC. Higher soil moisture (to a point), results in a higher respiration flux at any given temperature. However, higher soil temperatures can also lead to soil drying which can decrease soil microbial respiration. Soil moisture and temperature interact and the threshold of one affects the threshold of the other. It has been found that soil temperature determines the optimal soil moisture for respiration (Lellei-Kovács *et al.*, 2011). Increasing temperature can also decrease the pH of a system, although the changes may be small (Hong *et al.*, 2019). Therefore, temperature is a major factor that needs to be investigated when trying to understand microbial respiration changes.

2.4 Modelling Temperature Responses

To understand the impacts of climate change it is important to understand how the environment will respond to changes in global temperature. For soil environments, it is important to determine whether the increases in global temperatures will lead to sustained or temporary feedback loops. Therefore, to understand, predict and model the temperature responses of respiration rates over a range of temperatures, various models have been developed, including the Arrhenius and the Lloyd and Taylor models (Fang & Moncrieff, 2001). None of these models include a temperature optimum, instead, they predict continuously increasing rates of respiration with increasing temperature. A more recent way of modelling temperature responses that includes this optimum is the Macromolecular rate theory (MMRT; (Hobbs *et al.*, 2013; Schipper *et al.*, 2014)). In this

section, the applicability and relevant background of the Arrhenius-like models and MMRT approaches will be discussed.

2.4.1 Relative and absolute sensitivity

Temperature sensitivity is a measure of how quickly a rate increases for every degree increase in temperature (Robinson *et al.*, 2017). Respiration rates, decompositions rates, $Q_{10,}$ and turnover time are all common measures used to assess the sensitivity of organic matter decomposition (Sierra, 2012). The temperature sensitivity of organic matter is determined by its properties (e.g. the C pool it resides in) (Davidson & Janssens, 2006). The temperature sensitivity of the organic matter helps to determine the temperature response of respiration rates. The influence of temperature on these rates can be described in terms of relative or absolute temperature sensitivity. These two sensitivity measurements have contrasting behaviour, therefore, to understand the sensitivity of respiration rates to environmental change, it is important to distinguish between them (Sierra, 2012).

Relative sensitivity expresses the change in k (e.g. decomposition or respiration rate) with a given change in temperature, relative to the actual value of k. In other words, it expresses the ratio of rates $(1/k)\,\partial k/\partial T$ (Sierra, 2012). In contrast, absolute sensitivity expresses an absolute change in k for a given change in temperature ($\partial k/\partial T$;(Sierra, 2012)). Here, decomposition rates will be the focus of this section since both decomposition rates and respiration rates are calculated similarly.

Arrhenius kinetics and thermodynamics are widely accepted to describe reaction rates (equation (2-5); discussed in section 2.4.3). The analysis completed by Sierra (2012), which is the focus of this subsection, used the Arrhenius function as a backbone. However, here the general concept of relative vs absolute temperature sensitivity using work by Sierra (2012) will be described in brief (see Sierra (2012) and section 2.4.3 for further detail). A key to understanding temperature sensitivity is to understand the contrasting behaviour of relative and absolute temperature sensitivity. The figure below (**Figure 2.8**) illustrates the opposing temperature sensitivities in simplified terms of the Arrhenius function.

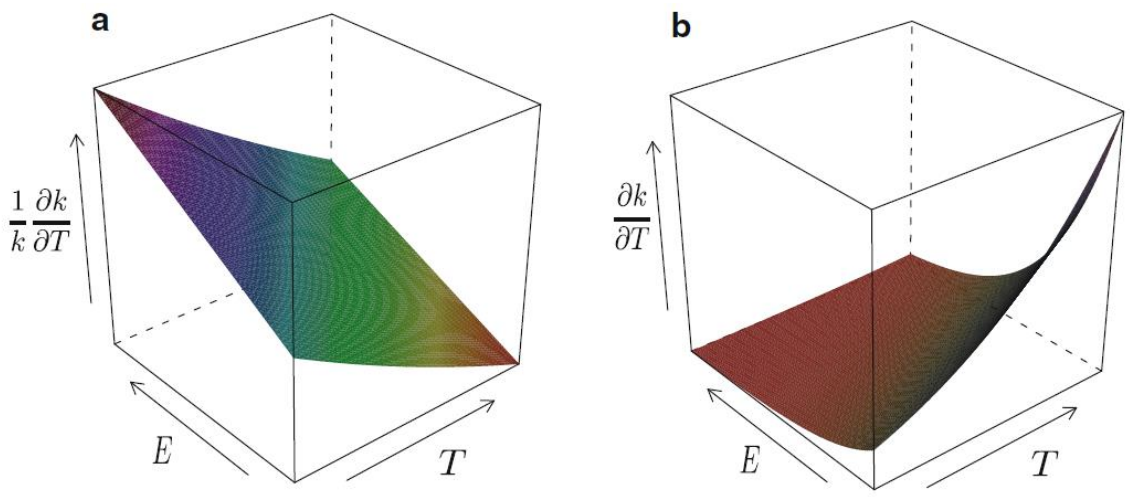

Figure 2.8 The temperature sensitivity of decomposition rates (k) as a function of temperature (T) and activation energy (E). Panel a shows the relative sensitivity of decomposition rates ($1/k$) $\partial k/\partial T$. Panel b shows the absolute sensitivity of decomposition rates $\partial k/\partial T$. Image from (Sierra, 2012).

In general, both relative and absolute sensitivity measurements agree that low-quality substrates have low decomposition rates. However, in relative terms, low-quality substrates are shown to have greater temperature sensitivity. In contrast, in absolute terms, the high-quality substrates are more sensitive to temperature changes. Sierra (2012) found that 70% of studies they looked at agreed with these statements.

The two sensitivities of decomposition rates behave in opposite directions when substrate quality decreases (Sierra, 2012). Sierra (2012) used activation energy (E) as a measure of substrate quality, whereby higher activation energies are required for lower quality substrates. Relative sensitivity shows linear increases toward infinity as substrate quality decreases (equation (2-3)), whereas absolute sensitivity exponentially decreases toward zero (equation (2-4)). These opposing behaviours are applicable under any given temperature for any given substrate (Sierra, 2012).

$$\lim_{E\to\infty} \frac{1}{k}\frac{\partial k}{\partial T} = \infty \tag{2-3}$$

$$\lim_{E\to\infty} \frac{\partial k}{\partial T} = 0 \tag{2-4}$$

As mentioned earlier, turnover time is another metric of temperature sensitivity. Turnover time (τ) is the inverse of the decomposition rate; it can be also referred to as the mean residence time (Sierra, 2012). In relative terms, both the turnover time and decomposition

rates behave similarly with increasing temperature, however, in absolute terms these measures produce contrasting results.

When investigating global climate system effects on soil C, it is the absolute changes in these stocks that are of most importance (Sierra 2012). Ultimately, it is insufficient to study global soil C changes looking at relative changes alone, when it is the absolute change in global C stocks that matters most. Using these two sensitivities in combination is recommended by Sierra (2012) when looking at the sensitivity of substrates with temperature changes.

The most widely used measure of relative temperature sensitivity (Q_{10}) will be described in detail below (section 2.4.1.1). Further details on absolute temperature sensitivity will be discussed in the context of established temperature models in later sections (sections 2.4.3-2.4.4).

2.4.1.1 Q_{10}

Q_{10} is the most widely used parameter to describe temperature sensitivity around the world (Sierra, 2012). Q_{10} is a factor that is used to describe the increases in respiration rate with a 10 ^{o}C rise in temperature (Davidson & Janssens, 2006). This factor is used as a proxy to describe the relative temperature sensitivity of SOM decomposition with variations in temperature (Fang & Moncrieff, 2001). Q_{10} provides a similar measure of relative sensitivities to decomposition rates and turnover times (Sierra, 2012). In some situations, Q_{10} can be an advantageous measure to use because it provides values of sensitivity independent of the absolute rate or C amount available. However, it does not provide information on which soil C pools are involved (Sierra, 2012).

There are multiple ways of calculating Q_{10} proposed in the literature. The use of multiple different functions to calculate Q_{10} can limit inter-comparisons through the production of different estimates (Sierra 2012). There is also a possibility that some of these functions may introduce biases through the addition of random variables across many models (Sierra, 2012). Another issue with multiple functions in the literature is that some assume Q_{10} behaves as a universal or single constant, which in most cases Q_{10} does not. Many studies set Q_{10} to a value of 2 and hold this constant across temperatures (Davidson & Janssens, 2006). However, other studies have found that Q_{10} varies above and below a value of 2 (e.g. Schindlbacher *et al.* (2010)). Evidence from theoretical and experimental

bases shows that Q_{10} only equals a value of 2 under specific conditions (Davidson & Janssens, 2006).

It has been shown by many studies that Q_{10} decreases with increasing temperature and that Q_{10} itself is temperature dependent (Lloyd & Taylor, 1994). Some temperature models, such as the exponential model, do not account for this phenomenon (Lellei-Kovács *et al.*, 2016). The observation that Q_{10} decreases with increasing temperature is commonly observed in nature (Davidson & Janssens, 2006). This observation is important to account for when investigating and extrapolating microbial processes with environmental change.

Ultimately, interpreting Q_{10} temperature coefficient should be treated with caution and comparisons between Q_{10} derived from different temperature response functions should be avoided (Sierra 2012).

2.4.2 Intrinsic and apparent sensitivity

Intrinsic and apparent temperature sensitivity are both determinants of temperature responses (Davidson & Janssens, 2006). Intrinsic sensitivity expresses the direct temperature effect on microbial decomposition (Schipper *et al.*, 2014). Apparent temperature sensitivity is the observed response of microbial decomposition under environmental constraints (Davidson & Janssens, 2006; Dash *et al.*, 2019). A complex relationship exists between these two temperature sensitivities (Dash *et al.*, 2019) so it is important to distinguish between the two when interpreting temperature responses.

The inherent kinetic properties (activation energy & structure) or the inherent response of a soil C pool to temperature is called its 'intrinsic temperature sensitivity (Davidson & Janssens, 2006; Dash *et al.*, 2019). The intrinsic sensitivity is expressed as the partial derivative, which measures absolute changes in reaction rate with changes in temperature (Sierra *et al.*, 2015). This sensitivity is primarily dependent on the ambient temperature, the chemical structure, and kinetic properties of the soil C pool (Dash et al. 2019; Sierra et al. 2015). Arrhenius functions and MMRT can be used to calculate intrinsic temperature sensitivity of organic matter decomposition with respect to temperature (Davidson and Janssens 2006).

The 'apparent' temperature sensitivity of soil C pools is the observed (measured) response to changes in temperature under environmental constraints (Davidson and Janssens 2006).

Apparent sensitivity expresses the absolute change in reaction rate with directional changes all in the driving variables (Sierra et al. 2015). The apparent sensitivity includes environmental constraints on rates and it is these environmental controls (see below for examples) that lead to the apparent temperature sensitivity (Dash et al. 2019).

Environmental constraints are factors or processes that slow down the decompositions rates of soil organic C (Dash et al. 2019). These constraints typically result in lower sensitivities (the apparent sensitivity) than the real intrinsic temperature sensitivity. There are four broad classifications of environmental constraints which protect soil organic C decomposition; physical, biological, chemical, and biochemical (Dash et al. 2019). Environmental constraints include things such as physical and chemical protection, flooding, freezing, drought, soil aggregation, microbial excretions and clay associated C (Dash et al. 2019; Davidson and Janssens 2006). Environmental constraints are themselves sensitive to management practices, climate and temperature changes (Dash et al. 2019; Davidson and Janssens 2006). These complex interactions form a complex relationship between intrinsic and apparent sensitivity. The relationship between intrinsic and apparent temperature sensitivities is shown in **Figure 2.9**, while an example of factors influencing apparent sensitivity can be found in **Figure 2.10**.

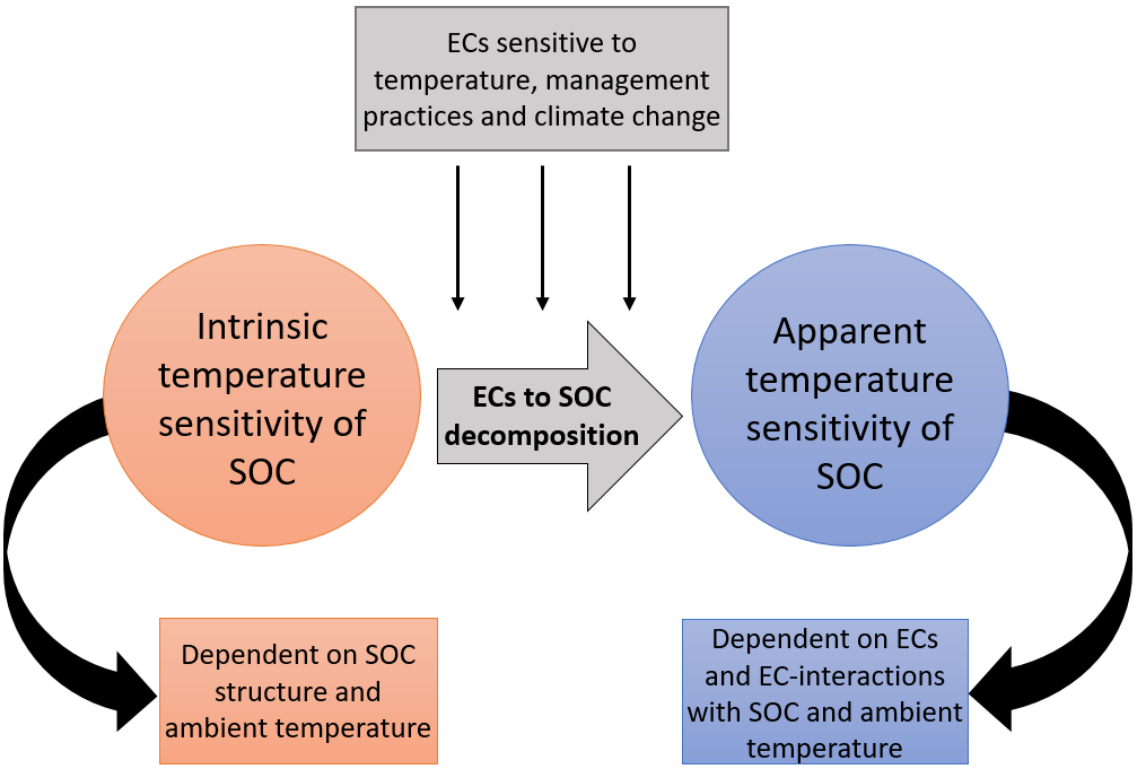

Figure 2.9 The relationship between intrinsic and apparent temperature sensitivity of soil organic carbon (SOC). The environmental constraints (ECs) influence the intrinsic sensitivity giving the apparent (measured) sensitivity. Adapted from Dash et al. (2019).

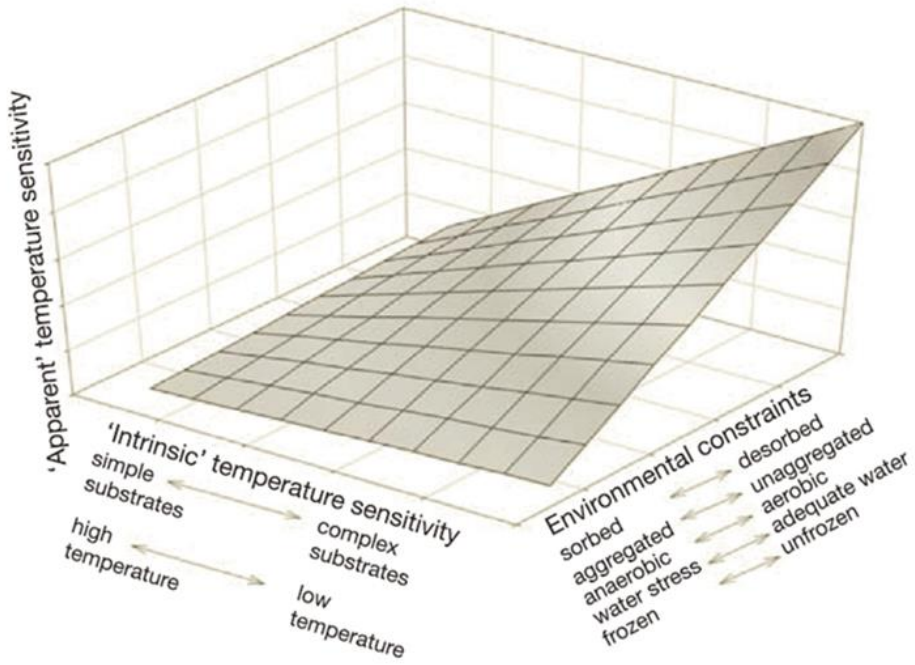

Figure 2.10 The diagram illustrates the factors affecting the apparent sensitivity of SOM decomposition. In general, more complex molecules have higher activation energies and temperature sensitivities than simple molecules. Environmental constraints dampen the intrinsic sensitivity often by reducing the availability of substrate, leading to a lower apparent sensitivity than would be expected. Image from Davidson and Janssens (2006).

2.4.3 Arrhenius model

Svante Arrhenius noticed that biochemical reactions often require a 'push' for the process to proceed, this 'push' is called the "activation energy" of the reaction (Davidson & Janssens, 2006). The activation energy helps substrates undergo transformation, which typically involves bond making or breaking in a 'transition state' (Schipper *et al.*, 2014). Considering this activation energy term and thermodynamic principles, the Arrhenius equation (equation (2-5)) was created in the 19th century to describe the relationship between temperature and reaction rate (Hobbs et al. 2013, Fang and Moncrieff 2001).

$$k = A\, e^{E_A/RT} \qquad (2\text{-}5)$$

Where: k is the reaction rate constant, A is a pre-exponential factor, E_A is the reactions required activation energy, R is the universal gas constant (8.314 J K^{-1} mol^{-1}), T is the temperature in Kelvin (K) (Davidson & Janssens, 2006; Hobbs *et al.*, 2013).

In relation to temperature, the Arrhenius model describes changes in the relative rates of reaction (Davidson and Janssens 2006). The Arrhenius model predicts that with increasing temperature, the rate of reaction will increase in a continuous exponential fashion (Robinson et al. 2017). This model is commonly used for describing the relationship between soil respiration and temperature. The first derivative (dk/dT) of the Arrhenius model describes at any particular temperature, the absolute temperature sensitivity (Schipper *et al.*, 2014).

In a review by Fang and Moncrieff (2001) of various temperature models, the Arrhenius equation was favoured based on its performance and theoretical basis. Although, despite its good performance, the Arrhenius equation has been found by many to underestimate respiration rates at low temperatures (e.g. (Lloyd & Taylor, 1994; Fang & Moncrieff, 2001). Even variations of the Arrhenius function, such as the Lloyd and Taylor model, still highly underestimate the relative temperature sensitivity at low temperatures (Schipper et al. 2014). However, despite these limitations, the Lloyd and Taylor and Arrhenius models are still widely used and accepted by the scientific community. These models have been very useful for expanding our knowledge in this area.

The Arrhenius equation was designed to describe the rates of physical chemistry, not necessarily to describe biochemical processes that involve large macromolecules (Hobbs *et al.*, 2013). A study by Robinson *et al.* (2020), investigating the interactions between labile and stable C pools, found that SOM tended to follow an Arrhenius-shaped curve. Schipper *et al.* (2019) also argued that the physical chemistry processes (desorption/sorption/diffusion) of SOM followed the Arrhenius model. The respiration rates of SOM with temperature mostly fit with the Arrhenius function, whereas enzymatic processes tend to be better fitted with MMRT (Schipper *et al.*, 2019; Robinson *et al.*, 2020; Numa *et al.*, 2021). A study by Numa *et al.* (2021) found that this statement was true for multiple soils and C substrates.

Due to this poor representation of enzymatic processes, there is caution against the use of the Arrhenius model and derived factors such as Q_{10} in biochemical modelling (Alster *et al.*, 2020). Therefore, the use of Arrhenius models should be for physical chemistry and the use of MMRT should be incorporated for understanding enzymatic processes. For context, the image below illustrates the Arrhenius model compared to the Arrhenius derived Lloyd & Taylor model and MMRT with different heat capacity parameters (**Figure 2.11**).

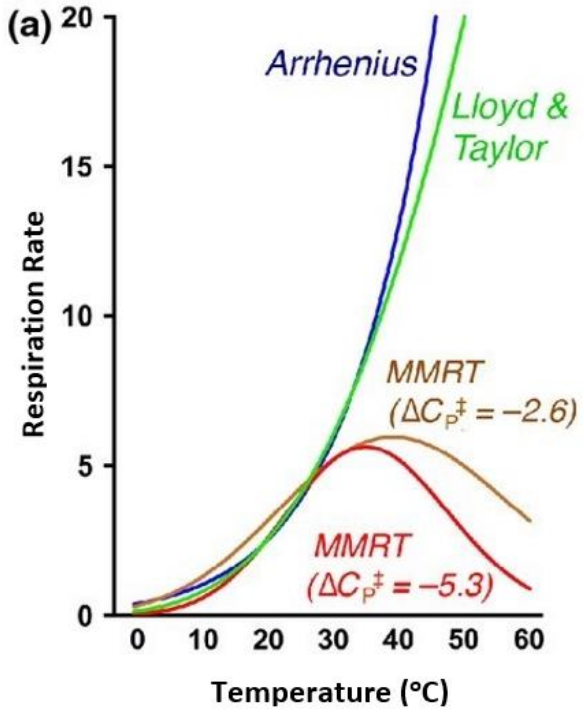

Figure 2.11 Comparison between Arrhenius model, the Lloyd & Taylor model, and MMRT outputs with differing heat capacities. Image taken from Schipper *et al.* (2014) Figure 1 (a).

2.4.3.1 *Arrhenius and temperature sensitivity*

The partial derivative of the Arrhenius equation gives an appropriate measure of absolute sensitivity (Sierra, 2012). The absolute sensitivity of decomposition is described in the simplified equation (2-6). The partial derivative implies that the decomposition rate will increase for constant values of activation energy with increasing temperature (Sierra, 2012). According to Sierra (2012), the logarithmic form of equation (2-6) can be used to evaluate the relative sensitivity of decomposition rates (equation (2-7)).

$$\frac{\partial k}{\partial T} = k\frac{E}{RT^2} \tag{2-6}$$

$$\frac{\partial \ \mathrm{In}\ k}{\partial T} = \frac{E}{RT^2} = \frac{1}{k}\frac{\partial k}{\partial T} \tag{2-7}$$

Where: k is the decomposition rate, T is the absolute temperature (K), E is the activation energy, A is a pre-exponential factor and R is the universal gas constant (8.314 J K^{-1} mol^{-1}).

2.4.3.2 *The Arrhenius model and Q_{10}*

Q_{10} can be calculated from the Arrhenius equation as a relative measurement of temperature sensitivity. One advantage of the model is that it accounts for decreasing Q_{10} value with increasing temperature. The Q_{10} equation used in the Arrhenius model is shown in equation (2-8) below which has been derived from the Arrhenius equation (Sierra, 2012).

$$Q_{10} = \frac{K_{T+10}}{K_T} \quad (2\text{-}8)$$

Where: K is either decomposition rate (*k*) or respiration rate (R).

As mentioned previously, Q_{10} can be influenced by substrate availability and quality in nature (Davidson & Janssens, 2006). When substrate availability is variable the applicability of Arrhenius kinetics may be limited (Davidson & Janssens, 2006). However, when substrate availability is abundant, Arrhenius kinetics are followed by enzyme-catalysed reactions. When substrate availability is low, these reactions follow Michaelis-Menten Kinetics (equation (2-9)).

$$k = \frac{V_{max} \times [S]}{(K_m + [S])} \quad (2\text{-}9)$$

Where: k is the reaction rate, V_{max} is the reaction rate maximum at a given temperature, [S] is the substrate availability and K_m is the Michaelis–Menten constant (Davidson & Janssens, 2006).

As predicted by the Arrhenius relationship, higher amounts of recalcitrant organic matter leads to higher Q_{10} values. In contrast, predictions from Michaelis Menten Kinetics suggest that diminishing substrate amounts could lead to a decrease in Q_{10} (Davidson & Janssens, 2006; Hamdi *et al.*, 2013). These concepts are important to consider when interpreting the results of temperature response work using the Arrhenius model.

2.4.4 Macromolecular rate theory

Macromolecular rate theory (MMRT) was developed from thermodynamics and first principles (Hobbs *et al.*, 2013; Schipper *et al.*, 2014). A key part of the MMRT theory is that the activation energy of reactions catalysed by enzymes is temperature dependent (Schipper et al. 2014). The MMRT model accounts for the initial exponential increases in rate that have been observed with increasing temperature, but the model then curves to fit an optimum (Alster *et al.*, 2016; Alster *et al.*, 2018; Robinson *et al.*, 2020). The temperature optimum (T_{opt}) of any reaction/process is the temperature where the activity is at its maximum rate (Hobbs *et al.*, 2013). Above this T_{opt}, the rate of activity beings to decline. This phenomenon is commonly seen in biological temperature responses, although, it is not always accounted for (e.g. the Arrhenius model; (Schipper *et al.*, 2014; Robinson *et al.*, 2017)). The MMRT function was developed to incorporate this T_{opt} and to provide a better method of modelling temperature responses.

In the early 20th century, the Arrhenius theory was developed further by Eyring and Polyani who quantified the pre-exponential term 'A' from the Arrhenius equation (equation (2-5)). The result was equation (2-10) which was termed the 'transition state theory' (Schipper et al. 2014).

$$k = \frac{k_B T}{h} e^{\left(\frac{-\Delta G^{\ddagger}}{RT}\right)} \qquad (2\text{-}10)$$

Where: k is the rate constant, k_B is Boltzmann's constant, T is the temperature (K), h is Planck's constant, $\Delta G^{\ddagger}$ is the change in Gibbs free energy (‡ superscript denotes transition state) and R is the universal gas constant.

To simplify equation (2-10) above the natural log can be taken for both sides of the equation, giving equation (2-11).

$$\ln(k) = ln\left(\frac{k_B T}{h}\right) - \frac{\Delta G^{\ddagger}}{RT} \qquad (2\text{-}11)$$

The equation has remarkable accuracy at describing chemical reactions over large temperature ranges (Hobbs *et al.*, 2013; Schipper *et al.*, 2014; Arcus *et al.*, 2016). However, biological reactions typically rely on enzymes that have a high heat capacity (C_p; Cooper (2005)). Heat capacity is defined as the amount of heat that is required to

raise a substance's temperature by 1 °C (Hanrahan, 2012). Large heat capacity changes can be hugely influential for the temperature dependence of Gibbs free energy ($\Delta G^{\ddagger}$) for the reaction and so needs to be accounted for (Oliveberg *et al.*, 1995). This heat capacity term was added into the model through the Gibbs free energy equation in the formation of MMRT (equation (2-12) & (2-13); (Hobbs *et al.*, 2013; Arcus & Pudney, 2015; Arcus *et al.*, 2016)). It is important to note that changes in heat capacity ($\Delta C_P^{\ddagger}$), enthalpy ($\Delta H_{T_0}^{\ddagger}$), and entropy ($\Delta S_{T_0}^{\ddagger}$) are in reference to the difference between the ground state and the transition state of the reaction (Hobbs *et al.*, 2013).

$$\Delta G^{\ddagger} = \Delta H^{\ddagger} - T\Delta S^{\ddagger} \tag{2-12}$$

$$\Delta G^{\ddagger} = \left[\Delta H_{T_0}^{\ddagger} + \Delta C_P^{\ddagger}(T - T_0)\right] - T\left[\Delta S_{T_0}^{\ddagger} + \Delta C_P^{\ddagger}(lnT - lnT_0)\right] \tag{2-13}$$

Where: $\Delta H_{T_0}^{\ddagger}$ is the change in enthalpy (J mol^{-1}), $\Delta S_{T_0}^{\ddagger}$ is the change in entropy (J mol^{-1} K^{-1}) both at reference temperature T_0 (309 K, 36 °C), $\Delta C_P^{\ddagger}$ is the change heat capacity (J mol^{-1} K^{-1}) (Robinson et al. 2020).

Combining the natural log of the transition state theory equation (equation (2-11)) and the extended Gibbs free energy equation (equation (2-13)) above gives the MMRT equation (equation (2-14)). Originally this was tested for enzymes and shown to have strong explanatory power (Hobbs *et al.*, 2013; Arcus & Pudney, 2015; Arcus *et al.*, 2016). Schipper *et al.* (2014) also applied this MMRT equation across a wide range of soil science studies and found it to describe the temperature response of a wide variety of processes.

$$ln(k) = ln\left(\frac{k_B T}{h}\right) - \frac{\Delta H_{T_0}^{\ddagger} + \Delta C_P^{\ddagger}(T - T_0)}{RT} + \frac{\Delta S_{T_0}^{\ddagger} + \Delta C_P^{\ddagger}(lnT - lnT_0)}{R} \tag{2-14}$$

Hobbs *et al.* (2013) initially developed the MMRT equation to model the reaction rates of enzymes in response to temperature. The model can further be scaled to model microbial growth rates. Since the initial development of the MMRT model, it has been applied to irrigated and unirrigated soils (Schipper et al. 2019), investigations of labile

and stable C pools responses including leaf litter (Robinson et al. 2020) and multiple different C substrates (Numa *et al.*, 2021), it has also been applied to multiple soil types and moisture contents (Robinson *et al.*, 2017; Numa *et al.*, 2021). MMRT model has also been applied to many other areas, including work on plants and leaf respiration, and to describe global respiration and photosynthesis (Liang *et al.*, 2017).

The schematic in **Figure 2.12** shows the general response output when applying MMRT to soil respiration/decomposition. As mentioned previously multiple studies have found that SOM decomposition generally follows an Arrhenius-like curve (e.g. Robinson *et al.* (2020); Numa *et al.* (2021)).

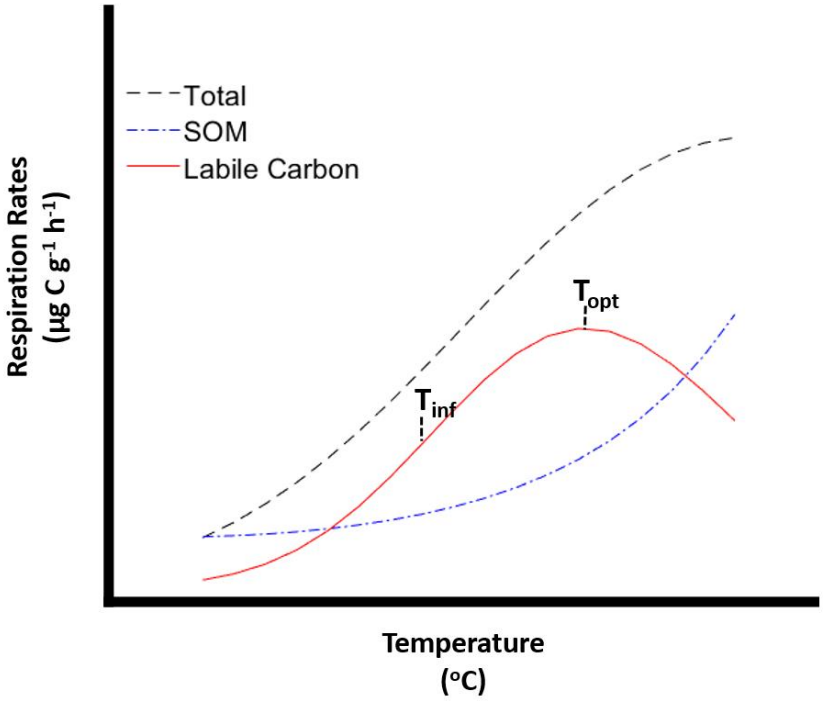

Figure 2.12 A schematic diagram of general MMRT respiration outputs (µg C g^{-1} h^{-1}) with temperature (°C). The SOM (blue) follows an Arrhenius curve. Both total respiration (combining labile and SOM; black) and labile C (red) follow MMRT curvatures. The temperature optimum (T_{opt}) and inflection point (T_{inf}) are marked for the labile C curve.

2.4.4.1 *Temperature sensitivity in MMRT*

Similar to the Arrhenius model, taking the first derivative of the MMRT equation gives the absolute temperature sensitivity (Robinson *et al.*, 2017).

The relative temperature sensitivity for this model is preferably calculated through equation (2-15), which was derived directly from the MMRT equation (Schipper *et al.*, 2014). The equation gives the Q_{10} as a proxy for the relative temperature sensitivity. This

equation for Q_{10} predicts decreasing Q_{10} with increasing temperature (Schipper *et al.*, 2014) which is an important aspect of Q_{10} in nature (Davidson & Janssens, 2006).

$$Q_{10} = e^{\left(\frac{10\Delta H^{\ddagger} - 5\Delta C_P^{\ddagger}}{RT^2}\right)} \quad (2\text{-}15)$$

2.4.4.2 *Temperature optima*

The T_{opt} for biological reactions identifies the temperature of the maximum rate. Beyond this optimum, the rate of reaction declines as enzymes become dysfunctional at higher temperatures and large negative values of heat capacity (C_p) occur for the enzyme catalyst (Hobbs *et al.*, 2013). The T_{opt} in the MMRT model constrains the curvature of the temperature response curve even before the T_{opt} resulting in a departure from exponential models (e.g. the Arrhenius model; (Robinson *et al.*, 2017)). The T_{opt} for a reaction can be calculated using equation (2-16) (Schipper *et al.*, 2019). This T_{opt} equation is derived from when the first derivative of the MMRT equation equals zero.

$$T_{opt} = \frac{\Delta H_{T_0}^{\ddagger} - \Delta C_P^{\ddagger} T_0}{-\Delta C_P^{\ddagger} - R} \quad (2\text{-}16)$$

Work by Numa *et al.* (2021) looking at a variety of C substrates and three different soil types, showed that six labile C substrates (glucose, yeast, arginine, lysine, glutamine & maltose), consistently had a T_{opt} of around 37 ^{o}C when incubated at a range of temperatures. Whether this is true for a wider range of soil types or climate regimes remains unanswered.

2.4.4.3 *The inflection point - hypothesis*

The inflection point (T_{inf}) of respiration is the temperature at which this process is the most sensitive to temperature increases, that is, where the change in respiration rate is greatest (Schipper *et al.*, 2014; Schipper *et al.*, 2019). This T_{inf} is the steepest part of the fitted curve (Prentice *et al.*, 2020). The T_{inf} can be calculated using equation (2-17) (Schipper *et al.*, 2019). This T_{inf} equation is derived from when the second derivative of the MMRT equation equals zero.

$$T_{inf} = \frac{\Delta H^{\ddagger}_{T_0} - \Delta C^{\ddagger}_P . T_0}{-\Delta C^{\ddagger}_P \pm \sqrt{-\Delta C^{\ddagger}_P . R}} \quad (2\text{-}17)$$

While T_{opt} is relatively intuitive, the T_{inf} is also critical for understanding the temperature response of an organism. Recently, the inflection point hypothesis proposed by Prentice *et al.* (2020) suggested that the T_{inf} of enzymes involved in biological reactions coincided with the T_{opt} of the parent organism. The hypothesis proposes that T_{inf}, not T_{opt} is evolutionarily selected for when enzymes adapt to environmental temperatures. The hypothesis suggests that the T_{inf} of metabolic enzymes is aligned at the average environmental temperature of the parent organism. This alignment allows for enzymes to maintain intrinsic homeostasis across a range of fluctuating environmental temperatures. Multiple metabolic enzymes align at the T_{inf} to allow for collinearly of enzyme reaction rates across short time scale changes in environmental temperature (Prentice *et al.*, 2020).

Having enzymes aligned to the T_{inf} decreases the need for precise alignments of enzyme temperature profiles due to the approximately linear relationship between temperature and rate at this point (d2k/dT2 = 0). If enzymes were aligned to the T_{opt} then enzymes would be restricted to a small temperature range where the rate either side of the T_{opt} declines. According to the hypothesis, aligning T_{inf} to the environmental temperature allows for less precision and more flexibility to variations in environmental temperature. The figure below shows the results of Prentice *et al.* (2020) when applying MMRT to the rate of E.coli metabolic enzymes to changes in temperature (**Figure 2.13**).

With regards to soil, the hypothesis suggests that enzymes inside microorganisms living in soil will set their T_{inf} at the temperature of their parent organism's soil environment. The microorganisms would benefit from this as soil environmental temperature can fluctuate variably over time. Enzymes following this hypothesis will remain flexible over these variable soil temperatures.

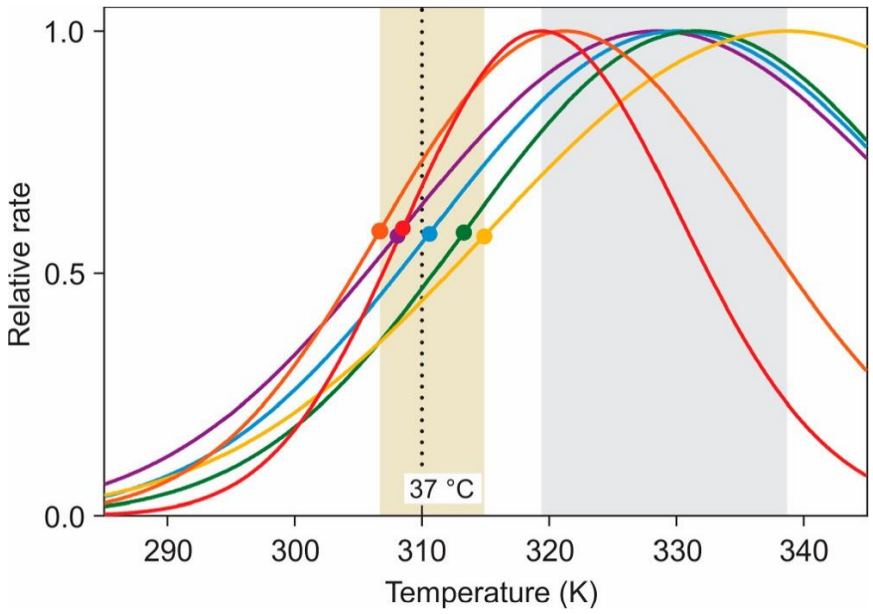

Figure 2.13 The relative temperature profiles of *E.coli's* glycolytic enzymes. Note the temperature is in Kelvins. Each enzyme response has been fitted with MMRT. The filled-in circles represent the T_{inf} point of the corresponding enzyme. The temperature range of the T_{inf} points are shaded in beige. The grey shaded area shows the range of T_{opt} values. The dotted line indicates *E.coli's* optimum growth temperature (37 ^{o}C; 310 K). Image from Prentice *et al.* (2020).

2.4.4.4 *MMRT application – key points*

Presented below is a summary of key findings produced from working using MMRT theory in soil environments:

- Schipper *et al.* (2019) determined that irrigated soils, compared to unirrigated soils, had lower respiration rates and higher Q_{10} values. They attributed this difference to the lower C availability in the irrigated soils from disproportionate past losses of C. This study showed that land management can influence the temperature dependence of soil respiration when other factors are controlled.

- A study by Robinson *et al.* (2017) observed that the temperature sensitivity and T_{inf} was not dependent on soil type.

- Robinson *et al.* (2020) observed that respiration from fresh litter inputs (liable C) had a lower T_{opt} and were less temperature sensitive than more stable C.

- Numa *et al.* (2021) measured the respiration of highly available C compounds to have an average T_{opt} ~37 ^{o}C and an average T_{inf} ~22 ^{o}C.

2.5 Microbial Communities and Geothermal Activity

A major challenge for studying temperature responses of soil microbes is finding soils with different environmental temperatures while also not varying in many other factors such as soil type, rainfall and vegetation. Geothermal sites may offer a potential approach for exploring the temperature response of soil processes.

Geothermal sites are characteristic of pH extremes, steep temperature gradients, steam exposure, highly mineralised soil/waters, slow-growing vegetation and having overall stressful environmental conditions (Boothroyd, 2009). Some adapted organisms require these conditions to survive (Satyanarayana *et al.*, 2005). Other species which are not adapted are unable to survive the environmental conditions. Microbial adaptation to environmental changes is important to understand as it will determine how communities will respond to sustained changes, such as climate change.

Geothermal soils can be used as a proxy for warming soils with climate change (Peterse *et al.*, 2009; Sigurdsson *et al.*, 2016; Parts *et al.*, 2019). Geothermal soils have been used in the past to investigate microbial adaptation to soil warming (Walker *et al.*, 2018). Geothermal soils make a great proxy for soil warming because they are naturally warmed, can be studied *in situ* as a whole ecosystem and are confined in space which reduces other confounding environmental factors (O'Gorman *et al.*, 2014; Sigurdsson *et al.*, 2016). Often geothermal features have been in place for decades and presumably the soil ecosystem has had time to adapt to this wide range of temperatures. Along with geothermal gradients, other natural warming gradients have been used as proxies for soil warming, these include, elevation gradients (Xu *et al.*, 2013; Boscutti *et al.*, 2018) and latitudinal gradients (De Frenne *et al.*, 2013). Geothermal gradients can be advantageous over these other gradients because they can function similarly to latitudinal gradients or large elevational gradients in a spatially confined space (Sigurdsson *et al.*, 2016). With the right experimental design, geothermal gradients can help to tease apart responses to warming across time, space and biological complexity (O'Gorman *et al.*, 2014). Geothermal gradients pose a range of warming scenarios projected by the IPCC (Inter-governmental Panel on Climate Change) which make them important tools for investigating the effects of climate change (Marañón-Jiménez *et al.*, 2018).

Of interest to this work is the temperature dependence of microbial respiration along a geothermal temperature gradient and evaluating the concept of thermal adaptation in this

context. The following subsections investigate the current knowledge around these key concepts.

2.5.1 Microbial communities and thermal adaptation

The concept of thermal adaptation is becoming increasingly critical to understanding the response of natural ecosystems to the effects of climate change. In this context, thermal adaptation can be defined as, adjustments to the rate of heterotrophic soil respiration in response to sustained temperature increases or decreases (Bradford *et al.*, 2008). Thermal adaptation theory posits that with increasing temperature, the microbial respiration rates per unit microbial biomass will decrease as they adapt to the new environmental temperature (Bradford *et al.*, 2008). This is due to evolutionary trade-offs between the function and structure of an organism's enzymes in response to temperature (Hochachka & Somero, 2002; Bradford *et al.*, 2008; Alster, 2019). This attenuation of heterotrophic soil respiration to temperature stimulation over time has been referred to as thermal 'acclimation', 'acclimatization' or 'adaptation' (Tucker *et al.*, 2013), although some authors use these terms with separate meanings. The term acclimatization is typically used due to the similarity of plant respiration acclimation to ambient temperatures (Atkin & Tjoelker, 2003; Tucker *et al.*, 2013). It is worth noting that previous studies working on thermal adaptation theory have used the Arrhenius equation and Q_{10} metrics of absolute rates, which have been found to be relatively poor metrics of soil temperature sensitivity and biological processes (Alster *et al.*, 2020).

There are three competing hypothesises in thermal adaptation theory, summarized in **Figure 2.14** (Alster, 2019). Alster (2019) summarized two studies (Bradford *et al.*, 2019; Dacal *et al.*, 2019) that combined looked at four different biomes, 4 years of warming experiments, global sampling, and >130 sites with temperatures ranging ~1.8 ^{o}C to 28 ^{o}C. These two studies contain large temporal and spatial differences but both found the same conclusion for supporting the compensatory hypothesis, where a dampening effect on CO_2 losses occurs in response to thermal adaptation. However, even with large support for thermal adaptation theory overall, there is still large debate among the literature as to whether thermal adaption occurs or whether the observed effects are a function of substrate depletion or other contributing factors (Hartley *et al.*, 2007; Bradford *et al.*, 2008; Hartley *et al.*, 2008; Walker *et al.*, 2018).

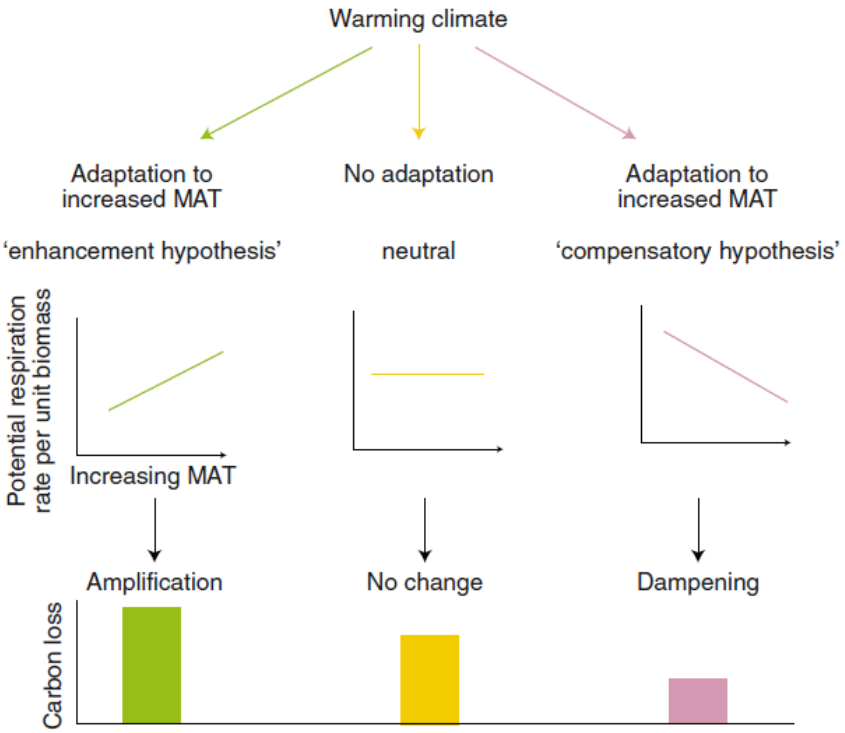

Figure 2.14 Three hypotheses proposed in thermal adaptation theory. MAT stands for mean annual temperature. Enhancement hypothesis – increasing MAT results in increased respiration rates and larger C losses. Neutral hypothesis – no adaptation occurs and so no changes occur to respiration rate or expected C losses. Compensation hypothesis – increased MAT results in decreasing respiration rates as microbes adapt, resulting in dampened soil C losses. Image taken from Alster (2019).

A study by Luo *et al.* (2001) found that a 2 ^{o}C increase in soil temperature was enough to decrease the temperature sensitivity of the soil respiration to higher temperatures, suggesting thermal adaptation occurred. Whereas, a study by Nottingham *et al.* (2020) increased soil temperature in the tropics by 4 ^{o}C and found no evidence of acclimation of respiration rates, no changes in temperature sensitivity or C use efficiency.

Bradford *et al.* (2008) found the after > 15 years of experimental soil warming, thermal adaptation, reductions in soil C pools and microbial biomass all contributed to the reduction of microbial respiration rates with higher seasonal temperatures. However, research by Hartley *et al.* (2007) suggests that substrate availability is the controlling factor to lower respiration rates not thermal adaptation.

To investigate the evidence for thermal acclimation of soil respiration, Carey *et al.* (2016) completed a meta-analysis of a global database (>3800 observations) consisting of 27 individual warming experiments and up to 22 years of experimental warming, spanning across nine different biomes. The results of this meta-analysis found limited evidence for

acclimation of soil respiration to experimental soil warming across these several significant biome types.

Support for both the occurrence and non-occurrence of thermal adaptation is significant and valuable to understanding the interactions between temperature and soil C cycling. The concept of thermal adaptation is important because if microorganisms adapt to rising soil temperatures with increases in global temperatures then the acceleration of CO_2 losses due to positive feedback loops will weaken (**Figure 2.15**, Luo *et al.* (2001)). If this is not the case then as air and soil temperatures rise, respiration rates will continue to increase with increasing temperature, accelerating C losses and climate change (Hartley *et al.*, 2008).

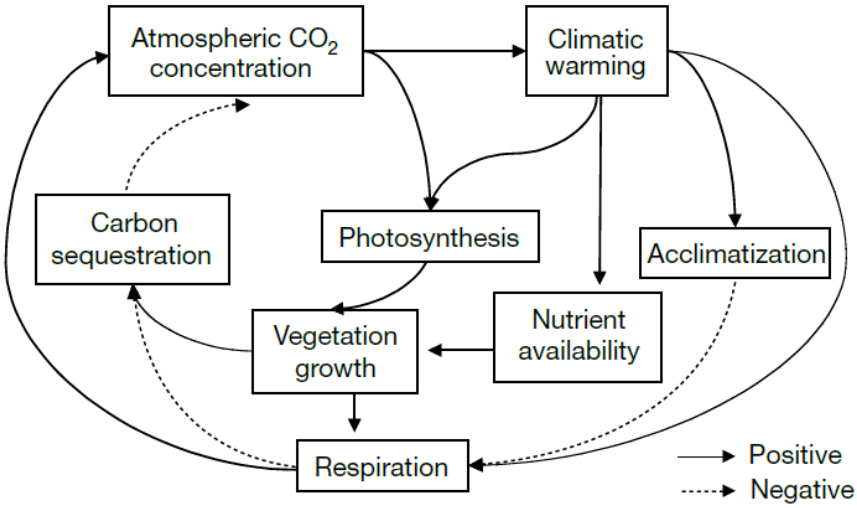

Figure 2.15 A schematic diagram of the positive and negative feedbacks in the climate-carbon cycle. Global warming has the potential to trigger both loops. Positive feedbacks result in increased outputs, negative feedbacks result in reduced outputs. Image taken from Luo *et al.* (2001), see this study for more details.

2.5.1.1 *Thermal adaptation, soil microbial respiration and MMRT*

The adaptation of soil microbial respiration and its effect on climate change is important to understand for making future decisions around climate management. To understand the adaptation of soil microbial respiration there needs to be a basis of informed ideas to help guide experimental findings. As discussed previously, the Arrhenius model and Q_{10} metrics have dominated the work completed in thermal adaptation theory, both of which do not account for a temperature optimum observed in soil processes. Recently, Alster *et al.* (2020) contributed further developments to thermal adaptation theory and proposed

three thermal adaptation hypotheses specifically for the MMRT framework. This subsection will summarize the key points of this article.

In the literature, it is still uncertain how respiration rates or enzymatic V_{max} from Michaelis-Menten kinetics (equation (2-9), section 2.4.3.2) should adapt to temperature change. However, it is expected that V_{max} will become more temperature responsive with soil warming (Alster *et al.*, 2020). In Arrhenius theory of thermal adaptation, enzyme catalyst rates adapted to cold environments should have lower activation energies to compensate for the lower kinetic energy of these environments (Alster *et al.*, 2020). The opposite should then be true for warm adapted enzymes (increase activation energy for reactions, **Figure 2.16a**). However, the support for the Arrhenius-based thermal adaptation theory is still contradictory and the theory has its limitations.

Alster *et al.* (2020) proposed three new hypotheses that fit with the MMRT framework. These hypotheses focus on V_{max} and how this adapts to temperature changes. The hypotheses focus on the $\Delta C_p^{\ddagger}$ and T_{opt} temperature response terms. In general, more negative $\Delta C_p^{\ddagger}$ results in a steeper temperature response curve that reflects larger changes in rate with temperature, whereas a flatter curve expresses the opposite and has a less negative $\Delta C_p^{\ddagger}$. Thermal adaptation in Alster *et al.* (2020) refers to changes in $\Delta C_p^{\ddagger}$ and T_{opt} to shifts in temperature experienced by organisms. The basis of these hypotheses are biochemical and physiological (Alster *et al.*, 2020).

1) Enzyme Rigidity hypothesis (**Figure 2.16b**): Warming temperatures cause C_p of the enzyme to become less negative, T_{opt} increases. The temperature response curve may shift upward with increasing temperature.

2) Optimum-driven hypothesis (**Figure 2.16c**): The T_{opt} will increase with warming but C_p will remain the same. T_{opt} increases to match the new environmental temperature more closely. At more negative C_p values this hypothesis is unlikely following predictions from the Enzyme Rigidity hypothesis.

3) Thermal Breadth hypothesis (**Figure 2.16d**): The temperature range of the environment influences changes in C_p. Greater temperature variation would result in a flatter temperature response curve for the enzymes. Flatter curves allow for more constant rates in environments with varying temperatures. Multiple C_p values can correspond to the same T_{opt} (Alster *et al.*, 2018).

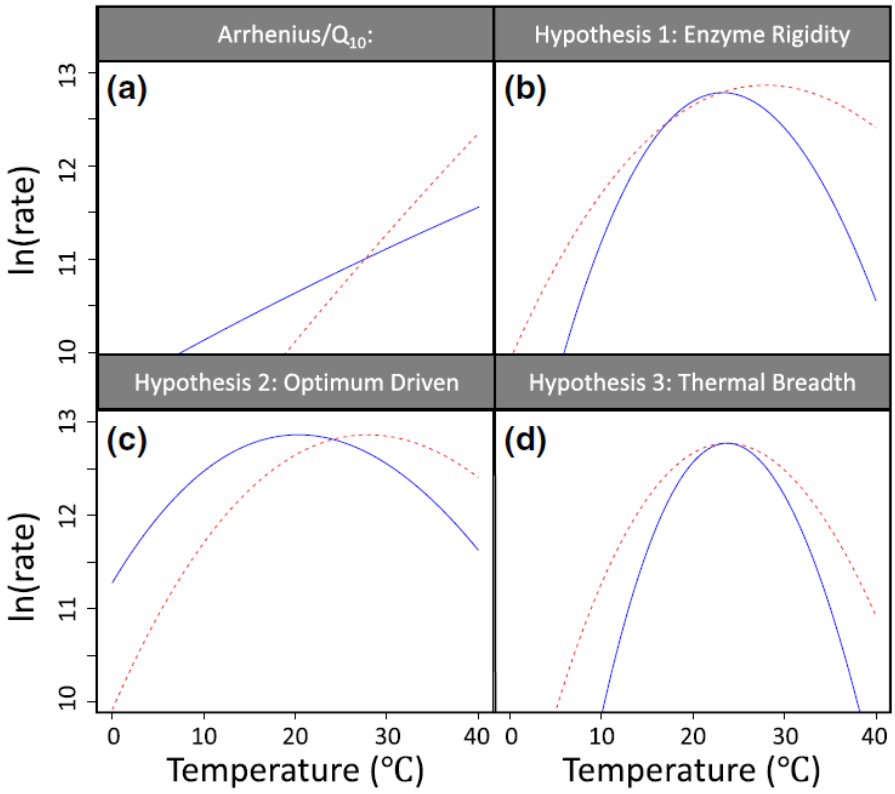

Figure 2.16 Hypothesises for thermal adaptation of temperature response curves. The red dashed lines represent warm-adapted and the blue lines represent cold-adapted biological reactions. Panel (a) shows the Arrhenius thermal hypothesis. Panel (b)-(d) illustrate the hypothesis generated for MMRT adaptation theory. Image from Alster *et al.* (2020).

2.5.2 Using geothermal gradients to assess thermal adaptation

There are few studies that have used geothermal gradients in soil environments to look at the effect of natural and artificial warming. Here, two studies are briefly presented to identify current findings.

A study in Iceland by Walker *et al.* (2018) looked at the respiration rates of microbial populations from stable geothermal gradients with >50 years of natural field warming. The experiment used soil from this stable geothermal gradient and investigated up to +6 ^{o}C of warming from ambient temperature through the use of artificial heating. The study investigated both short-term and long-term warming effects. The study found that microbial respiration rates, along with growth rates, turnover, and C uptake, did not acclimate to warming (+6 ^{o}C) over weeks or decades. A study by Marañón-Jiménez *et al.* (2018) also completed studies on a different geothermal gradient in Iceland. This study investigated a 7-year warming period of 1.8-15.9 ^{o}C in the topsoil. The study looked at two *in situ* treatments, the addition of substrate and no substrate addition. The study found

that in both cases no thermal acclimation or compensatory adaptation of the microbial communities had occurred.

These studies suggest that thermal adaptation does not occur along these geothermal gradients, although Maljanen *et al.* (2019) suggests these results may be confounded by abiotic CO_2 sources. In either case, more work needs to be completed in this area under different climatic regimes in order to support or reject these findings.

2.6 Priming Effects

When investigating the implications of climate change on the soil environment, all factors need to be considered and understood to accurately model and predict future impacts. To do so in the soil environment, a process called 'Priming' needs to be accounted for. Priming effects (PEs) are becoming recognised as playing a significant role in soil nutrient cycling and as a mediator of responses/feedbacks of many ecological processes related to global climate change (Luo *et al.*, 2016). However, PEs are not well understood and so more work needs to be completed to develop our understanding of the processes involved. An overview and summary of soil priming will be covered below.

2.6.1 Priming properties

When an exogenous C substrate is added to soil, this C is liable and widely available to the microbial community. The microbial community mineralises the exogenous C, producing CO_2 as an output. The majority of measured CO_2 from the soil will be the result of exogenous C mineralization (respiration). However, this amendment of C to the system and the stimulation of microbial activity can cause short-term changes to the turnover/decomposition rate of SOM (Kuzyakov *et al.*, 2000; Bastida *et al.*, 2013; Sun *et al.*, 2019). This results in the extra decomposition of SOM in response to the addition of exogenous C substrate into the soil (Dalenberg & Jager, 1989; Kuzyakov *et al.*, 2000). This phenomenon is called the "Priming effect" (PE) and was first discovered by Lohnis (1926) during a study on the decomposition of green manure in soil. The general definition of PE is short-term changes in SOM turnover caused by treatments of the soil (Kuzyakov *et al.*, 2000). PEs have been found not only for C compounds but also for nitrogen, phosphorus and sulphur, following the addition of substrate (Kuzyakov *et al.*, 2000). The PEs of C will be the focus of this thesis.

The C priming has been demonstrated in numerous studies in the last few decades. A meta-analysis by Sun *et al.* (2019) of 2048 comparisons highlighted the inconsistency of results in the literature, the majority of studies showing positive PEs (69.6%), some showing negative PEs (7.3%), and some showing neutral PEs (23.1%). A positive PE occurs when there is an acceleration of SOM decomposition in response to the addition of substrate, such as glucose (Kuzyakov *et al.*, 2000). A negative PE occurs when the addition of a substrate causes a reduction in the decomposition of SOM (Guenet *et al.*, 2010). A neutral PE occurs when no change in SOM decomposition is observed. The concept of positive and negative PEs is visualised in **Figure 2.17**. The naturally complex interactions between abiotic (e.g. moisture, incubation temperatures) and biotic factors are the likely cause of these inconsistencies between previous studies, as these interactions influence the direction and magnitude of PEs (Kuzyakov, 2010; Sun *et al.*, 2019).

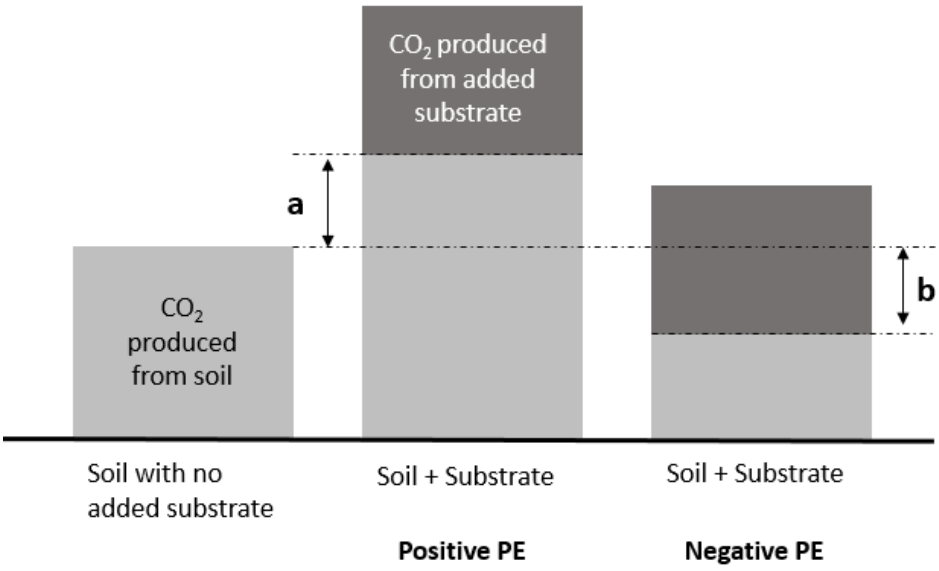

Figure 2.17 A schematic diagram of positive and negative PEs for the addition of exogenous C substrate into the soil: (a) shows the acceleration of SOM decomposition induced by C addition and (b) shows the deceleration of SOM decomposition induced by C addition. Image adapted from Kuzyakov *et al.* (2000).

2.6.2 Potential drivers and controls of priming

Several environmental factors can influence the type and amplitude of PEs. Some general potential influences can include, increasing temperature, increasing turnover rates, soil management, and soil moisture deficits (Kuzyakov, 2010). It is suggested that positive PEs can be stimulated by the addition of mineral fertilisers, readily available organic

substances, plant rhizodeposition, salts or soluble substances, and even soil drying – rewetting (Kuzyakov *et al.*, 2000). In contrast, negative PEs can be stimulated by the addition of easily decomposable C, living plant roots, toxic substances, mineral-N fertilisers, and the addition of organic substances with C\N ratios less than 16 (Kuzyakov *et al.*, 2000). However, it is important to note that the effects of environmental conditions on soil priming are not well understood (Kuzyakov, 2010).

Other potential influences on PE include; substrate quality, soil properties and texture, SOM content and nutrient availability (Kuzyakov *et al.*, 2000; Kuzyakov, 2010; Sun *et al.*, 2019). Sun et al. (2019) found that PE magnitude was dependent on soil properties, ecosystem type, and experimental conditions. For laboratory studies, the incubation duration, temperature, addition rate of substrate, and soil moisture can also influence PEs (Sun *et al.*, 2019).

Substrate type and soil pH can also affect the outcome of PEs. For example, a study by Zhang *et al.* (2019) found that the addition of glucose (labile) and tannin (recalcitrant) compounds to soil produced positive PEs. However, the addition of oxalic acid resulted in negative PEs. The acid treatment was found to have lowered the pH of the soil, negatively affecting microbial growth and reproduction. Soil pH is, therefore, likely to be a key factor in influencing PEs.

2.6.3 Apparent and real PEs

Apparent PEs are the result of an acceleration of microbial metabolism and biomass turnover due to the addition of a fresh C substrate (Blagodatskaya & Kuzyakov, 2008). Real PEs occur when said microbial activity enhances the decomposition of SOM in response to an added substrate (Blagodatskaya & Kuzyakov, 2008). Even with the use of isotopes, disentangling and identifying, apparent or real priming, is difficult or near impossible (Kuzyakov, 2010). Some of the difficulty in distinguishing between these PEs comes from the ability for both effects to occur simultaneously (Blagodatskaya & Kuzyakov, 2008). However, without the use of labelled C substrates using ^{14}C or ^{13}C one cannot evaluate the real PEs occurring in a system (Blagodatskaya & Kuzyakov, 2008). Although there remains debate around the type of PEs detected (apparent or real), most studies agree that real PEs can be inferred when using isotopic traces (Nottingham *et al.*, 2009).

An article by Blagodatskaya and Kuzyakov (2008) suggested the possible mechanisms occurring when PEs result from the addition of exogenous substrates. They suggested a handful of mechanisms that can occur to produce apparent and/or real PEs (**Figure 2.18**). The mechanisms are presented for C cycling and are presented as a successional sequence of processes that can occur during PE. These mechanisms (Blagodatskaya & Kuzyakov, 2008) are summarized below and are often sequential.

1a) Triggering effect – When the added substrate amount is far less than the microbial biomass C, there is a "triggering effect" which produces apparent PEs. The result is a small and brief increase in CO_2 production. There is no change to SOM decomposition, enzyme production, or microbial communities.

1b) Pool substitution – Pool substitution is when labelled C takes the place of unlabelled C in a particular soil pool, where the unlabelled C would have otherwise been used (Jenkinson *et al.*, 1985). After the triggering action has occurred, pool substitution may then cause higher CO_2 production. There is still no change to SOM decomposition at this stage.

1c) Preferential substrate utilization – If the added substrate amount is higher than the microbial biomass C, then the fresh exogenous C substrate is utilised by soil microbes. This may temporality lead to a decrease in SOM decomposition (Negative PE). This can be counterbalanced by pool substitution which produces positive PEs.

2) Microbial activation – Soil microbial community increases their activity; communities grow and change utilising the added substrate.

3) After the usage of readily available substrates (added exogenous liable C), the microbial communities produce extracellular enzymes to find and utilise other sources of C. It is this co-metabolism that promotes the additional SOM decomposition.

4) Eventually microbial activity will return to its initial state and the equilibrium between SOM pools and microbial communities will be restored.

It is generally accepted that apparent priming is often experienced shortly after the addition of available substrate (hours to days), whereas, real priming requires more time (weeks to months) to produce effects (Blagodatskaya & Kuzyakov, 2008; Kuzyakov, 2010; Luo *et al.*, 2016; Bastida *et al.*, 2019). Blagodatskaya and Kuzyakov (2008) suggested that the high microbial turnover after the addition of substrate leads to apparent PEs and not real PEs early on.

The sequence of priming processes can be visualised in a contextual diagram for simplicity (**Figure 2.19**). The diagram represents a situation in the natural environment where the input of labile C originates from plant roots. In a laboratory context, this would be analogous to adding exogenous C substrates such as ^{13}C labelled glucose.

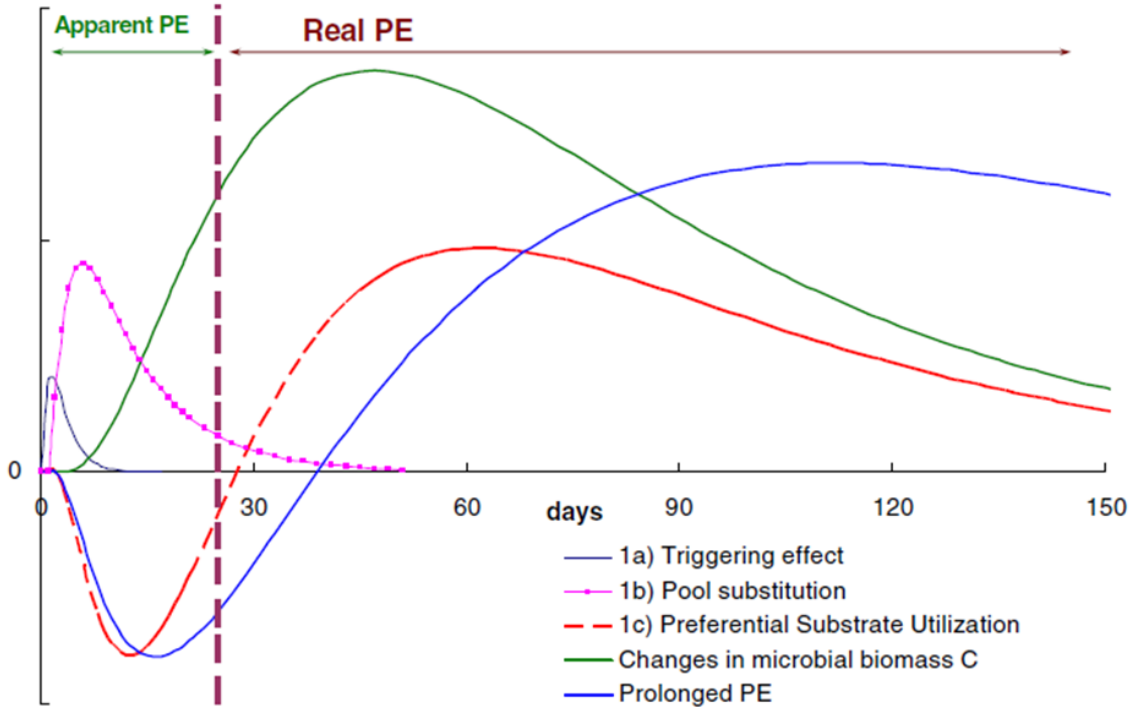

Figure 2.18 Visual representation of the mechanism sequence. Image from Blagodatskaya and Kuzyakov (2008). Note: The first two mechanisms produce apparent effects and are completed in 1-5 days.

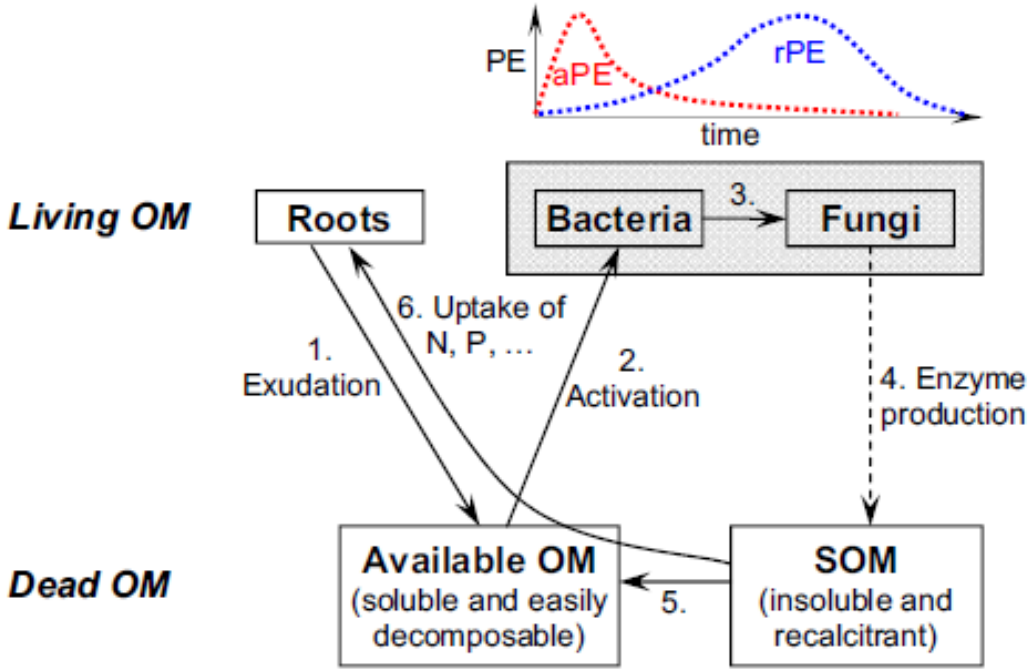

Figure 2.19 Sequential processes in nature that induce real and apparent PEs. 1) Inputs from roots (addition of C substrates); 2) Activation of microbial communities (r-strategists); 3) Activation of k- strategists; 4) Extracellular enzyme production for SOM decomposition; 5) SOM decomposition creates available C substrates. 6) Root uptake of nutrients (not occurring in laboratory incubations). Image from Kuzyakov (2010).

2.6.4 Using isotopes to understand PEs

Using isotopically labelled C substrates to determine soil priming has become a common and widely used approach. Isotopes are alternate forms of the same element that have the same chemical properties and the same atomic number but differ in atomic mass and physical properties. C has three naturally existing isotopes; ^{12}C is the most abundant and the lightest, followed by ^{13}C and ^{14}C which are rarer and heavier. The ratios of these isotopes' changes across ecosystems and scales. Spiking a system with isotopes has allowed scientists to identify and highlight certain processes occurring.

For investigating soil priming, a simple and common way of determining PEs is using the concept of equation (2-18) (Bastida *et al.*, 2019). This method uses a simple two-pool model for the structure of the soil C pools.

$$PE = (Total\ CO_2 - Substrate\ CO_2) - SOM\ CO_2 \quad (2\text{-}18)$$

Where, Total CO_2 is the total amount of CO_2 produced from the treatment soil (which includes CO_2 from added substrate, CO_2 from the SOM and CO_2 from priming), Substrate CO_2 is the CO_2 derived from the added substrate (isotopically separated from other processes) and SOM CO_2 is the total CO_2 that comes from an unamended control soil. When these CO_2 rates are subtracted from one another we are left with the CO_2 produced from priming.

Some studies have incorporated the use of multiple C isotopes to investigate C soil priming, such as Shahbaz *et al.* (2018), who used ^{14}C-labelled glucose, ^{13}C-labelled plant residues and unlabelled SOM to study soil priming at ~22 ^{o}C over a 62-day incubation. This study found that the addition of glucose to soil increased the decomposition rate of SOM by 1- to 4-fold the amount of glucose-C added to the system (Shahbaz *et al.*, 2018). Glucose is the most commonly used sugar in these types of studies because it has a low molecular weight, is water-soluble, and a readily available carbohydrate that is a universal substrate used in heterotrophic processes (Bastida *et al.*, 2019).

From priming studies using isotopes, it has been found that PEs do not seem to be affected by the C/N ratio of the substrate (Sun et al. 2019). However, Sun et al. (2019) suggests one should consider temporal variations in PE when estimating long-term effects on SOM dynamics.

A global study by Bastida et al. (2019) looked at the apparent priming of 86 globally distributed locations using ^{13}C isotopes. These sites varied in climate, soil and biotic conditions. This study found that apparent priming was often negative in moist soil environments (mesic) with high soil organic C and positive in areas of low soil organic C and more arid conditions (e.g. croplands, shrublands). It has also been found that positive PEs were more likely to occur and be observed in nutrient-poor soils (Fontaine *et al.*, 2004). These study findings give an insight into the potential global responses of soil priming.

Multiple studies have completed similar methods where they use an isotopically labelled substrate and incubated at only a few temperatures (1-3) for days to months (e.g. Bastida *et al.* (2019), Garcia-Pausas and Paterson (2011)). Of these multiple studies, no study has looked at the temperature dependence of priming at a wide range of temperatures, except preliminary studies by Numa (2020) using MMRT modelling.

Numa (2020) utilised ^{13}C labelled glucose to investigate priming at 40 temperatures over a 5-hour incubation period. When applying the MMRT model to a control soil and a supplemented soil (with added substrate) the result is three curves; SOM respiration, total respiration and respiration for the added substrate (Labile C). When a ^{13}C labelled C substrate is added to the soil, we can separate the labile C and priming from one another and plot the temperature response of priming. Preliminary results from Numa (2020) suggest that priming follows an MMRT curve response (**Figure 2.20**). However, these findings need to be investigated further to make any solid conclusions.

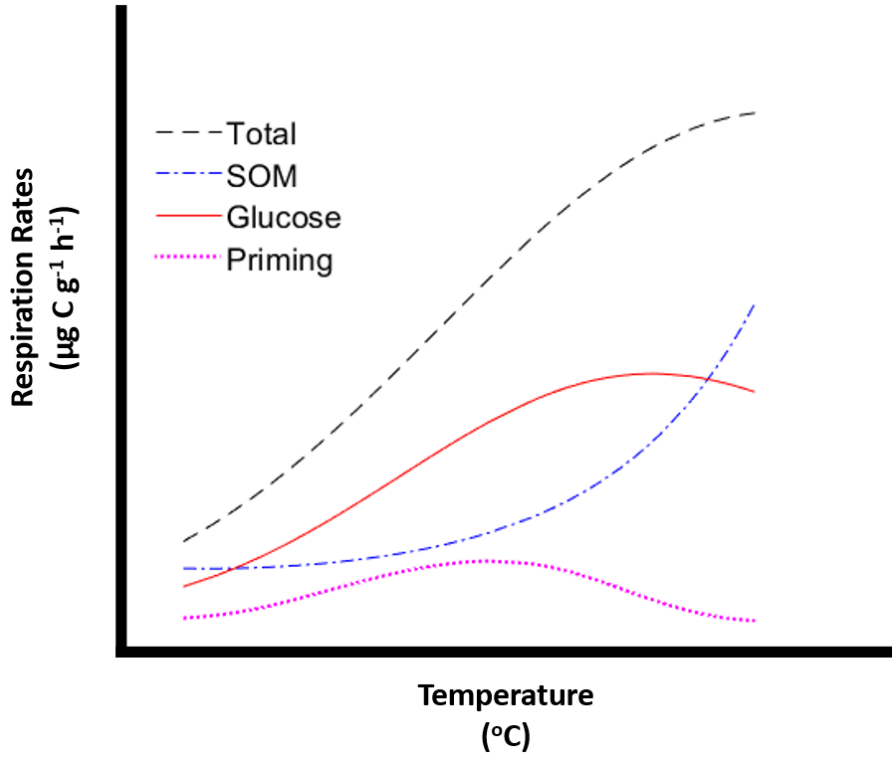

Figure 2.20 A general schematic of the MMRT model fits with temperature (°C) and the respiration rates (µg C g^{-1} h^{-1}) of priming. See Numa (2020) for further information.

2.7 Literature Review – Key Points

1) Soil C cycling is important at global scales.
2) Soil respiration is a key component of this cycling and its response to temperature is still not well defined despite a great deal of work.
3) There are many temperature response models but most are exponential without T_{opt}. MMRT provides an opportunity to reassess the temperature response of soil respiration for stable C, added labile C substrates, and potential priming.

4) Understanding how soil respiration will respond to increasing temperature is difficult but geothermal gradients offer an opportunity to explore soil warming in greater detail.

2.8 Future Work

The understanding of microbial responses to environmental pressures such as climate change remain poorly understood. The research presented here aimed to target gaps in some of these areas through incubation studies of soil and measurements of respiration in response to temperature. Below is a summary of the future work needed and attempted by this thesis:

- Many temperature dependence studies only have a small number of incubation temperatures (e.g. Fierer *et al.* (2005)) and so completing laboratory incubations at more temperatures is needed. This work has used 40 incubation temperatures spanning from ~1.8-53 ^{o}C in an attempt to capture the true temperature response of soil respiration.
- Previous work has found that labile C substrates exhibit very similar temperature responses with a T_{opt} around 37 ^{o}C and a T_{inf} ~ 22 ^{o}C (Numa *et al.*, 2021). This result has been found for three soils under one uniform temperature regime. This thesis aimed to determine if these findings were also observed along the length of a geothermal gradient with a range of soil temperatures, representative of temperate and tropical soils.
- The T_{inf} hypothesis has not yet been applied in a soil environment. If the hypothesis is true for geothermal gradients then an increase in T_{inf} should be observed with increasing environmental temperature (Prentice *et al.*, 2020). This hypothesis was investigated at an ecosystem scale as part of this thesis.
- Minimal work on the thermal adaptation of microbes have used geothermal gradients in soil as a test site. Of these studies, none of them have applied MMRT as a descriptor of temperature response. This thesis used MMRT to investigate the potential thermal adaptation occurring along a geothermal gradient with a focus on T_{opt} and T_{inf}.
- Many studies have attempted to understand the processes of soil PEs. However, most of these studies did not examine how PEs vary with a range of temperatures. Furthermore, none of these previous studies have characterised the temperature

response of priming in full or used MMRT to do so. This thesis aimed to further preliminary work completed by Numa (2020) to characterise the temperature response of soil priming.

Chapter 3
Site Description and Characterisation

3.1 Site Description and Location

Arikikapakapa (38º09'39.10"S, 176º14'57.47"E) is a geothermal golf course located in Rotorua, Bay of Plenty, New Zealand (**Figure 3.1**). Rotorua is a part of the Taupo Volcanic Zone (TVZ) which has been active for thousands of years. The Arikikapakapa Golf Course is located within the Arikikapakapa geothermal zone which spanned a surface area of 45,566 m^2 in 2014 (Reeves & Rae, 2016). The Arikikapakapa zone contains only steam-heated geothermal features, which includes, mud features, hot pools, thermal lakes and steam vents (Reeves & Rae, 2016). The geothermal feature used in this study is classed as 'heated ground' by GNS surveys (Seward *et al.*, 2015) and is located on the southern side of the golf course (38º09'46.54"S, 176º14'56.90"E; See **Figure 3.1**).

The geothermal feature is about 5.1 m long and 3.8 m wide (**Figure 3.2**). Old aerial images of the Arikikapakapa site (See Appendix A) showed that this feature has been present since at least 2003 (~17 years old). There is evidence that this feature has been present longer, with potential aerial sightings in the 1970s and 1980s (Retrolens, Historical Image Resource, Appendix A). Although some of the aerial images are of low quality, it is possible that this feature could be at least 40 years old. The area where the site is located was under native bush until 1972 and so it is not possible using aerial photographic records to determine whether this feature was present before that year.

The Arikikapakapa Golf Course was mapped by Landcare Research's S-MAP Online resource (https://smap.landcareresearch.co.nz/). The soil type was classified as an inactive hydrothermal recent soil, consisting of two sibling types; Tikitere_1a.1 (40%) and Tikitere_2a.1 (60%). The soil is a tephra based soil originating from rhyolitic rock, this soil type is weakly developed with a sandy loam texture. The soil is moderately well-drained, with moderate permeability and soil moisture, a deep rock depth and low topsoil phosphorus retention. Between the two types of soil present, the area has a moderate soil water holding capacity. These descriptions are generalised to the wider Arikikapakapa area and are not necessarily specific to the field site.

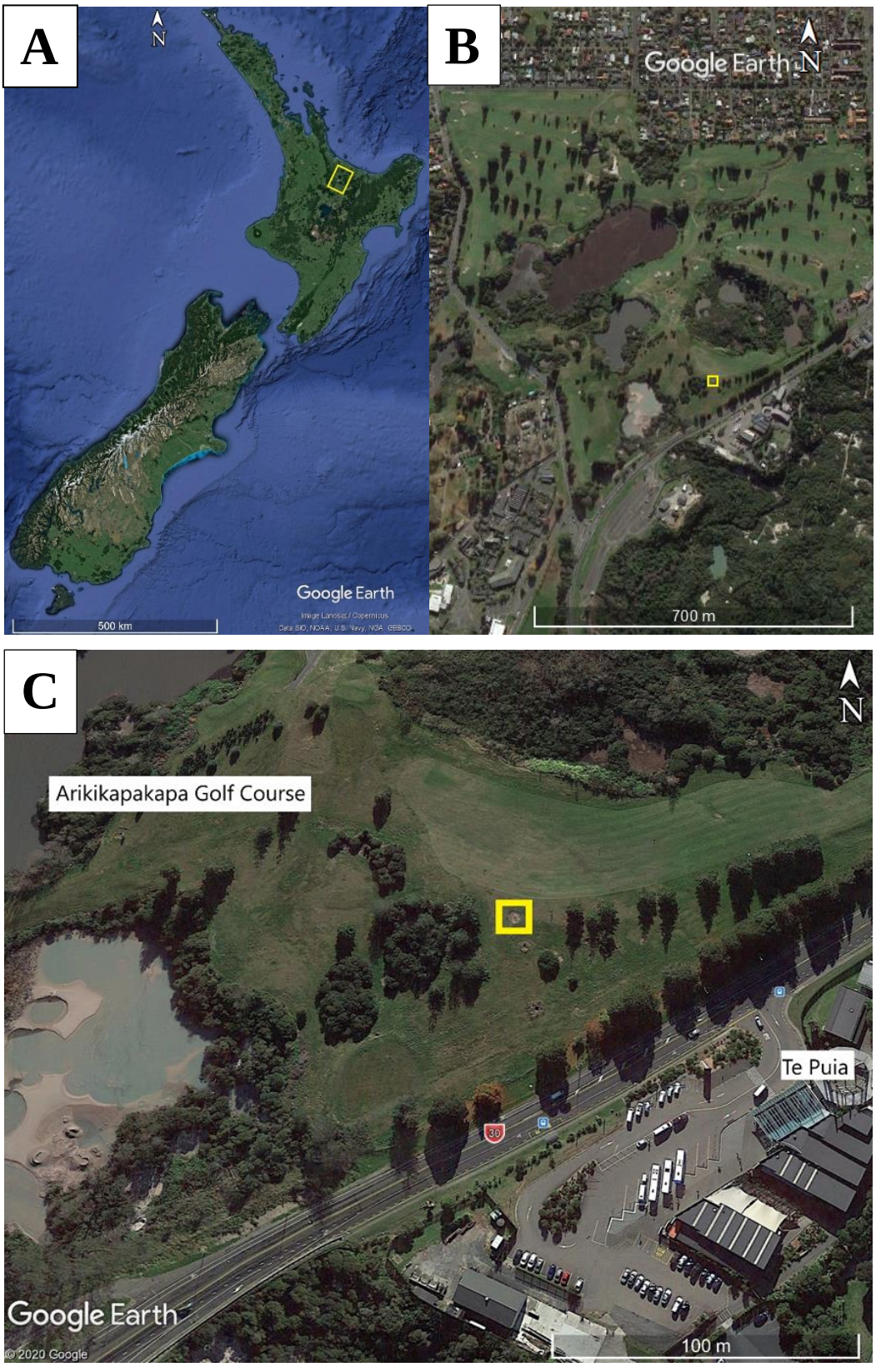

Figure 3.1 A) Map of New Zealand with a yellow box surrounding the Rotorua region. B) An aerial view of the Arikikapakapa Golf Course in Rotorua with the field site located in the yellow box. C) Close up location of the field site as indicated by the yellow box. All images from Google Earth 2020.

The field site used in this study was relatively uniform in terms of vegetation. The vegetation consisted of grasses and unidentified scattered mosses (37 % of ground cover). The grasses were identified as *Axonopus affinis* (carpet grass) and possibly *Elymus repens* (couch grass) at about 40 % and 15 % ground cover, respectively. Also, present was the common weed *Hypochaeris radicata* (catsear) and small sprouting's of *Leptospermum scoparium* (Manuka) which covered about 5 % and 3 % of ground cover, respectively. The vegetation around the field site was consistently managed on the same mowing regime and the area was not fertilised or limed. The main external influences on the site are primarily geothermal and weather-related.

Figure 3.2 Image of the geothermal feature and site area used for this research (20th November 2020).

3.2 Site Characterisation

3.2.1 Temperature

We measured the natural thermal gradient in the soil surrounding the geothermal feature. To characterise the field site in terms of soil temperature we used two simple methods. The first involved the use of a 3 m by 3 m grid (**Figure 3.3**) where the temperatures at 2 cm and 10 cm soil depths were measured using soil temperature probes. The grid was used to map the temperature along a 16 m gradient moving away from the geothermal source. The temperature measurements decreased with distance as the soil temperature began to stabilise further from the geothermal feature.

Three brands of temperature probes were used during the duration of this study. These consisted of a Dostmann electronic GmbH P700 temperature probe, a Brannan digital thermometer and a Greisinger electronic digital thermometer (GTH 175 / Pt). Differences in sensitivity and measurement were found to be negligible between each of the temperature probes used.

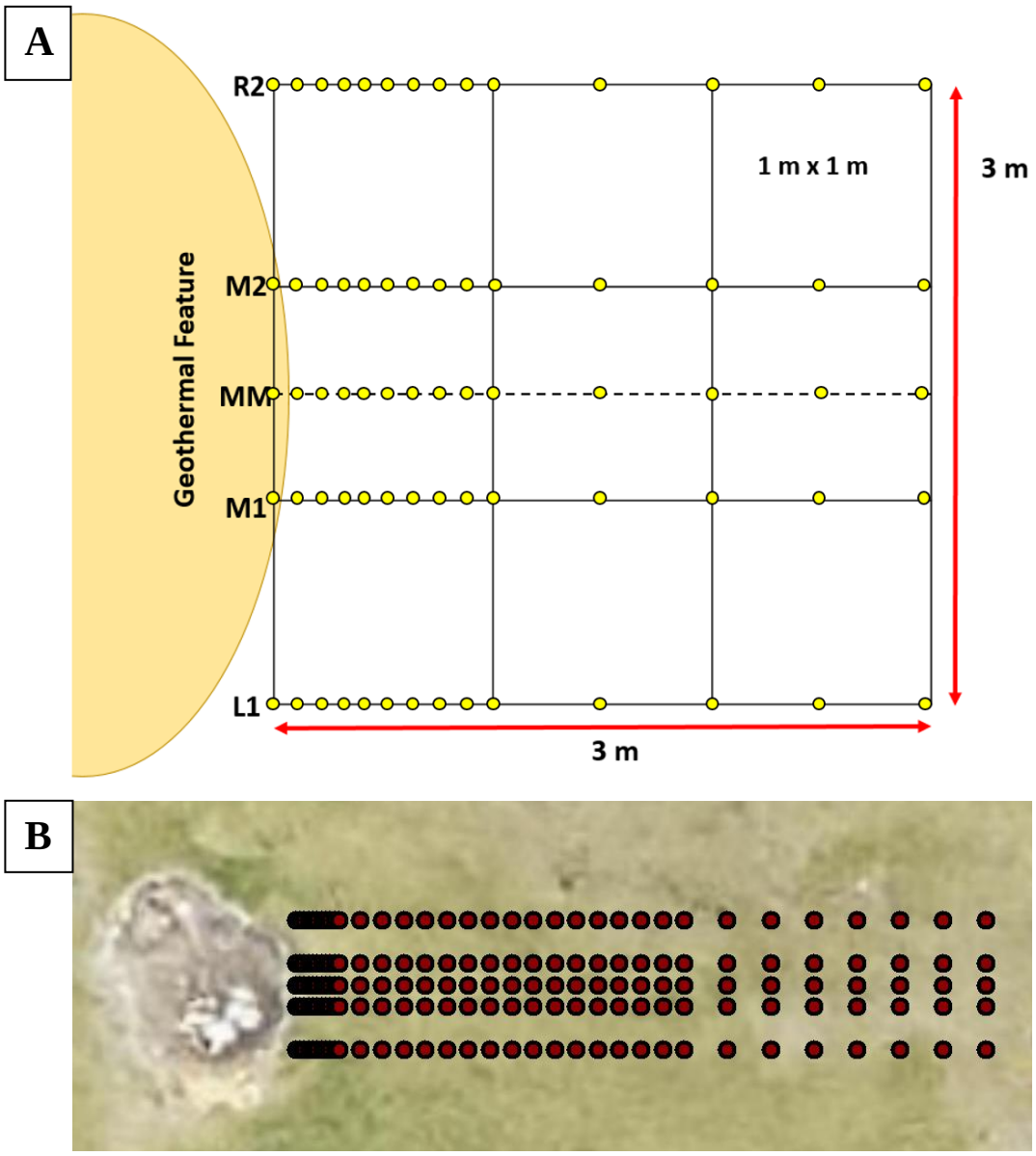

Figure 3.3 A) The basic 3 m by 3m grid layout used to map the temperature gradient moving away from the geothermal feature. Each line (L1, M1, MM, M2 & R2) represents a line where measurements were taken along the 16 m length. The yellow dots show the first 3 m of temperature measurement distances taken along each of the lines. At 9 m, the sampling distance increased to every 1 m for each of the lines. A total of 340 temperature measurements taken on each grid sampling occasion (68 total per line). B) An aerial image of the geothermal site with all the sampling locations located as red dots. Data mapped using ArcGIS 10.7.

The second way of characterising the site temperature involved the use of iButtons (manufacturer). iButtons are temperature loggers that have been designed to run for long periods of time in relatively harsh conditions. The iButtons used were DS1922L iButton thermochrons from iButtonLink Technology. The software used to set up and collect data from the iButtons was called 1-Wire Viewer from Maxim. Five iButtons were buried at a soil depth of 7.5 cm along the gradient at 10 cm, 30 cm, 60 cm, 300 cm and 1600 cm distance from the geothermal source (**Figure 3.4**).

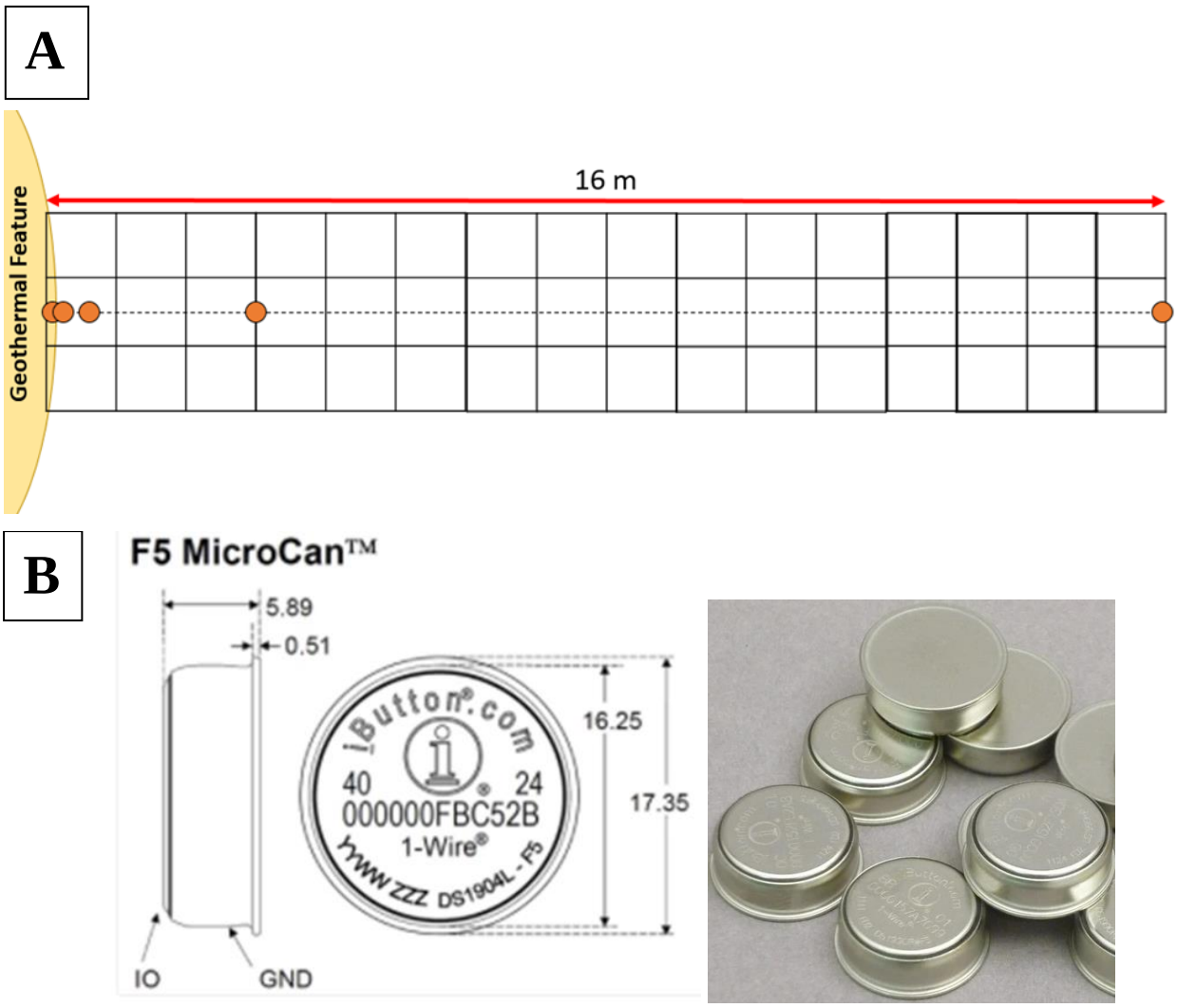

Figure 3.4 Image A shows the 16 m grid layout and the locations of the iButtons as indicated by the orange circles. Image B shows the iButton specifications (left) and physical appearance (right) (both images from https://www.ibuttonlink.com/products/ds1922l).

These iButtons made temperature measurements every hour, starting on the 5th August 2020. The data from these iButtons was downloaded every 3-4 weeks. Each iButton was coated in waterproofing spray before each deployment to improve water resistance and decrease the chances of water damage. Based on experiments by Roznik and Alford (2012), coating these iButtons in waterproofing spray should have minimal influence on

the temperature readings taken. The iButtons were redeployed a couple of hours after data collection to ensure the waterproofing spray had dried completely.

Both the grid data and the iButton convincingly showed that there was a thermal soil gradient present at this field site. The gird data is presented in **Figure 3.5** and shows the average temperatures along each line from the 26^{h} August 2020 to the 22nd June 2021. The greatest changes in temperature were found closest the geothermal source (within the first 3 m). The thermal gradient was consistent at the 10 cm depths but more variable at the 2 cm depths. This gradient, however, was sustained and persistent throughout the entire study.

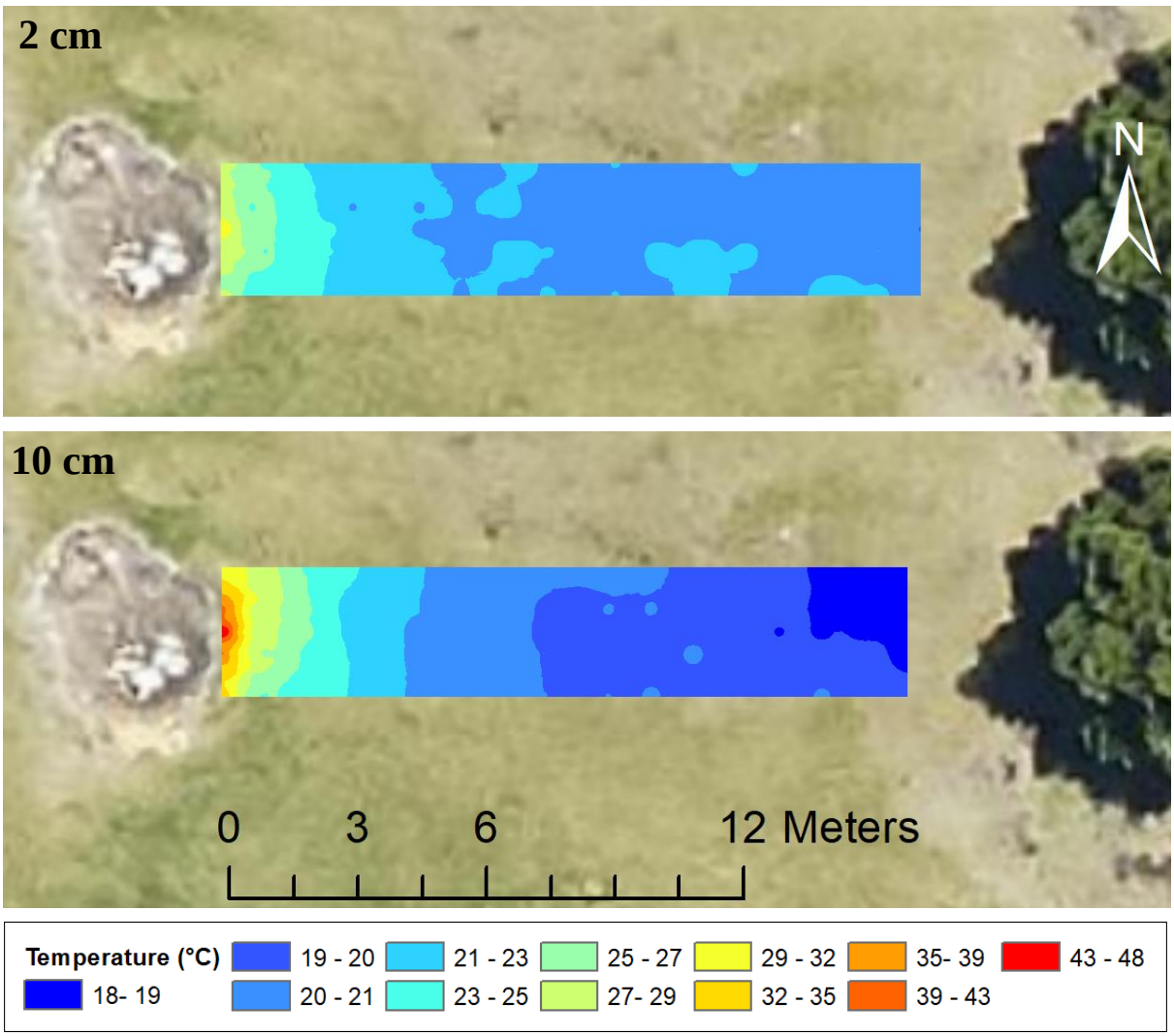

Figure 3.5 These images show the average gird data for each line over the period of 26th August 2020 to the 22nd June 2021 for both the 2 cm and 10 cm depths. Data averaged over 12 separate sampling visits during this time period. Data mapped using ArcGIS 10.7.

The iButton temperature data is shown in **Figure 3.6**, the data recordings begin on the 5th August 2020 and continue until the 22nd June 2021. Data gaps were due to iButton device failure, technology and software issues. The large temperature drops observed closest to the geothermal feature have all been linked to large rainfall events that occurred on the same day or the day before (BOPRC, Whakarewarewa EK577135 rain monitoring site). The variation in temperature at all iButton distances was strongest in the summer-spring period (Dec-Mar). The distances closer to the geothermal feature (10-60 cm) seemed to be more affected by rainfall events than the further distances (300-1600cm).

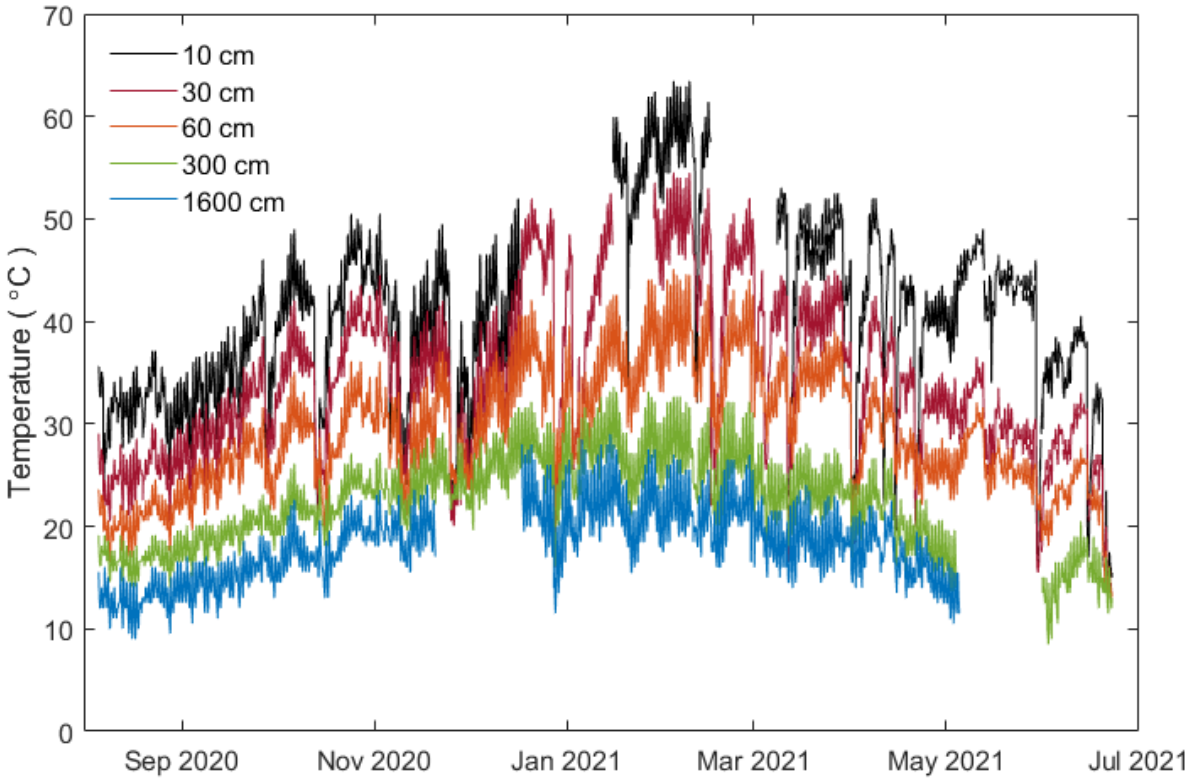

Figure 3.6 iButton temperature data (°C) from five distances along the gradient, 10 cm (black), 30 cm (red), 60 cm (orange), 300 cm (green) and 1600 cm (blue) from the geothermal source. Data begins the 5th August 2020 and ends 22th June 2021. Data measurements taken every hour.

3.2.2 Nutrients and pH

Alongside determining the changes in temperature along the gradient, soil sampling and characterisation was undertaken to identify other potential variables. Along the grid length, soil was collected on the 27th October 2020 and analysed for total C, total N, ^{13}C

and ^{15}N isotopes. The soil was collected at, 30 cm, 60 cm, 100 cm, 300 cm, 550 cm, 900 cm and 1600 cm. This nutrient data is summarized below (**Table 3.1**).

Table 3.1 Summary of pH, C and N properties at seven distances from the geothermal site.

Distance from Source (cm)	δ ^{15}N (‰)	δ ^{13}C (‰)	Total N (%)	Total C (%)	C/N ratio	pH
30	4.4	-21.3	0.27	4.4	16.0	4.0
60	6.1	-18.3	0.38	6.2	16.3	4.4
100	10.1	-18.6	0.58	10.0	17.3	4.7
300	13.0	-19.7	0.75	12.9	17.3	4.7
550	9.8	-21.0	0.56	9.7	17.2	4.8
900	10.2	-22.1	0.60	9.6	15.9	4.7
1600	7.8	-22.5	0.43	7.0	16.3	5.2

The ^{15}N values ranged from 4.4-13.0 ‰ and were relatively enriched for a grassland site, suggesting high N turnover, N cycling and losses (Mudge *et al.*, 2014). The ^{15}N values were much higher than ^{15}N values measured in pasture and plantation forest of 4.3‰ and 2.6‰, respectfully (Mudge *et al.*, 2014). Values found for dairy and cropping systems were also lower than the values found at this site, 5.4‰ and 6.2‰ respectively (Stevenson *et al.*, 2010). Since the site was not fertilised, this high N cycling was likely to be aided by the geothermal activity which brings with it high mineral-rich water and potential ammonia deposition. The C/N ratios measured at this field site ranged from 15.9 to 17.3. The percentages of C and N averaged 8.5 % and 0.51 %, respectively.

Values of ^{13}C are typically reflective of the plant community (Wynn & Bird, 2008). The δ ^{13}C range for C_3 plants ranges between –20 to –37‰ and for C_4 plants between –9 to –16‰ (Wynn & Bird, 2008; Kohn, 2010). Our findings suggest that the plants at this site were likely to be mostly C_3 plants. However, carpet grass found at the site is a well-known C_4 plant that is adapted to warmer soils and is usually found on north-facing dry slopes in pastures.

The average pH around the site was ~ 4.6, which is considered low for most soil systems. The pH was relatively stable along the gradient, see section 4.1.2 for more pH values.

Chapter 4
Methods

This chapter presents detailed descriptions of the full methods used in this research. These full methods will be summarized in the research chapter (Chapter 5). Additionally, a number of preliminary experiments are presented here in greater detail.

4.1 Temperature Dependence Methods

4.1.1 Preliminary experiment: Moisture content

Soil moisture (MC) is commonly described in three common ways; gravimetric MC (symbol: θ units: grams water/grams soil (gg^{-1})), soil water potential (SWP; symbol: $\boldsymbol{\Psi}$; units of pressure are used e.g. megapascals MPa), and volumetric water content (VWC; symbol: θ_V units: water volume/soil volume). Soil MC can also be expressed as percentages (%) and as water-filled pore space (WFPS; relationship between VWC and soil porosity).

Water holding capacity (WHC) is another measure used to describe soil MC. Soil WHC is the amount of water that a given soil can hold against gravity. The optimum MC for most organisms undergoing microbial respiration tends to be 60% of the maximum water holding capacity (MWHC) of the soil (i.e. the maximum amount the soil can hold). The MWHC can be determined using methods from Harding and Ross (1964). This general MC is typically ideal for maximum rates of microbial respiration where above or below this MC complications can occur.

The MC of soil can heavily influence the temperature response of microbial populations (Lellei-Kovács *et al.*, 2011). To determine the appropriate soil moisture for this research a set of preliminary experiments were completed. Often soil MC is adjusted after collection from the field to 60% MWHC, however, the objective was to disturb the soil as little as possible and so we tested how respiration changes with moisture at this site.

For the first test, the soil was wetted up to 60% MWHC for measuring respiration. To do this, a sieved bulk soil sample (top 7.5 cm taken using a bucket sampler) from the field site was used to determine the MWHC of the soil using methods from Harding and Ross

(1964). The MC of the bulk soil and at the MWHC was determined by taking three subsamples (~5 g each) and drying them in the oven at 105 ^{o}C for 24 hours. The MC at MWHC and of the bulk soil was calculated using equation (4-1). The MC needed at 60% MWHC was calculated using equation (4-2).

$$\theta_g = \frac{S_w - S_d}{S_d} \quad (4\text{-}1)$$

Where; θ_g is the gravimetric SMC (gg^{-1}), S_w is the wet weight of the soil before drying (g), S_d is the dry weight of the soil after drying at 105 ^{o}C in an oven (g).

$$\theta_{g60\%} = \theta_{g100\%} \times 0.6 \quad (4\text{-}2)$$

Where; $\theta_{g60\%}$ is the gravimetric soil moisture at 60% MWHC (gg^{-1}), $\theta_{g100\%}$ is the gravimetric soil moisture at MWHC (gg^{-1}).

When the bulk soil was wetted up to 60% MWHC, the soil was found to be visually too saturated for effective use in laboratory experiments, having formed clumps and surface puddles. Therefore, to identify the ideal MC of the soil used in this research, further preliminary investigations were undertaken.

Six MC values were used for this experiment; 0.3 gg^{-1}, 0.4 gg^{-1}, 0.5 gg^{-1}, 0.6 gg^{-1}, 0.7 gg^{-1} and 0.8 gg^{-1} MC. The 0.7 gg^{-1} and 0.8 gg^{-1} MCs were wetted up using the bulk soil already at 0.6 gg^{-1} MC. This was done by adding distilled water to 50 g subsamples. For the 0.3-0.5 gg^{-1} MCs the bulk soil was air-dried to below 0.3 gg^{-1} MC. These were wetted up using the air-dried soil and distilled water to their respected MCs.

The resulting MCs were checked following drying at 105 ^{o}C to constant weight as described above (equation (4-1)), before incubating the samples at three different temperatures. The MCs were close to their intended MC values (**Table 4.1**).

Table 4.1 The intended and real MC values of the soil involved in this MC experiment.

Intended MC value (gg^{-1})	Subsample soil weight (g)	Moisture added (g)	Resulting MC value (gg^{-1})
< 0.30	111	Air Dried Soil	0.07
0.30	37	11.3	0.27
0.40	37	12.1	0.38
0.50	37	15.8	0.51
0.60	Bulk	None	0.60
0.70	50	5.0	0.74
0.80	50	10.0	0.89

The same experiment was repeated using two slightly different methods. The first experiment utilised 24 mL hungate tubes and 3 g of soil. The second utilised 15 mL hungate tubes and 2 g of soil.

In both experiments, one tube from each MC was incubated at 7.89 ^{o}C, 25.8 ^{o}C and 51.4 ^{o}C for a total of five hours. After the five hours, 1 mL headspace gas samples were taken using a 1 mL insulin syringe. The needles were then inserted into a rubber bung to stop leakages before being injected into an Infrared Gas Analyser (IRGA; LI-COR, LI-7000 CO_2/H_2O Analyser) for CO_2 quantification (section 4.1.3). The results of both experiments were standardised by the average of each experiment. The data was plotted for each temperature (**Figure 4.1**).

The results of these MC experiments showed that there was little difference in respiration rates across the measured range of MCs. The results overall suggested that the soil produced CO_2 effectively across a wide range of MCs. Therefore, it was decided that working at field moisture (which ranged between 0.35-0.80 gg^{-1}) would be able to produce accurate results without negatively impacting the respiration rates from the soil. Thus, all soil samples taken from the field site were incubated at field MC for the rest of the experiments undertaken in this research.

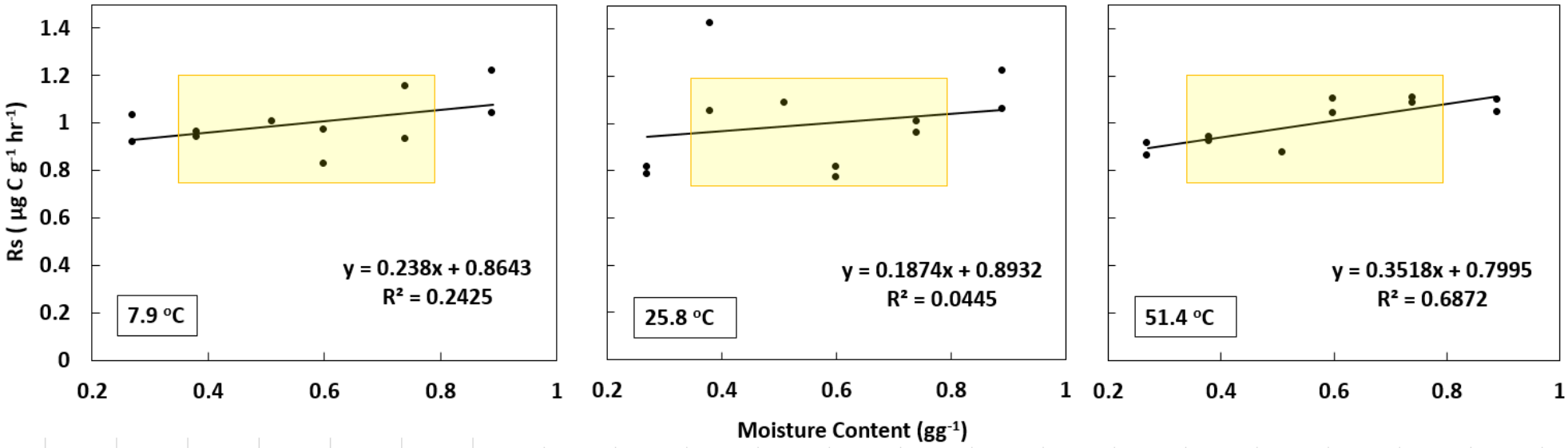

Figure 4.1 MC experiment results showing the respiration rates (µg C g^{-1} h^{-1}) of soils with varying moisture contents (gg^{-1}) measured at three temperatures (7.9 °C on the left, 25.8 °C in the middle and 51.4 °C on the right). The yellow box highlights the MC range found at the field site during the year of this research (range 0.35-0.80 gg^{-1}).

4.1.2 Preliminary experiment: Temperature and pH

As temperature increases, more hydrogen ions are released from soil surfaces, decreasing the pH of the system, although often only to a small degree. A short experiment was completed to test the effects of measuring pH at room temperature in the laboratory compared to the environmental temperature in the field. This experiment was used to determine if the laboratory measurements of pH were representative of the field site pH.

For this experiment, three soil samples at environmental temperatures of 30.1 ^{o}C, 28.4 ^{o}C and 24.8 ^{o}C were used, collected from 20 cm, 180 cm and 800 cm from the geothermal source, respectively. To measure the soil pH, 10 g of each soil (in triplicates) was placed into a 50 mL falcon tube with 25 mL of distilled water. These tubes were briefly mixed using a milkshake mixer until well combined, then left to sit for ~30 minutes, before measuring pH with the pH probe (Denver Instrument pH/mV meter UB-10) just resting on the soil surface.

Triplicates of each soil were measured at room temperature and triplicates of each soil were heated to the environmental temperature before measurement. After the pH of the heated triplicates was measured, the samples were left to cool, the pH was remeasured again once the samples reached room temperature. The temperature at each pH measurement was taken using Greisinger digital thermometer (GTH 175 / Pt). Overall, pH changed very little when comparing measurements at room temperatures and heated temperatures (**Table 4.2**).

Table 4.2 The average pH and temperature (^{o}C) measurements from the room, heated and cooled samples. The heated temperature is in the environmental temperature range for each sample. The cooled samples are the heated samples cooled to room temperature.

Distance from Source (cm)	Room Temperature (^{o}C)	Room pH	Heated Temperature (^{o}C)	Heated pH	Cooled Temperature (^{o}C)	Cooled pH
20	22.1	3.95	41.7	3.72	21.0	3.97
180	22.1	4.42	28.4	4.39	20.9	4.42
800	22.2	4.61	25.1	4.59	18.8	4.58

The results shown above suggest that within the temperature range experienced at the site the pH was relatively stable when measured at a lower temperature. The largest difference between pH values was 0.25 pH units' between the heated and cooled samples of the

20 cm sample. All differences were considered negligible and so it was decided that all pH values measured at room temperature could accurately represent the pH of the soil at the field site.

4.1.3 Geothermal soil – Glucose

The objective of this experiment was to determine the temperature response of glucose-induced respiration using soil from the geothermal site described in Chapter 3. Glucose-induced respiration here was used as a proxy for the respiration of labile C (Numa *et al.*, 2021). The geothermal soil was used to determine if the temperature optimum (T_{opt}) and inflection point (T_{inf}) of glucose-induced respiration was the same along an environmental temperature gradient. To complete this main objective, identical sets of laboratory incubation experiments were completed using a temperature block consisting of 40 different temperatures. In total, 20 soil samples were collected at different distances along the geothermal gradient on different occasions.

4.1.3.1 *Field collection*

The distances along the geothermal gradient used in this experiment were determined using the grid layout and iButton data (section 3.2.1). The samples were taken at a range of distances to capture the range of temperatures found along the natural temperature gradient (**Figure 4.2**).

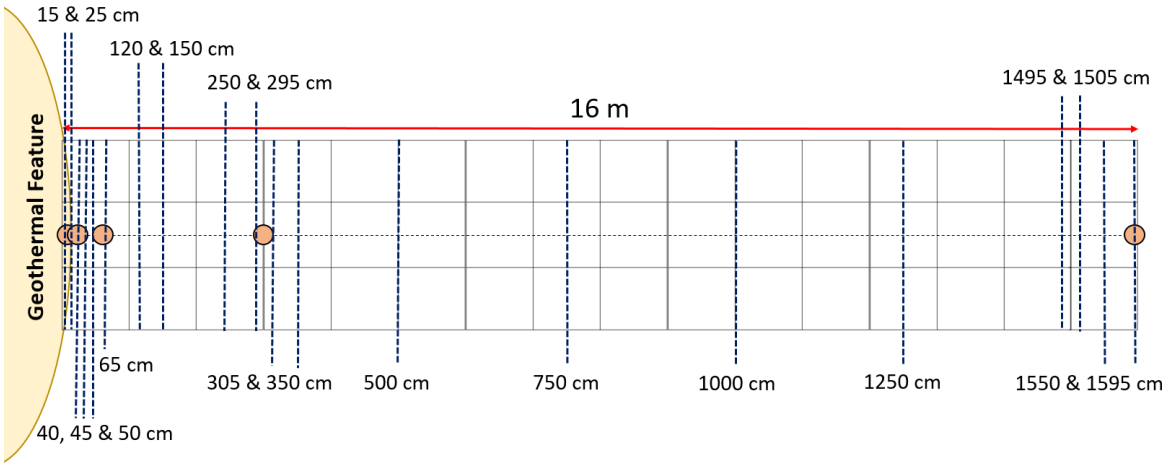

Figure 4.2 Diagram of the 16 m grid layout showing the iButton locations in orange circles and the sample sections in blue dotted lines. This diagram shows all 20 sample distances involved in this research experiment.

Soils collected along the grid transect were incubated within the same week of soil collection. To gather the samples, the 3 by 3 m grid was laid out to set the boundaries of sampling. The temperatures along the chosen grid distance were measured at 2 cm and 10 cm depths before soil cores were taken using a bucket sampler (7.5 cm depth, 2.5 cm diameter). Samples were taken along a transect of the grid where the temperature remained consistent. The soils cores were placed into zip lock bags, one bag for each sampling distance. The bucket sampler was wiped and dusted between each sampling distance to avoid soil transfer between samplings.

After each transect was sampled, the soil cores were taken back to the laboratory where they were passed through a 2 mm sieve. The sieve was cleaned thoroughly and dried between each soil bag. The sieved samples were then left to settle at room temperature in the sealed zip lock bag plugged with a ball of cotton wool.

A maximum of four soil incubations could be completed in a week and so sample collection and subsequent measurements were spread over 7 months. To determine the order in which samples were to be incubated the distances along the gradient were assigned a random number using the excel rand() function then rearranged in ascending order of these random numbers. The run order of these samples, their sampling dates and soil properties can be found in Appendix B.

As determined in the preliminary moisture content experiment the soils samples were kept at field moisture and no alterations were made to the soil except sieving. All samples were treated the same for all 20 incubation runs.

For 11 of the experimental sets, soil C and N were measured (**Table 4.3**). Samples from the middle of the grid had the highest amounts of C and N. The C:N ratio increased further away from the geothermal source.

Table 4.3 Soil properties of 11 sites taken from the geothermal grid.

Distance from source (cm)	δ ^{15}N (‰)	δ ^{13}C (‰)	Total N (%)	Total C (%)	C:N Ratio
15	-1.1	-20.3	0.24	3.7	15.4
25	-1.2	-19.7	0.30	4.8	16.2
40	-0.72	-19.0	0.34	5.3	15.4
50	-0.30	-18.4	0.35	5.8	16.4
150	0.04	-18.6	0.71	12.2	17.1
295	-0.53	-19.7	0.68	11.9	17.5
305	-0.63	-20.0	0.75	12.8	17.1
350	-0.84	-20.1	0.63	10.9	17.3
1495	-0.17	-22.8	0.49	8.9	17.9
1505	0.23	-22.6	0.51	9.3	18.5
1595	0.61	-22.1	0.39	6.8	17.4

4.1.3.2 *Incubation methods*

The method described below was completed for all 20 soil samples collected.

To incubate the collected soils at a range of temperatures, a temperature block was used (Robinson *et al.*, 2017; Robinson *et al.*, 2020). A temperature block is an insulated metal block (**Figure 4.3ab**) that is heated on one end and cooled on the other using a water bath. The heating and cooling of opposite ends creates a temperature gradient along the block. This temperature gradient can be altered to capture the desired range of temperatures needed for an experiment. For all incubations completed in this thesis, the water bath was turned to the lowest setting, producing temperatures as low as 1.8 ^{o}C. The hot end of the block was set to 62 ^{o}C which produced a maximum of 53 ^{o}C on average for the hottest incubation temperature. The temperatures along the block were recorded by thermistors connected to the block at seven different points spanned along the temperature gradient. The one-minute average of the temperature recorded at the sensor position was taken and later used to determine the temperatures along the length of the block.

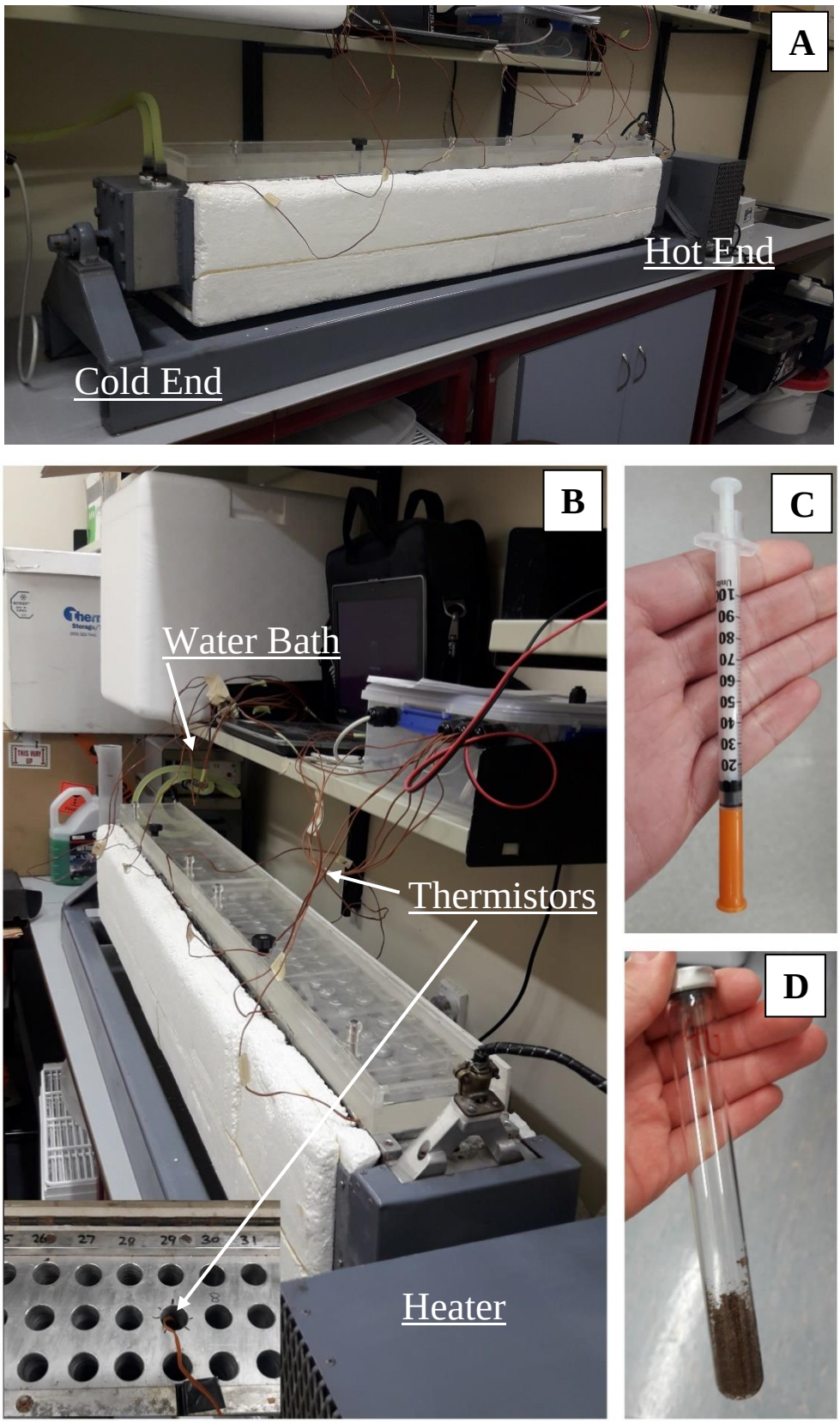

Figure 4.3 Images of the temperature block and equipment used for all incubation experiments. Image A shows the temperature block indicating the cold and hot ends. Image B shows the block from the hot end. The wires hanging down are connected to the block and act as thermistors to record the temperature. The small circles seen under the lid are caps of sealed tubes, the block contains three rows of 44 holes available for use. Image C shows the 1 mL syringes used to take samples. Image D shows an example soil tube.

The afternoon the day before each incubation, the temperature block was turned on to allow the block to equilibrate and come to temperature overnight. A total of 84, 24 mL hungate tubes were used for each incubation, 40 tubes for control soil, 40 for treatment soil (with added C source) and four tubes used as blanks (no soil).

To each of the 80 tubes, 2 g of soil (within 0.01 g) was added the morning of the incubation. Using an Eppendorf 1000 µl pipette, 0.25 mL of distilled water was added to the 40 control tubes following the ratio found by Numa *et al.* (2021) (1 g soil to 0.125 mL solution). For the treatment tubes, a glucose solution was added to represent a labile C source in soil. Adding glucose to the soil allows the separation of glucose-induced respiration, which can be used as a proxy for other labile C sources. Glucose is a monosaccharide (simple sugar) that has the chemical formula $C_6H_{12}O_6$. The sugar was chosen because it is a central part of metabolism for most organisms. Glucose also dissolves easily in water, which made it easy to distribute uniformly in the soil. Glucose has a diverse range of origins in soil, including plant/microbial residues and root/microbial excretions, and therefore, dominates cellulose and non-cellulose sugars found in soils (Gunina & Kuzyakov, 2015). To make the glucose solution, 0.2702 g of glucose powder (D-GLUCOSE, Ajax Chemicals UNIVAR 783-500G) was added to 20 mL of distilled water in a beaker and dissolved. The dissolved glucose solution (0.25 mL) was added to each of the 40 treatment tubes, following the same ratio as the control tubes (1 g: 0.125 mL).

The difference in CO_2 production between the control and treatment tubes allows the calculation of respiration produced from the decomposition of glucose. The control soil provides the respiration flux from just the soil and the distilled water. When the control fluxes are subtracted from the corresponding treatment tubes (i.e. each at the same temperatures) then we can get the respiration that has come from the addition of glucose. This respiration also includes the respiration from priming since the treatment tube contains the total respiration (**Figure 4.4**). Respiration from priming was not the main focus of this thesis but is also likely to be induced from the addition of labile C sources in soil. The separation of priming was explored in subsequent experiments (Section 4.2). This method used a simple two pool model where SOM consisted of more stable C and the glucose consisted of labile C.

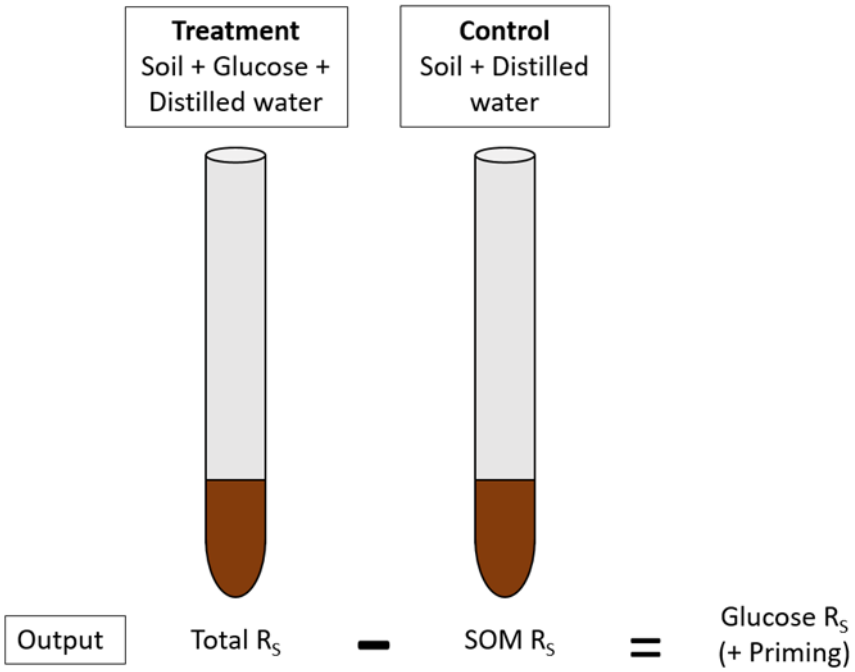

Figure 4.4 The method used to determine the respiration of glucose. Total respiration (Total R_S), soil respiration (SOM R_S) and glucose respiration (Glucose R_S). Subtracting the control tube's CO_2 outputs from the treatment tube's CO_2 outputs will give the CO_2 produced from the addition of glucose (+ priming).

All the tubes were sealed using a rubber septum and metal crimp caps. The four blanks with no soil were sealed at the same time as the samples to account for the background CO_2 concentration of the lab. After all the tubes were sealed, each tube was briefly mixed using a vortex mixer (Degens *et al.*, 2001).

All the tubes were placed along the 44 holes of the temperature block. The back and middle rows were used for every incubation. Each row consisted of 40 soil tubes, 2 blanks and two unoccupied holes. The tubes were incubated for a total of five hours, time beginning when the first tube entered the block.

A total of 40 different temperatures for each incubation were used in this study. Experiments using less than 20 different temperatures can be can more susceptible to errors and can deteriorate confidence in the model fit (Robinson *et al.*, 2017).

Before the end of the incubation period, the IRGA (LI-COR, LI-7000 CO_2/H_2O Analyser) used for analysis was set up in the lab. Triplicates of 1% CO_2 gas standards ranging from 2 mL to 0.1 mL were run on the IRGA to create a calibration curve. The peak size of the samples determined the highest and lowest standards run.

After five hours, the temperature block was turned off and the samples directly put on ice, gas samples were taken and immediately analysed for CO_2 using the IRGA (within 30-40 minutes of the 5-hour incubation ending). To measure the CO_2 flux, 1 mL of headspace gas from each tube was injected into the IRGA using a 1 mL insulin syringe (Becton-Dickinson and co, **Figure 4.3c**). The syringe needle was inserted through the rubber septum of the tube and the syringe was pumped up and down 3-4 times (keeping the syringe in the septum) before taking the 1 mL gas sample. A separate syringe was used for each sample set (control & treatment). After all samples, standards, and blanks had been run, the CO_2 peaks were analysed using custom code in Matlab R2019b.

4.1.4 Geothermal soil – Yeast

Since not all organisms can use glucose and it may be variably available in soil, a subset of incubations were completed using yeast extract. This secondary labile C source was used to determine if the results of glucose incubations could be representative of a wide range of C sources. Numa *et al.* (2021) showed that six different labile C sources all had the same respiration T_{opt} when incubated over five hours. Yeast extract was chosen from those six labile compounds to check if this would remain true at different environmental temperatures.

Yeast extract is a water-soluble concentrated powder of autolysed yeast cells, it is high in vitamins, amino acids and many other growth factors, and is commonly used as microbiological culture media (Condalab, 2021). Yeast extract contains a high substrate variety which suggests more organisms are able to use this labile C source.

These yeast extract incubations were carried out following the same methods as the glucose incubations. Since yeast extract does not have a molarity, the solution of yeast was made the same as the glucose solution (0.2702 g yeast powder & 20 mL distilled water) and added at the same ratio (1 g soil to 0.125 mL solution). The yeast extract used in this experiment was Condalab Yeast Extract (Cat. 1702).

Soil was collected for these runs on the 23rd March 2021 and the 29th March 2021 along the geothermal gradient. Two runs taken from 35 cm (run 1) distance and 1400 cm (run 2) distance were completed in the first week. Another run taken at 400 cm (run 3) was completed in the second week. This order of runs was randomised following the same method presented earlier (section 4.1.3.1). All three incubations were completed within

one week. The three distances were picked to characterise the grid along its length (**Table 4.4**). The distances chosen were based on those already sampled from the glucose experiments and the iButton data.

Table 4.4 Summary table of soil and environmental properties for yeast extract incubation samples. The average environmental temperature was averaged across the width of the 3 m grid for the sampling distance. Samples were collected on the 23rd and 29th March 2021 and run on the 24th March, 26th March and 30th March 2021.

Distance from Source (cm)	Moisture content (gg^{-1})	pH	Average temperature 2 cm depth (°C)	Average temperature 10 cm depth (°C)
35	0.51	4.0	27.7	36.2
400	0.65	4.6	22.0	25.1
1400	0.38	4.7	18.0	19.2

4.1.5 Data analysis

For all samples run, the respiration rates (R_S) for each sample gas was calculated using equation (4-3) using excel 2016. The triplicate standards were used to create a calibration curve taking the average of the three triplicates. The fours blanks were also averaged to give the background CO_2 concentration of the laboratory.

(4-3)

$$R_S = \left[\left(\left(\frac{H_s/V_i}{H_{st}/V_i}\right) - \left(\frac{H_b/V_i}{H_{st}/V_i}\right)\right) \times S \times V \times 10^3\right] \div (ODW \times t)$$

Where R_S is the respiration rate (µg C g $soil^{-1}$ $hour^{-1}$), H_s, H_{st} and H_b are the peak area of the sample (mm^2), standard (1% CO_2, mm^2) and blank (mm^2), respectively. V_i is the injection volume into the IRGA (mL), S is the concentration of CO_2 in the standard (1% CO_2 = 0.01 µg CO_2 mL^{-1} gas) (Robinson, 2016), V is the headspace volume (mL), ODW is the oven dried weight of the soil (g) and t is the incubation length (hr) (Robinson, 2016; Numa, 2020).

The respiration rates at different temperatures were fitted using MMRT to calculate T_{opt} and T_{inf}. All MMRT application and plotting is fully described in section 4.3. All fitted curves for the temperature response of glucose and SOM can be found in Appendix C.

4.2 Soil Priming Method

To determine the temperature dependence of soil priming and how it relates to glucose respiration, soils from the geothermal site were incubated with δ ^{13}C labelled glucose. The use of δ ^{13}C allows the separation of CO_2 output from priming from the CO_2 outputs from soil and glucose. The method presented below was developed by Robinson *et al.* (2020) and first used for priming by Numa (2020). The machine used for the measurements of δ ^{13}C was an Off Axis Integrated Cavity Output Spectroscopy (OA-ICOS) instrument (Los Gatos Research, CCIA-46, model 908-0021; **Figure 4.5**). The OA-ICOS instrument uses a continuous flow method which was developed by Barker *et al.* (2011). The custom machine modifications allow the machine mechanisms to be controlled using LabVIEW® software from an external computer. The machine is located in the Carbon Isotope Dating Lab at the University of Waikato. Due to the complexity of this method only a few example experiments could be completed.

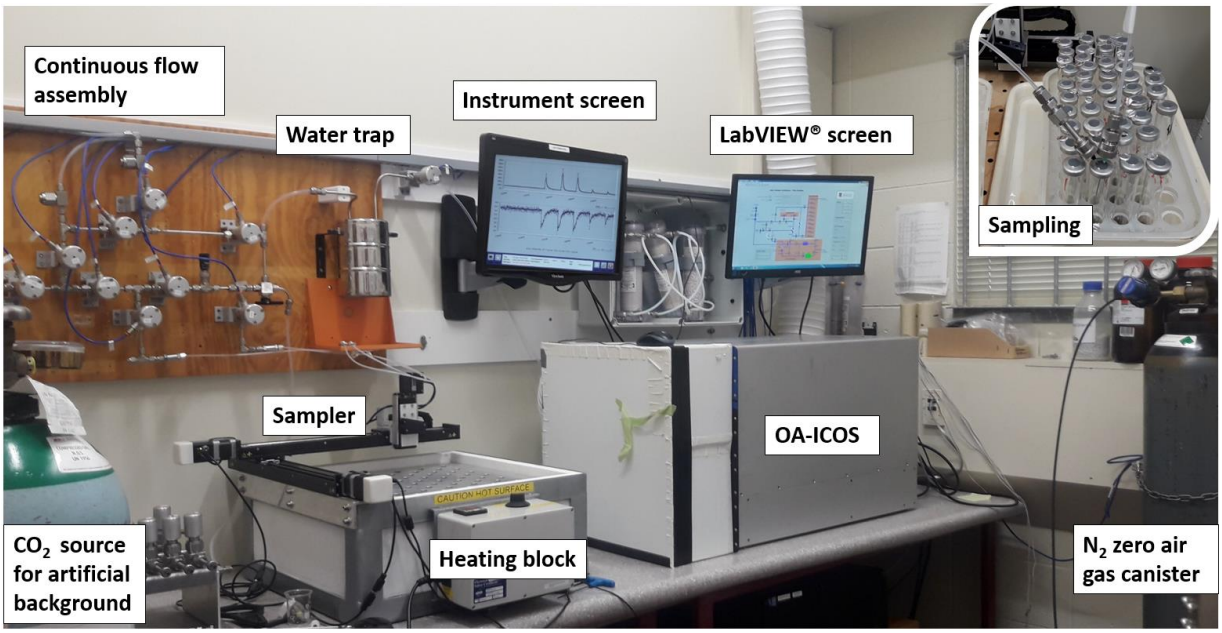

Figure 4.5 Lab setup of the LGR Off Axis Integrated Cavity Output Spectroscopy (OA-ICOS) CO_2 isotope analyser located at the University of Waikato. The samples are introduced into the continuous flow assembly (upper left) by two needles (shown in the upper right corner). The valves are controlled by the LabVIEW interface (upper right). The water trap consists of ethanol and dry ice (50:50).

4.2.1 Priming method

For this research, the same solution ratio (1:0.125) was used as in Numa (2020) but with only 2 g of soil instead of 3 g to reduce excessive CO_2 production that would exceed the detection limit of the OA-ICOS. Following the same incubation method (section 4.1.3.2), the priming runs used 40 24 mL hungate tubes for treatment, 40 for the control tubes and

four blanks. This amount of soil and glucose was found in preliminary experiments to be above the lower limits of the machine (160 ppm) and below the upper limits of the machine (2500 ppm), in which the data is reliable inside these limits.

The $\delta^{13}C$ treatment solution used in this research consisted of 0.01 g of $\delta^{13}C$ labelled glucose (D-GLUCOSE U-13C6, 99%, Cambridge Isotopic Laboratories Inc.) and 27 g of unlabelled glucose (D-GLUCOSE, Ajax Chemicals UNIVAR 783-500G) dissolved in 2 L of distilled water (Numa, 2020). The solution was kept sealed in the laboratory fridge (4 ^{o}C) and was not used after greater than 4-months of storage. The resulting isotopic signature of the solution was 29.92 ‰ (VPDB). This solution signature and the natural signature of $\delta^{13}C$ in the geothermal soil (-20.48 ‰ VPDB) were accounted for in the data processing calculations.

To the control tubes, 0.25 mL of distilled water was added, and to the treatment tubes 0.25 mL $\delta^{13}C$ labelled glucose solution was added, both following the same ratio as the unlabelled glucose samples (1:0.125). These solutions were added to 2 g of soil which had been collected following the method described in section 4.1.3.1

The treatment, control tubes and blanks were run in the temperature block at 40 temperatures for five hours on the day proceeding sample measurement. After the five hour soil incubation was completed the samples were put directly on ice and were frozen at -20 ^{o}C overnight. The incubation process and sampling process took two days in total to complete due to the longer time of ^{13}C-CO_2 analysis.

The next morning, the first set of samples, the treatment tubes and blanks, were run on the IRGA. Triplicates of 1% CO_2 gas standards ranging from 2 mL to 0.1 mL were run on the IRGA first. The samples were then run-in ascending temperature order. The headspace gas sample was taken using a 1 mL insulin syringe. The samples remained on ice for the duration of sampling both on the IRGA and OA-ICOS machines.

Once the first sample set was run, the samples were taken to the Carbon Isotope Dating Lab. Here, the OA-ICOS machine was set up for the run. The machine consists of two continuous gas flows, zero air and CO_2 gas, which remained on during the sampling duration. The gas pressure in the system was set to 39 psi and the CO_2 baseline set to ~183 ppm. An ethanol and dry ice water trap was used to cool the gas coil and keep the pressure stable. The baseline of 183 ppm was chosen as it sat between the lower limit (160 ppm) and the upper baseline limit (200 ppm) of the machine. The baseline for every sample run remained within the bounds of these values.

A drift correction sequence was set to run for 2 minutes at the beginning and end of sampling. A shorter drift correction (~40 secs) was also set to run between each sample. The sample flow valve was set to one turn (slower airflow) due to the large size of the hungate tubes.

Once the machine was set up, the sampling sequence was made and the samples were run manually through the machine. The sequence of the overall run can be found in **Table 4.5**. Each sample took around 2-3 minutes to run including drift correction. The samples were run in order of ascending incubation temperature. The sampling process was completed separately for both the treatment and control sample sets to minimise the time the samples were out of the freezer. Both sets were treated and run exactly the same on the IRGA and OA-ICOS machines.

Table 4.5 Run order of samples, standards, blanks and drift corrections.

Order	Sample Type	Number of Hungate Tubes
	Drift Correction Sequence	
1st	Standards	5
2nd	Glucose Soil Samples	40
3rd	Blanks	4
4th	Standards	5
	Drift Correction Sequence	
5th	Control Soil Samples	40
6th	Standards	5
	Drift Correction Sequence	

The OA-ICOS machine measures samples using a flushing system with a carrier gas of scrubbed nitrogen gas (N_2). Two needles comprising an inlet and outlet are inserted into the headspace of the incubated hungate tube. The carrier gas, pumped through the inlet needle, mixes with the respired CO_2 in the tube. Using an applied vacuum created by the OA-ICOS instrument, both gasses are drawn out of the tube by the outlet needle and into the measurement cavity (Barker *et al.*, 2011; Robinson *et al.*, 2020).

This priming method is technically challenging and time-consuming due to the largely manual component and technical machine setup. This manual sampling method can take

around 8-hours to complete. This method is incredibly labour intensive, attempts to automate this method were tried before the commencement of the work. These attempts were unsuccessful, for supplementary information of these experiments and details see Appendix D.

Overall, only three priming runs were able to be completed in the time frame available (**Table 4.6**). These were run in a random order determined using the rand() function in excel and the values placed into ascending order. The random order of sampling distance was 1) 800 cm, 2) 180 cm and 3) 20 cm.

Table 4.6 Summary table of soil and environmental properties for soil priming samples. The average environmental temperature was averaged across the width for the 3 m grid for the sampling distance. Samples run the 3rd March, 5th March and 10th March 2021.

Distance from Source (cm)	Moisture content (gg^{-1})	pH	Average temperature 2 cm depth (^oC)	Average temperature 10 cm depth (^oC)
20	0.50	4.0	30.1	40.6
180	0.57	4.4	28.4	32.1
800	0.43	4.6	24.8	25.1

4.2.1.1 *Standard preparation*

On the morning of sampling, $\delta\ ^{13}C$ standards for the OA-ICOS priming run were prepared in 24 mL hungate tubes. The $\delta\ ^{13}C$ standards were used to create a calibration curve to correctly adjust the measured sample results based on known standards. The standards used for all runs are presented in **Table 4.7**, the table order of these standards is the same as the run order. The sequence of these five standards was counted as one set (BDH, WCS, NBS-19, 17A, 68A). Three sets of standards need to be run for sample runs of 80 samples or less. These sets were run at the beginning, middle, and end of the incubated soil samples (see **Table 4.5**).

Table 4.7 Summary of δ ^{13}C reference and internal standards used in this research.

Standard name	Actual isotopic signature (‰ VPDB)
BDH	-24.95
WCS	-10.27
NBS-19	1.95
17A Bicarbonate	17
68A Bicarbonate	68

Approximately 0.1 mg of the powdered calcite international reference standards (BDH, WCS & NBS-19) was used in each corresponding standard tube. Three drops were used for each bicarbonate standard (17 ‰ & 68 ‰ which were standardized using the international reference standards (Robinson *et al.*, 2020)). Each standard tube was sealed using the same rubber stoppers and metal crimping caps as the soil tubes. Each standard was then acidified with 10 drops of orthophosphoric acid and left to acidify on a 73 ^{o}C heating block for at least 45 minutes.

4.2.1.2 *Data analysis*

Once all the samples were run on the IRGA and OA-ICOS machines, the data was collected and run through Matlab R2019b to identify peaks. The data produced four temperature responses including; Total-R_S which was measured directly from the treatment soil; Glucose-R_S which was calculated from the δ ^{13}C content of the labelled glucose respiration and using a two pool mixing model (see equation (4-4)); SOM-R_S was the CO_2 measured directly from the control soil (SOM_c), SOM respiration was also measured from the treatment soil which was hypothesised to also included priming (SOM_t); Priming-R_S was calculated as the difference between SOM_c and SOM_t CO_2 fluxes (Numa, 2020). A schematic diagram representing this explanation can be found in **Figure 4.6**.

The data gathered was analysed using a two pool mixing model that separated the total CO_2 produced into enriched δ ^{13}C glucose and soil derived components (equation (4-4); Robinson *et al.* (2020)). This mixing model then allowed the separation of SOM_t-R_S and Glucose-R_S from the Total-R_S (Numa, 2020).

$$f = \frac{(C_S - C_R)}{(C_G - C_R)} \quad (4\text{-}4)$$

Where, C_S is the $\delta\ ^{13}C$ value of the soil , C_R is the $\delta\ ^{13}C$ value of the respired CO_2 and C_G is the $\delta\ ^{13}C$ of the added glucose solution, all units as ‰ VPDB (Numa, 2020; Robinson *et al.*, 2020).

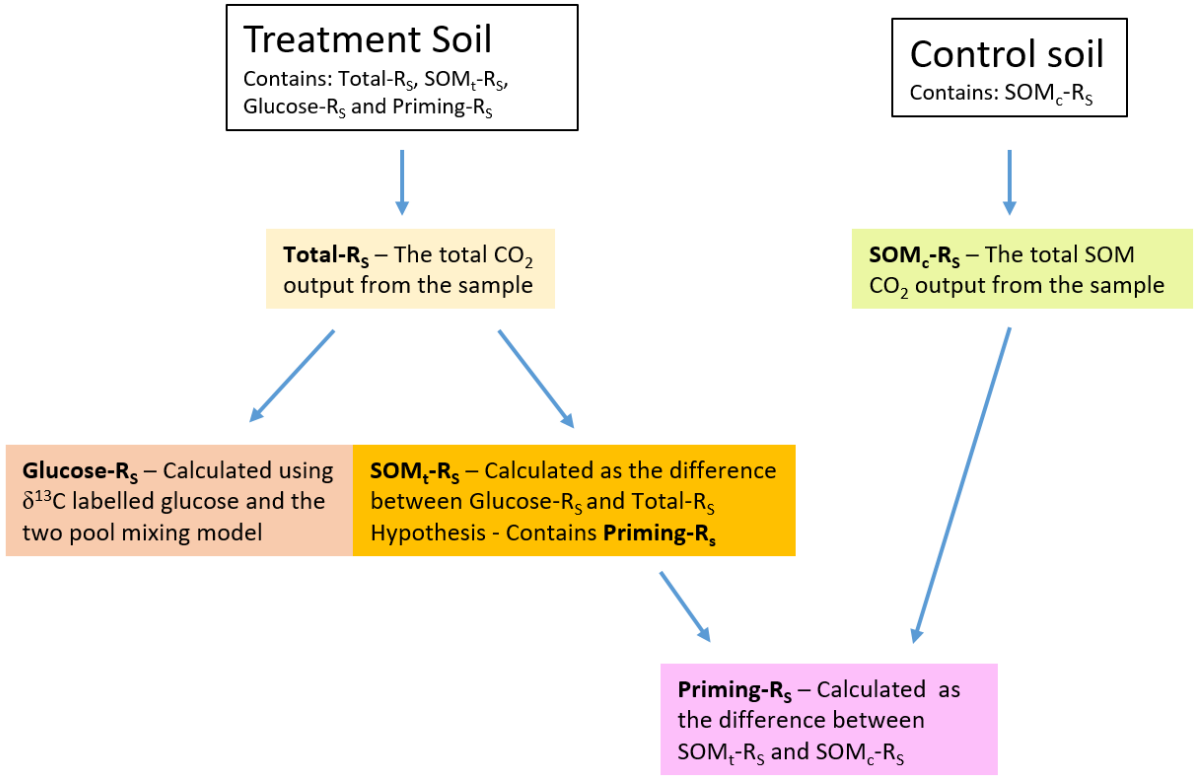

Figure 4.6 Schematic diagram of the approach used to determine the soil priming induced by the addition of glucose.

This data was analysed using the same principles in section 4.1.5 above using equation (4-3). The data was then interpreted using MMRT principles to determine the T_{opt} and T_{inf} of all the respiration parameters (section 4.3).

4.3 Curve Fitting

In this research, MMRT was used to capture the temperature response of microbial populations along a geothermal soil gradient. MMRT has the following equation (equation (4-5), chapter 2 equation (2-14)):

$$ln(k) = ln\left(\frac{k_B T}{h}\right) - \frac{\Delta H^{\ddagger}_{T_0} + \Delta C^{\ddagger}_P(T - T_0)}{RT} + \frac{\Delta S^{\ddagger}_{T_0} + \Delta C^{\ddagger}_P(lnT - lnT_0)}{R} \quad (4\text{-}5)$$

Where: k is the rate constant, k_B is Boltzmann's constant, T is the temperature (K), h is Planck's constant, R is the universal gas constant, $\Delta H^{\ddagger}_{T_0}$ (‡ superscript denotes transition state) is the change in enthalpy (J mol^{-1}), $\Delta S^{\ddagger}_{T_0}$ is the change in entropy (J mol^{-1} K^{-1}) both at reference temperature T_0 (309 K, 36 ^{o}C), $\Delta C^{\ddagger}_P$ is the change heat capacity (J mol^{-1} K^{-1}) (Robinson et al. 2020). The MMRT equation assumes that $\Delta H^{\ddagger}_{T_0}$, $\Delta S^{\ddagger}_{T_0}$ and $\Delta C^{\ddagger}_P$ are all constant with increasing temperature.

When fitting MMRT to the data, issues arose with the data fits where the MMRT model was not fully capturing the true curvature of the data points, resulting in under-estimations of the T_{opt} and T_{inf} parameters. One issue with MMRT is the assumption that $\Delta C^{\ddagger}_P$ is constant with changes in temperature, however, it has been found in many studies that $\Delta C^{\ddagger}_P$ itself is temperature dependent (Ghosh & McSween Jr, 1999; Darros‐Barbosa *et al.*, 2003).

To overcome this issue, the development of an updated MMRT version was undertaken. A version MMRT 2.0 is being developed, however, in this research the intermediate version MMRT 1.5 was used (Prentice *et al.*, 2020). The difference between MMRT 1.0 and the new MMRT 1.5 is that $\Delta C^{\ddagger}_P$ is able to change with increasing temperature (positive/negative linear relationship). The new MMRT 1.5 equation adds two new terms, A and B, the A and B parameters act like a linear equation (y=mx + c) and replace the $\Delta C^{\ddagger}_P$ term. The addition of parameters A and B adds complexity to MMRT but still allows the calculation of important microbial parameters T_{opt} and T_{inf}. The MMRT 1.5 equation can be found below (equation (4-6)). The parameters $\Delta H^{\ddagger}_{T_0}$ and $\Delta S^{\ddagger}_{T_0}$ are still held constant with increasing temperature as found in MMRT 1.0.

$$ln(k) = ln\left(\frac{k_B T}{h}\right) - \frac{\Delta H^{\ddagger}_{T_0}}{RT} - \frac{\Delta C^{\ddagger}_P (T - T_0)}{RT} + \frac{\Delta S^{\ddagger}_{T_0}}{R} + \frac{\Delta C^{\ddagger}_P (lnT - lnT_0)}{R} \quad (4\text{-}6)$$

Where $\Delta C_P^{\ddagger}$ is linearly dependent on temperature:

$$\Delta C_P^{\ddagger} = A(T - T_0) + B$$

Where: $\Delta C_P^{\ddagger}$ is the change heat capacity (J mol^{-1} K^{-1}), in this MMRT 1.5 equation $\Delta C_P^{\ddagger}$ is linearly dependent on temperature with slope A, and B is the value of $\Delta C_P^{\ddagger}$ at the reference temperature T_0 (309 K, 36 ^oC).

This equation was found to fit the data found in this research more visually accurately than the MMRT 1.0 equation. Therefore, for all MMRT analyses completed in this work, MMRT 1.5 was used as it more accurately represented the data. The first derivative of the MMRT 1.5 equation was used to calculate the T_{opt} of each curve and the second derivative was used to calculate T_{inf} of each curve. MMRT 1.5 equation was applied to the data using R software version 4.0.2. A comparison between the fits of both MMRT models can be found in Appendix E.

Chapter 5

The Temperature Dependence of Microbial Respiration and Soil Priming along a Geothermal Gradient

5.1 Abstract

Soil carbon (C) has the potential to be lost under a changing climate particularly through increasing temperatures and the acceleration of feedback loops by microbial populations. To understand the potential responses of microbial populations to soil warming, the temperature responses of microbial respiration and soil priming were investigated along a geothermal gradient in Rotorua, New Zealand, which ranged in temperatures from 18-36 ^{o}C. This geothermal gradient was used as a proxy for soil warming with climate change. Soil from this site was incubated for five hours in the laboratory at 40 different temperatures (~1.8-53 ^{o}C) and the headspace CO_2 production measured using an Infrared Gas Analyser (IRGA). The results were fitted using Macromolecular rate theory (MMRT) to characterise the temperature response in terms of the temperature optimum (T_{opt}) and temperature inflection point (T_{inf}). Soils were incubated with and without glucose which was used as a general surrogate for labile C in soil. Consequently, the temperature response of two pools in soil were calculated (i) a labile C pool and (ii) soil organic matter (SOM) considered to represent a more stable C pool. The results measured only small increases in the T_{opt} of labile C respiration and the T_{inf} of SOM respiration with increasing environmental temperature. These changes were small with average changes no larger than 0.198 ^{o}C per ^{o}C change in environmental temperature (^{o}C ^{o}C^{-1}) and 0.263 ^{o}C ^{o}C^{-1}, respectively. Soil priming followed an MMRT temperature response and may be negatively impacted by warming temperatures. These results suggest the microbial populations may adapt to climate change through different mechanisms and that feedback loops in response to climate change may be small.

5.2 Introduction

Soil is the largest terrestrial carbon (C) pool, containing more C than the atmosphere and biosphere combined (Jobbágy & Jackson, 2000; Scharlemann *et al.*, 2014). Soil C is a function of inputs through photosynthesis (primary production) and outputs through

heterotrophic decomposition (microbial respiration) and autotrophic respiration (Schlesinger, 1977; Janzen, 2004). Climate change and rising global temperatures have the potential to negatively impact our soil C stocks through the acceleration of microbial respiration (Davidson & Janssens, 2006). Therefore, understanding the temperature dependence of microbial respiration and its interactions with soil C is important for future climate change predictions, policies, and management.

There are many different ways to partition different pools of C in soil, including physical or biochemical pools (Davidson & Janssens, 2006). One approach views soil C as separated simply into two pools, labile C (readily available to microbes) and stable C (less available) (Kirschbaum, 2004). These pools have different temperature sensitivities which influence how they respond to temperature changes (Davidson & Janssens, 2006; Craine *et al.*, 2010). Temperature sensitivity is a metric of how respiration changes with increasing temperature (Robinson *et al.*, 2017). These temperature sensitivities can be measured in relative (ratios of rate changes) and absolute terms (absolute rate change at a given temperature) (Sierra, 2012). Past studies looking at the temperature sensitivity of soil C and microbial processes have typically used equations such as Q_{10} and the Arrhenius equation (e.g. Fang and Moncrieff (2001), Lloyd and Taylor (1994), Schindlbacher *et al.* (2010), Sierra (2012)). However, these metrics were originally created to primarily model the temperature response of chemical processes and therefore, may have substantial limitations when examining biological temperature responses (Hobbs *et al.*, 2013; Schipper *et al.*, 2014; Arcus *et al.*, 2016; Robinson *et al.*, 2020; Numa *et al.*, 2021). Equations based on the Arrhenius function assume continuous and exponential increases in rate with increasing temperature, whereas biological (enzymatic) processes are well known to have a temperature optimum (T_{opt}) (Hobbs *et al.*, 2013).

Macromolecular rate theory (MMRT) is a recently developed temperature model derived from thermodynamics and first principles to specifically model the response of enzymatic processes with temperature (Hobbs *et al.*, 2013; Schipper *et al.*, 2014; Arcus & Pudney, 2015). A key part of the MMRT theory is that the activation energy of reactions catalysed by enzymes is temperature dependent (Hobbs *et al.*, 2013; Arcus & Pudney, 2015; Arcus *et al.*, 2016). Unlike the Arrhenius model, MMRT accounts for the natural phenomenon that biological reaction rates increase with temperature until a T_{opt}, after which reaction rates decline with increasing temperature even in the absence of enzymatic denaturation (Hobbs *et al.*, 2013; Schipper *et al.*, 2014; Alster *et al.*, 2016; Xu & Shang, 2016; Liang *et al.*, 2017; Robinson *et al.*, 2017; Alster *et al.*, 2018; Robinson *et al.*, 2020). The fitting

of MMRT allows the calculation of metrics including T_{opt}, the infection point of the fitted curve (T_{inf}), and change in heat capacity of the enzyme-substrate complex ($\Delta C_P^{\ddagger}$) (Hobbs *et al.*, 2013). T_{inf} is the temperature at which a process (e.g. respiration) is the most sensitive to temperature increases, that is, where the change in rate is greatest (Schipper *et al.*, 2014; Schipper *et al.*, 2019). The importance of T_{opt} is that it defines the temperature at which the rate is maximised. It has recently been argued that the T_{inf} of enzymes involved in biological reactions determines the T_{opt} of the parent organism (Prentice *et al.*, 2020). In soil environments, this hypothesis suggests that the enzymes of soil microorganisms will set their T_{inf} at the temperature of their soil environment (Prentice *et al.*, 2020). This hypothesis remains to be tested.

MMRT was used in this study to model the temperature response of microbial respiration of both stable (soil organic matter; SOM) and labile C sources in soil. Previous studies using MMRT have looked at labile and stable C pools responses including the use of more complex and polymeric C such as leaf litter (Robinson *et al.*, 2020) and multiple simpler C substrates (Numa *et al.*, 2021). MMRT has also been applied to multiple soil types and moisture contents (Robinson *et al.*, 2017; Numa *et al.*, 2021). Numa *et al.* (2021) showed that glucose-induced respiration, along with five other labile substances (maltose, dextran, yeast extract, lysine, arginine), had the same temperature response with a T_{opt} of ~37 ^{o}C and a T_{inf} of ~ 22 ^{o}C across three very different soil types. These findings suggested that temperature response of labile C respiration was highly conserved across soils and substrates, however, these soils were all collected from a single farm and experienced the same climatic regime. These findings have not yet been tested for soils under different temperature regimes.

Here, these findings that the T_{opt} of labile C respiration tends to be ~37 ^{o}C and the T_{inf} ~ 22 ^{o}C were investigated for soil along a natural thermal gradient. Natural thermal gradients in soil environments can be used as proxies for soil warming and can help give insight into the warming effects of climate change (Peterse *et al.*, 2009; Sigurdsson *et al.*, 2016; Marañón-Jiménez *et al.*, 2018; Parts *et al.*, 2019) . Types of thermal gradients used in proxy studies include, artificial warming, elevational, latitudinal and geothermal (De Frenne *et al.*, 2013; Xu *et al.*, 2013; Walker *et al.*, 2018; Parts *et al.*, 2019). Geothermal gradients can be advantageous over other natural gradients because they are confined in space which reduces other confounding environmental factors, such as vegetation changes (O'Gorman *et al.*, 2014; Sigurdsson *et al.*, 2016). Often geothermal features have been in place for decades and presumably the soil ecosystem has had time to adapt to this

wide range of temperatures. A geothermal gradient located in Rotorua, New Zealand, was used to investigate if, and to what extent, the respiration of different C pools changes with environmental temperature and to explore potential thermal adaptation by microbial communities (Walker *et al.*, 2018). Thermal adaptation can be summarized as the adjustment of an organism's metabolic rates (e.g. respiration) to sustained temperature increases or decreases (Bradford *et al.*, 2008). Whether thermal adaptation occurs in response to climate change will influence the magnitude and type of potential feedback loops (Luo *et al.*, 2001).

The main focus of this study was to examine the temperature response of labile C (using glucose & yeast extract) and more stable C (determined from bulk soil respiration (c.f. Numa *et al.* (2021)). Our experimental approach added glucose to soil to determine the labile C response. Adding labile C to a system promotes soil priming and so soil priming was another factor to consider when investigating the temperature response of C cycling in soil. Soil priming effects (PE) are well recognised as playing an important role in soil C and nutrient cycling, as well as a mediator of responses/feedbacks of many ecological processes related to global climate change (Sulman *et al.*, 2014; Finzi *et al.*, 2015; Keiluweit *et al.*, 2015; Luo *et al.*, 2016). Priming effects are the increased or decreased response of soil microbial respiration to the addition of an exogenous C compound (Kuzyakov *et al.*, 2000). Measuring PEs can be methodically challenging and obtaining the temperature response of PEs even more so (Numa, 2020), consequently, a full exploration of the temperature response of PEs here was not possible. Soil PEs along the geothermal gradient were investigated briefly in this research.

The main goal of this work was to determine if the T_{opt} and T_{inf} of microbial respiration in soil changed along the length of a geothermal gradient located in Rotorua, New Zealand. This soil gradient was relatively uniformly vegetated and managed. The temperature gradient in the soil spanned on average from ~18 to ~36 ^{o}C and could be considered to represent a wide range of soil systems from temperate to tropical ecosystems. Added glucose and yeast extract were used as proxies for labile C substrates in soil. To determine the temperature response of labile C, respiration rates from soil incubations with added C were subtracted from respiration rates of soil incubated alone. These measurements were simultaneously made for 40 different temperatures (ranging ~1.8-53 ^{o}C) over a five hour incubation period. Here, the respiration of glucose (Glucose-R_S) and yeast extract (Yeast Extract-R_S) will be referred to collectively as labile C respiration. The two main objectives of this study were; to characterise the microbial respiration of SOM and

glucose (and yeast extract) along the geothermal gradient using T_{opt} and T_{inf}, and to determine the temperature response of priming along a geothermal gradient and characterise it in terms of T_{opt} and T_{inf}.

5.3 Methods

5.3.1 Field site and sample collection

The geothermal gradient used in this study was located on the Arikikapakapa golf course in Rotorua, New Zealand (38º09'39.10"S, 176º14'57.47"E). The Arikikapakapa golf course is located in the Taupo Volcanic Zone which has been geothermally active for thousands of years. The geothermal feature selected at this location was a heated ground feature ~5.1 m long and ~3.8 m wide, situated just off the main golf course (Seward *et al.* (2015); **Figure 5.1**). The soil at this site consisted of Tikitere siblings, which is an inactive hydrothermal recent soil of sandy loam texture (Landcare Research S-MAP). The gradient length and surrounding areas were all under the same vegetation of grasses, identified as *Axonopus affinis* (carpet grass) and *Elymus repens* (couch grass), and unidentified mosses. As this gradient was located on the side of the driving range, the grasses were not fertilised or limed, and the only known land management was frequent mowing.

To characterise the soil temperatures at the field site, the site was monitored using DS1922L iButton thermochrons (iButtonLink Technology) and periodic gird measurements along a 16 m by 3 m grid on the east side of the geothermal feature. Data collection occurred every 3-4 weeks beginning August 2020 and ending June 2021. The iButton monitoring found a long-term temperature gradient that varied both seasonally (highest in summer) and daily by about 5.0 ºC presumably in response to radiation inputs during the day (**Figure 5.2**). We observed rapid temperature decreases near the geothermal source that were linked to large rainfall events occurring on the same day or the day before the drop in temperature was observed (BOPRC, Whakarewarewa EK577135 rain monitoring site). The 16 m by 3 m grid data was obtained using a 3 m by 3 m grid template, which consisted of 5 lines of temperature measurements (1 m apart & 1 down the centre; see **Figure 5.3a**). The grid data identified that the temperature gradient was somewhat variable at 2 cm depth but more stable at 10 cm depth along the length of the gradient (**Figure 5.3b**).

For respiration measurements, soil samples were collected using a bucket sampler (7.5 cm depth, 2.5 cm diameter). Bulk soil samples (~15 separate cores) were taken from transects that were perpendicular to the temperature gradient (**Figure 5.3a**). The soil samples were passed through a 2 mm sieve in the laboratory on the same day of collection. Surfaces, such as the sampler, gloves, and the sieve were wiped down between samples to minimise cross-contamination. Soils were stored at room temperature in sealed zip lock bags plugged with cotton wool until tested. Soils collected were incubated within the same week of collection. Based on preliminary experiments it was found that the soil was capable of producing consistent and measurable respiration rates at a range of moisture contents. Therefore, all experiments were completed at field moisture to minimise disturbance (see results section 5.4.1). Samples were collected along the 16 m by 3 m geothermal gradient grid at distances informed by the iButton data to capture a wide range of environmental temperatures. A maximum of four soil samples could be run in a week and consequently, sampling and analyses were distributed over several months. The run order of soil collection and analysis from different distances along the gradient were randomly allocated using the rand() function in excel (Appendix B).

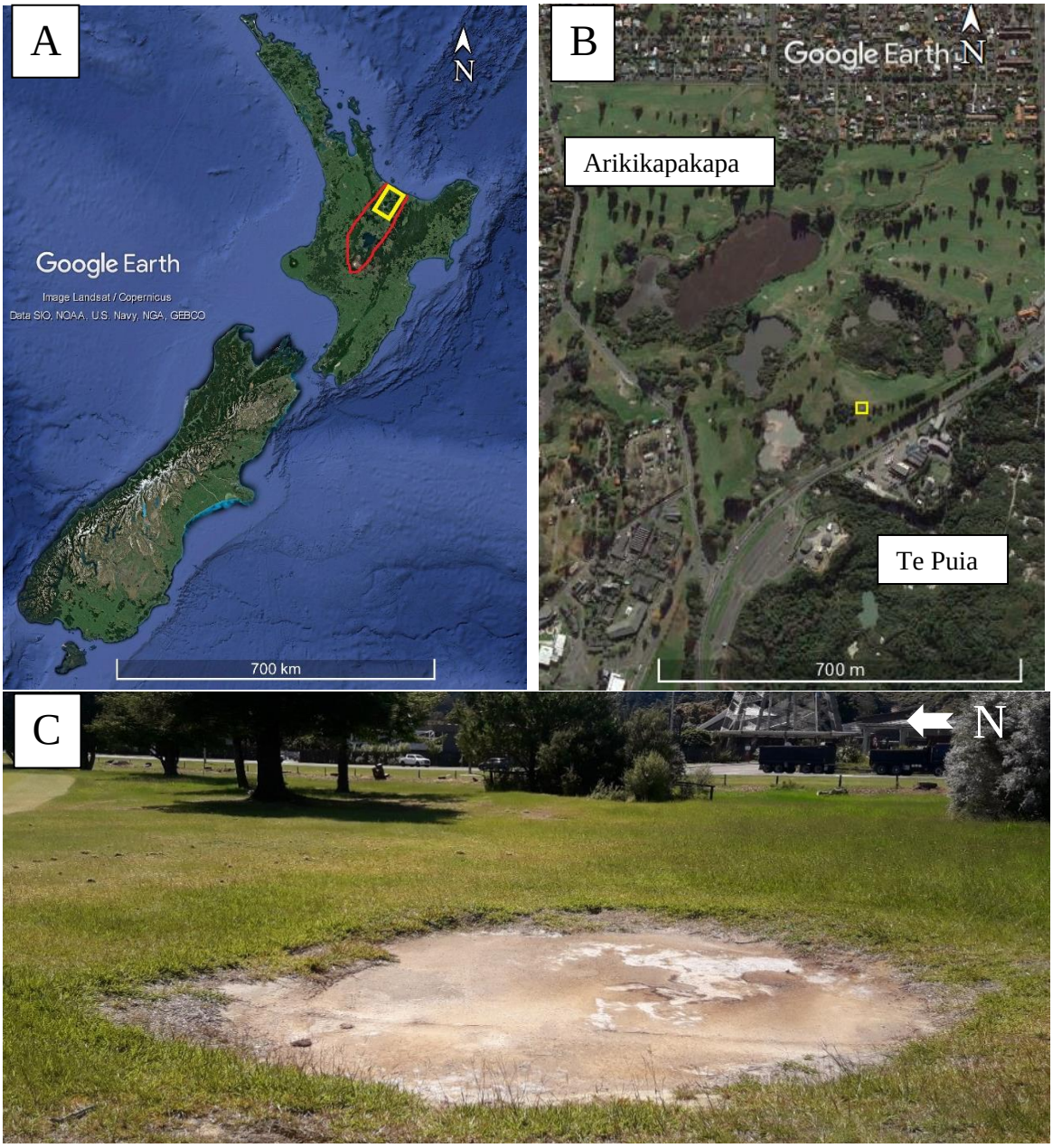

Figure 5.1 A) Map of New Zealand showing the Taupo Volcanic Zone in red and the Rotorua region in the yellow box. B) An aerial view of the Arikikapakapa Golf Course in Rotorua with the field site located in the yellow box. C) A ground photo of the field site used in this research taken on the 20th November 2020. Images A and B from Google Earth 2020

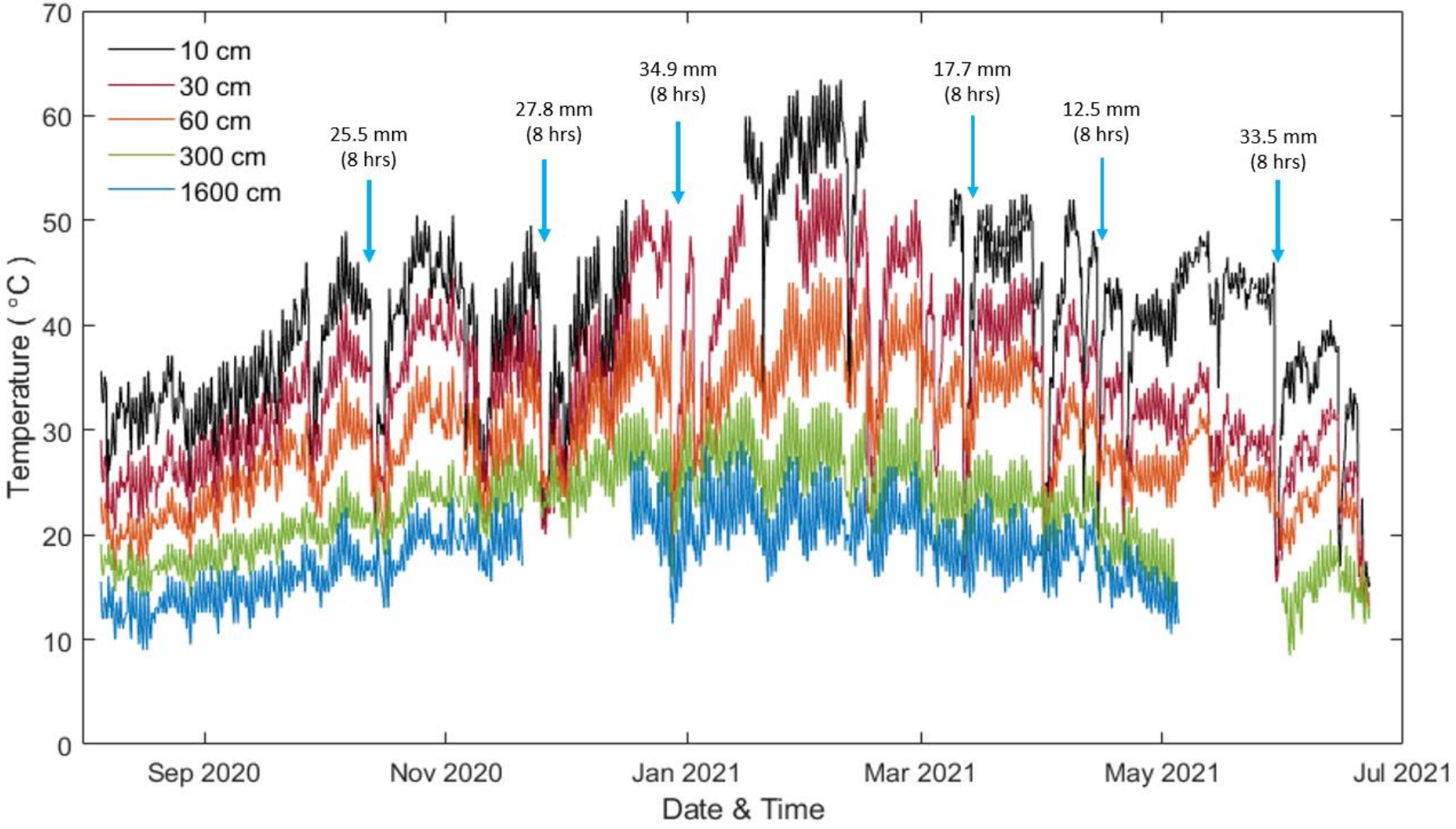

Figure 5.2 Hourly iButton temperature data (°C) at 7.5 cm depth, beginning the 5th August 2020 to the 22nd June 2021 at five distances along the geothermal gradient, 10 cm (black), 30 cm (red), 60 cm (orange), 300 cm (green), 1600 cm (blue), distances away from the geothermal source. The light blue arrows denote examples of large rainfall events (mm in 8-hours) that were associated with rapid temperature declines potentially due to the cooling effects of water.

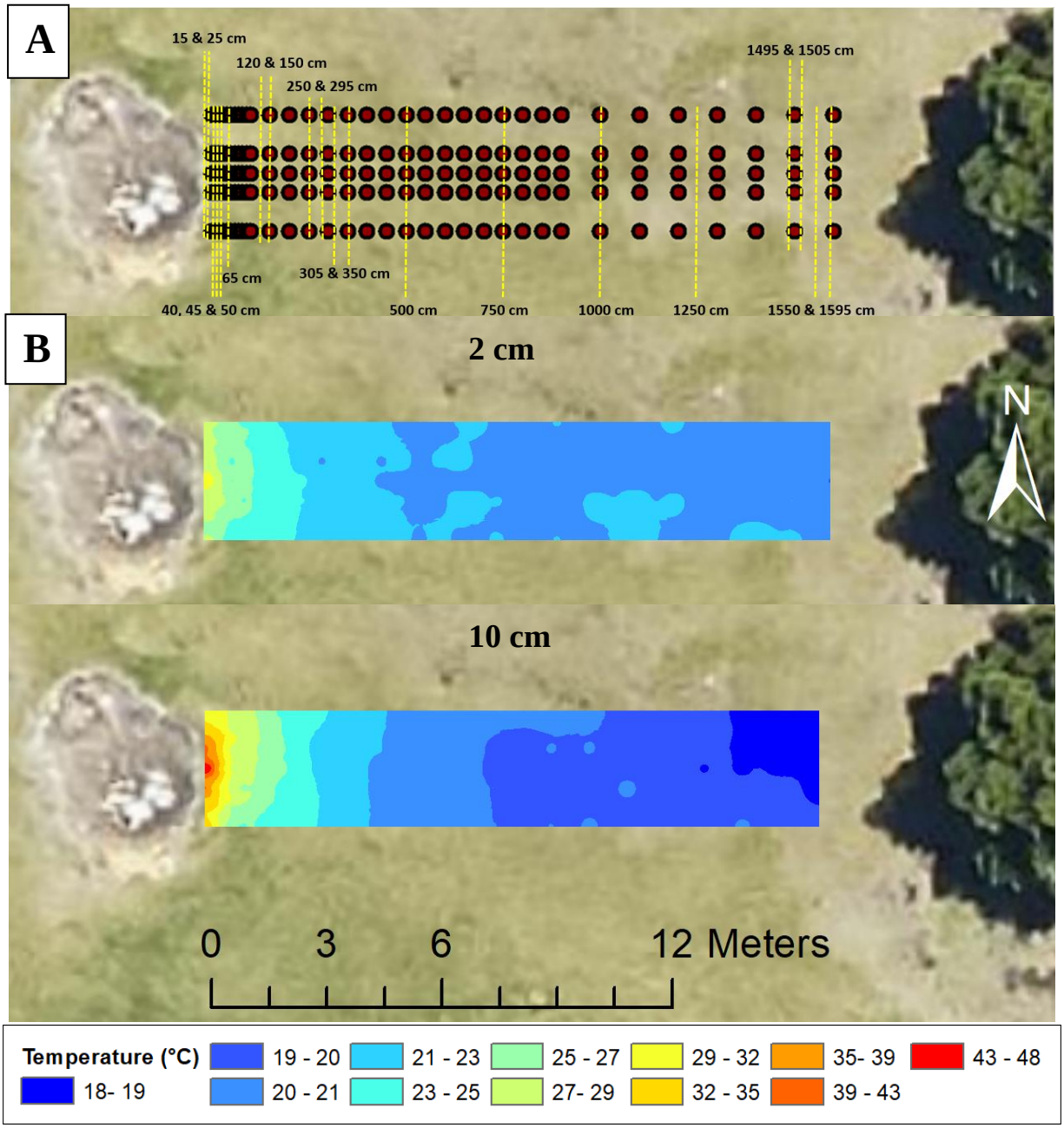

Figure 5.3 A) The red dots show the locations of temperature measurements taken along the 16 by 3 m grid. Data taken every 10 cm for the first metre, every half metre from 1-9 m and every metre from 10-16 m. The yellow lines indicate sampling distances for the glucose experiments. B) The averaged grid from data along the geothermal gradient at 2 cm and 10 cm depths. All grid data was averaged from the 26th August 2020 to the 22nd June 2021 from 12 sampling visits. Data mapped using ArcGIS 10.7.

5.3.2 Labile C incubations

To determine the temperature response of respiration from SOM and of labile C (using glucose as proxy), 20 separate laboratory incubations were carried out over a 7-month period beginning November 2020. The soil was collected from 20 different locations spaced along the temperature grid (**Figure 5.3a**). A temperature block consisting of 40

different temperatures was used for all incubations in this study (see **Figure 5.4**; temperatures ranging from ~1.8-53 ^{o}C in ~1.5 ^{o}C increments). The incubation method used here was based on work completed by Numa *et al.* (2021) and Robinson *et al.* (2017).

A total of 84, 24 mL hungate tubes were used for each incubation. Four of these tubes were blanks (containing no soil) to account for the background CO_2 concentrations of the laboratory atmosphere during the experimental setup. The other tubes consisted of 40 control tubes containing 2 g soil and 0.25 mL of distilled water, and 40 treatments tubes containing 2 g soil and 0.25 mL of glucose solution. The soil was weighed to within 0.01 g of intended weights. The ratio of soil to solution (1 g:0.125 mL) was based on findings from Numa *et al.* (2021). The glucose solution used for the treatment tubes comprised of 0.2702 g of glucose powder (D-GLUCOSE, Ajax Chemicals UNIVAR 783-500G) to 20 mL of distilled water. All tubes were plugged with a rubber septum and sealed using metal crimp caps. Once sealed, the tubes were briefly mixed using a vortex mixer following methods by Degens *et al.* (2001).

Once sealed and mixed, all 84 tubes were placed along the length of the temperature block and left to incubate for five hours. After five hours, the tubes were placed on ice to minimise additional CO_2 production. From each tube, 1 mL headspace samples were taken and run through an Infrared Gas Analyser (IRGA; LI-COR, LI-7000 CO_2/H_2O Analyser) for the determination of CO_2 concentrations. Standards of 1% CO_2 were also run to create a calibration curve for analysis. The CO_2 peaks were analysed using custom Matlab 2019b extraction code. Concentrations here are presented in µg C g soil^{-1} hour^{-1}.

To check whether the results obtained from glucose addition were comparable to other labile C compounds, the same incubation experiment was completed using added yeast extract, following the same method and ratios. Only three distances were completed along the geothermal gradient for this treatment.

The treatment tubes (soil & added glucose) were used to determine the Total-R_S (total respiration) at each incubation temperature. The control tubes (soil only) were used to determine the SOM-R_S (SOM respiration) and by subtraction calculate the Labile-R_S (glucose/yeast respiration). This Labile-R_S theoretically also includes the potential CO_2 production from soil priming which was investigated in later experiments.

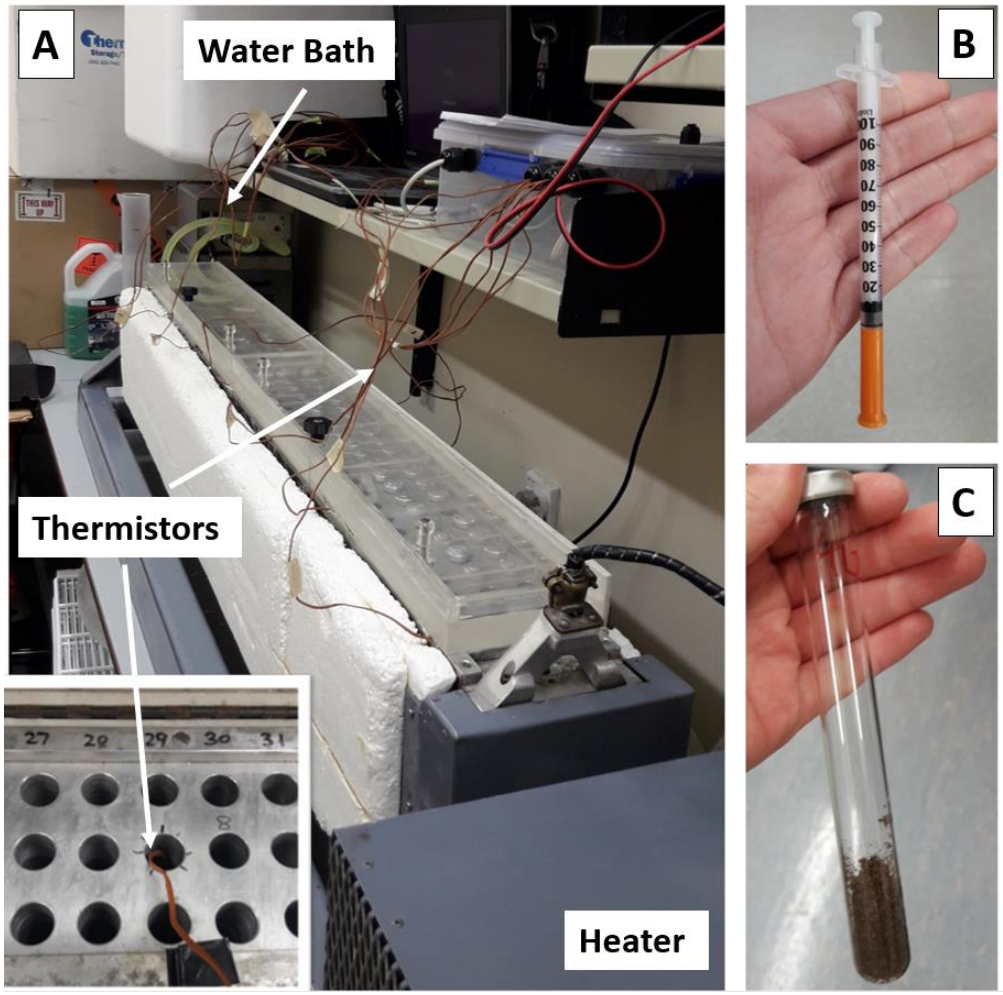

Figure 5.4 A) View of the temperature block from the hot end. The wires hanging down are connected to the block and act as thermistors to record the temperature at eight points. The small circles seen under the lid are the caps of sealed tubes, the block contains three rows of 44 holes available for use. B) Shows the 1 mL syringes used to take samples (Becton-Dickinson and co). C) Shows an example soil tube used.

5.3.3 Priming experiments

To investigate the soil priming occurring in the system $\delta^{13}C$ labelled glucose was used to separate the respiration responses (**Figure 5.5**). A total of three soils runs were completed using this method due to time constraints and the technically challenging nature of the manual method. This method was developed by Robinson *et al.* (2020) and first used for priming by Numa (2020) where a full method description can be found.

The $\delta^{13}C$ labelled glucose treatment solution used comprised of 0.01 g of $\delta^{13}C$ labelled glucose (D-GLUCOSE U-13C6, 99%, Cambridge Isotopic Laboratories Inc.), 27 g of unlabelled glucose (D-GLUCOSE, Ajax Chemicals UNIVAR 783-500G) and 2 L of distilled water (Numa, 2020). The same setup method described earlier was used in these experiments (2 g soil, 0.25 mL solution), but the $\delta^{13}C$ labelled glucose solution was added

to the 40 treatment tubes (same ratio 1:0.125). All 84 tubes (40 control, 40 treatment, 4 blanks) were incubated for five hours, once the incubation was completed the samples were put on ice and transferred to a -20 ^{o}C freezer where they were left overnight.

The following morning, the headspace samples were run through the IRGA and then subsequently on a modified Off Axis Integrated Cavity Output Spectroscopy (OA-ICOS) instrument (Los Gatos Research, CCIA-46, model 908-0021) described by Barker *et al.* (2011) and Beinlich *et al.* (2017). The samples were kept on ice for the duration of the sampling to minimise microbial activity. These samples were run in two batches on a single day to minimise time out of the freezer.

The OA-ICOS measurements for the samples were run at a CO_2 baseline of ~183 ppm and a pressure of 39 psi. A baseline drift correction was run between each sample and standard. The OA-ICOS machine measured samples using a flushing system with a carrier gas of scrubbed nitrogen gas (N_2). Two needles comprising an inlet and outlet were inserted into the headspace of the incubated hungate tube. The added CO_2 ensured the CO_2 concentration is in the measurement chamber was high enough for detection. The carrier gas, pumped through the inlet needle, mixed with the respired CO_2 in the tube. Using an applied vacuum created by the OA-ICOS instrument, the gas was drawn out of the tube by the outlet needle and into the measurement cavity. The internal valves of the machine were controlled using LabVIEW ® software from an external computer (Barker *et al.*, 2011; Robinson *et al.*, 2020).

Five standards were used for the analysis, both international reference standards (NBS-19 1.95 ‰, BDH -24.95 ‰, WCS -10.27 ‰; Beinlich *et al.* (2017)) and internal carbonate standards (bicarbonate standards 17 ‰ and 68 ‰, which were standardised using the international reference standards (Robinson *et al.*, 2020)). Before sampling, these standards were acidified using O-phosphoric acid and heated at 73 ^{o}C until fully dissolved (~45 minutes). These standards were run in triplicates at the beginning, middle, and end of the total run. These standards were used to adjust the $\delta\ ^{13}C$ measured from the samples to $\delta\ ^{13}C$ relative to Vienna Pee Dee Belemnite (VPDB; Robinson *et al.* (2020)).

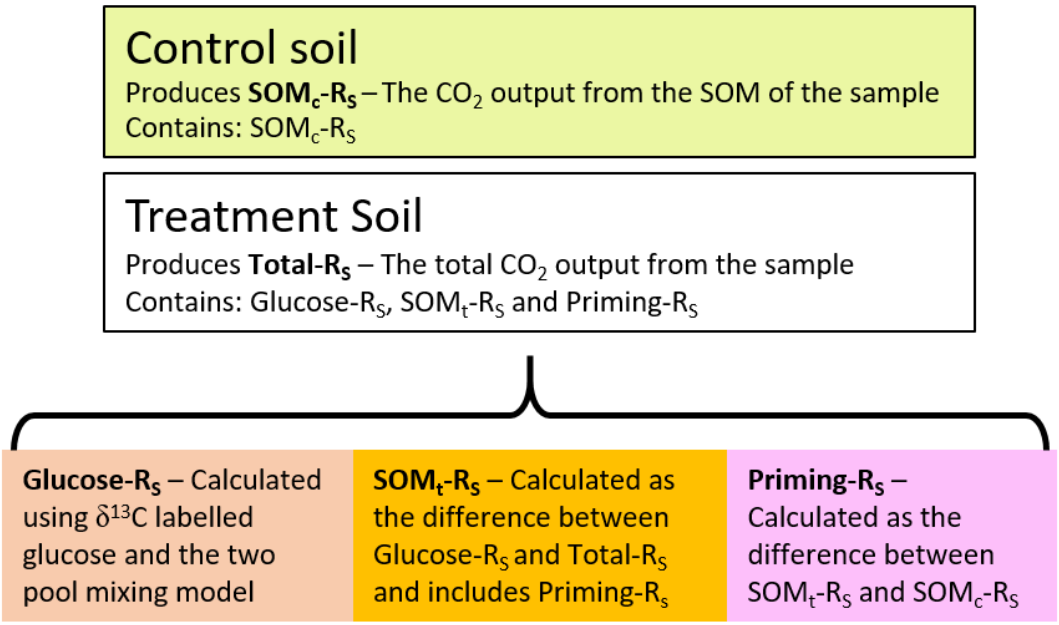

Figure 5.5 A summary of the approach used to determine the temperature response of priming. SOM- R_S is the soil organic matter respiration; Total-R_S is the total respiration of the system including from added glucose; Glucose-R_S is the respiration produced from glucose (labile C); Priming-R_S is the respiration contributed by priming. Adapted from Numa (2020).

5.3.4 Data analysis

The temperature response of SOM, priming, and microbial respiration of labile C, was investigated using MMRT. However, when initially applying the MMRT equation to the data, issues arose with the fit of the curves with the true nature of the curve not being captured (see supplementary material for examples; Appendix E). The MMRT equation underestimated the T_{opt} and T_{inf} parameters of the data. MMRT assumes $\Delta C_P^{\ddagger}$, $\Delta H_{T_0}^{\ddagger}$ and $\Delta S_{T_0}^{\ddagger}$ are held constant with increasing temperature, however, it has been shown that $\Delta C_P^{\ddagger}$ is temperature dependent (Ghosh & McSween Jr, 1999; Darros - Barbosa *et al.*, 2003). To account for this changing $\Delta C_P^{\ddagger}$ with temperature, a new intermediate version of MMRT called MMRT 1.5 was used in this research (equation (5-1)) (Prentice *et al.*, 2020). The new MMRT 1.5 equation adds two new terms, A and B. The A and B parameters act like a linear equation (y=mx + c) and replace the $\Delta C_P^{\ddagger}$ term.

$$ln(k) = ln\left(\frac{k_B T}{h}\right) - \frac{\Delta H^{\ddagger}_{T_0}}{RT} - \frac{\Delta C^{\ddagger}_P (T - T_0)}{RT} + \frac{\Delta S^{\ddagger}_{T_0}}{R} + \frac{\Delta C^{\ddagger}_P (lnT - lnT_0)}{R} \quad (5\text{-}1)$$

Where $\Delta C_P^{\ddagger}$ is linearly dependent on temperature:

$$\Delta C_P^{\ddagger} = A(T - T_0) + B$$

Where: k is the rate constant, k_B is Boltzmann's constant, T is the temperature (K), h is Planck's constant, R is the universal gas constant, $\Delta H^{\ddagger}_{T_0}$ (‡ superscript denotes transition state) is the change in enthalpy (J mol^{-1}), $\Delta S^{\ddagger}_{T_0}$ is the change in entropy (J mol^{-1} K^{-1}) both at reference temperature T_0 (309 K, 36 °C), $\Delta C_P^{\ddagger}$ is the change heat capacity (J mol^{-1} K^{-1}) (Robinson et al. 2020). $\Delta C_P^{\ddagger}$ in this equation is linearly dependent on temperature with slope A, and B is the value of $\Delta C_P^{\ddagger}$ at the reference temperature T_0.

To a degree, MMRT 1.5 reduces the direct interpretability of $\Delta C_P^{\ddagger}$, but in this experiment, MMRT was mainly being used to allow the calculation of T_{opt} and $T_{inf.}$ The T_{opt} was calculated using the first derivative of MMRT 1.5 and the T_{inf} was calculated using the second derivative of the equation. This analysis was completed in R version 4.02.

5.3.4.1 *Priming study*

A two-pool mixing model was used to separate the total CO_2 produced into enriched δ ^{13}C glucose and soil-derived components (equation (5-2)).

$$f = \frac{(C_S - C_R)}{(C_G - C_R)} \quad (5\text{-}2)$$

Where, C_S is the δ ^{13}C value of the soil , C_R is the δ ^{13}C value of the respired CO_2 and C_G is the δ ^{13}C of the added glucose solution, all units as ‰ VPDB (Numa, 2020; Robinson *et al.*, 2020).

5.3.4.2 *General statistics*

A regression analysis between the T_{opt} and T_{inf} values and environmental temperature was completed for the labile C experiment data. The slope significance and standard error was calculated for each regression. Data from this study and previous studies were compared using simple t-tests of the means.

5.4 Results

5.4.1 Preliminary experiments

5.4.1.1 *Soil properties*

Soil samples were initially collected for site characterisation at 30 cm, 60 cm, 100 cm, 300 cm, 550 cm, 900 cm and 1600 cm from the geothermal source, and were analysed for total C, total N, $\delta^{13}C$, $\delta^{15}N$ and pH. The nutrients at the site were low-moderate, with total N and total C ranging from 0.27-0.75 % and 4.38-12.93 %, respectively (see chapter 3, section 3.2.2). The soil nutrients peaked in the middle of the geothermal gradient (150-500 cm from the geothermal feature). The site was enriched in $\delta^{15}N$ with a range of 4.35 to 12.98 ‰ and depleted in $\delta^{13}C$ with a range of -22.27 to -18.26 ‰. The pH at the site was stable along the grid length with an average of 4.6.

Along with these preliminary site characterisation samples, eleven of the glucose samples along the geothermal transect were also tested for the same nutrients, along with pH and moisture content (MC: grams of water per gram soil (gg^{-1})) at field moisture (**Figure 5.6**). The $\delta^{15}N$ values from these samples had a very different isotopic range than the preliminary samples, -1.09 to 0.61 ‰. However, the other nutrients had similar ranges including $\delta^{13}C$ range -20.3 to -18.35 ‰, total N range 0.24-0.75 % and total C range 3.7-12.8 %. The pH average remained the same.

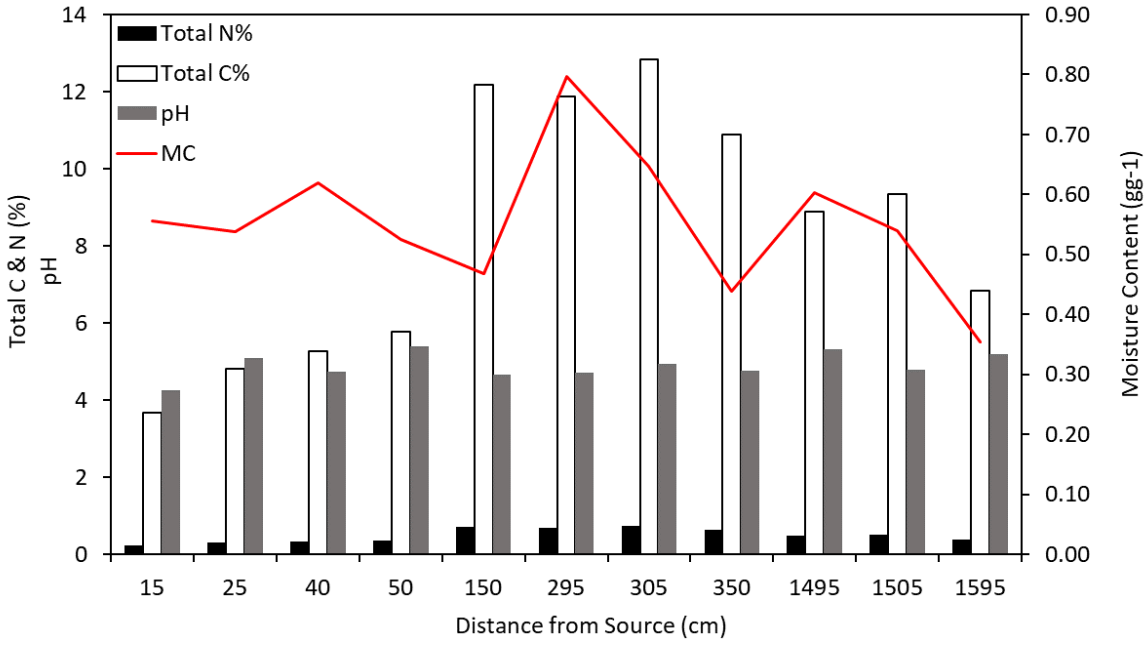

Figure 5.6 The total C and N (%), pH and moisture content (MC; gg^{-1}) at eleven difference distances (cm) along the geothermal gradient. The MC is the MC on the day of incubation, presumably analogous to the field moisture (see Appendix B for dates).

5.4.1.2 *Soil moisture effects on respiration*

To investigate the effects of soil moisture on respiration a preliminary study was completed. This study incubated a bulk soil sample from the geothermal site at three different temperatures, 7.9 ºC, 25.8 ºC and 51.4 ºC for five hours. Each temperature had a sample at one of six adjusted MCs, 0.3 gg^{-1}, 0.4 gg^{-1}, 0.5 gg^{-1}, 0.6 gg^{-1}, 0.7 gg^{-1} and 0.8 gg^{-1}. Two experiments were completed using 2 g soil in 15 mL hungate tubes and 3 g soil in 24 mL hungate tubes. The individual results were standardised by the average of the corresponding experiment. The CO_2 concentration in the headspaces were taken using a 1 mL insulin syringe and measured using an IRGA. The results for both experiments were plotted on the same plots (**Figure 5.7**). The results suggested that the soil produced similar amounts of CO_2 across a wide range of soil MCs. Therefore, all experiments here were completed at field MC. Furthermore, the key objective of this work was to establish the shape of the temperature response curves with less concern about the magnitude of rates, so long as there was no evidence of moisture limitations.

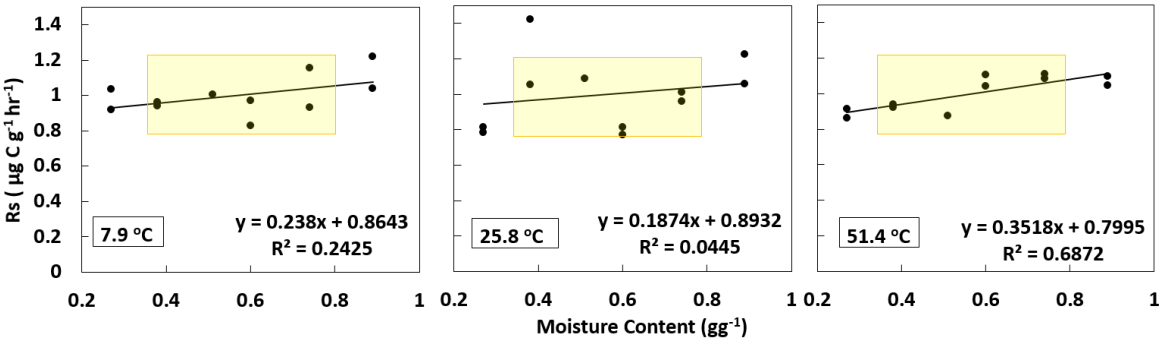

Figure 5.7 MC experiment results showing the respiration rates (µg C g^{-1} h^{-1}) of soils with varying moisture contents (gg^{-1}) measured at three temperatures (7.9 ºC on the left, 25.8 ºC in the middle and 51.4 ºC on the right). The yellow box highlights the MC range found at the field site during the year of this research (range 0.35-0.80 gg^{-1}).

5.4.2 Labile C experiment - Glucose

Although the overall temperature gradient at the site was relatively stable, the temperature did fluctuate daily. Therefore, selecting the most appropriate environmental temperature was more complex than simply using the soil temperature on the day of sampling. This is particularly important when determining the importance of environmental temperature on respiration metrics T_{opt} and T_{inf}. To understand the relationship between T_{opt} and T_{inf} with environmental temperature, it was important to determine the potential scale of

temperature influence (e.g. long-term or short-term). Therefore, to find the most representative temperature at each sampling location, the T_{opt} and T_{inf} relationship with environmental temperature was plotted for different temperature averaging periods and the goodness of fit calculated. The R^2 values from these regression plots were plotted against their averaging periods (**Figure 5.8**). The averaging periods were calculated using the long-term iButton data and the temperature on the day of sampling. The maximum averaging period was 117 days as this was the longest period of data for the first samples taken. The graph suggested that after ~20 days the R^2 value stabilised with temperature and so the environmental temperatures from the averaging period of 30 days (a month) was chosen to best represent the T_{opt}/T_{inf} relationship with temperature with time. In simple terms, the 30-day averaging period temperature was the average environmental temperature over the 30 days prior to the day of sampling.

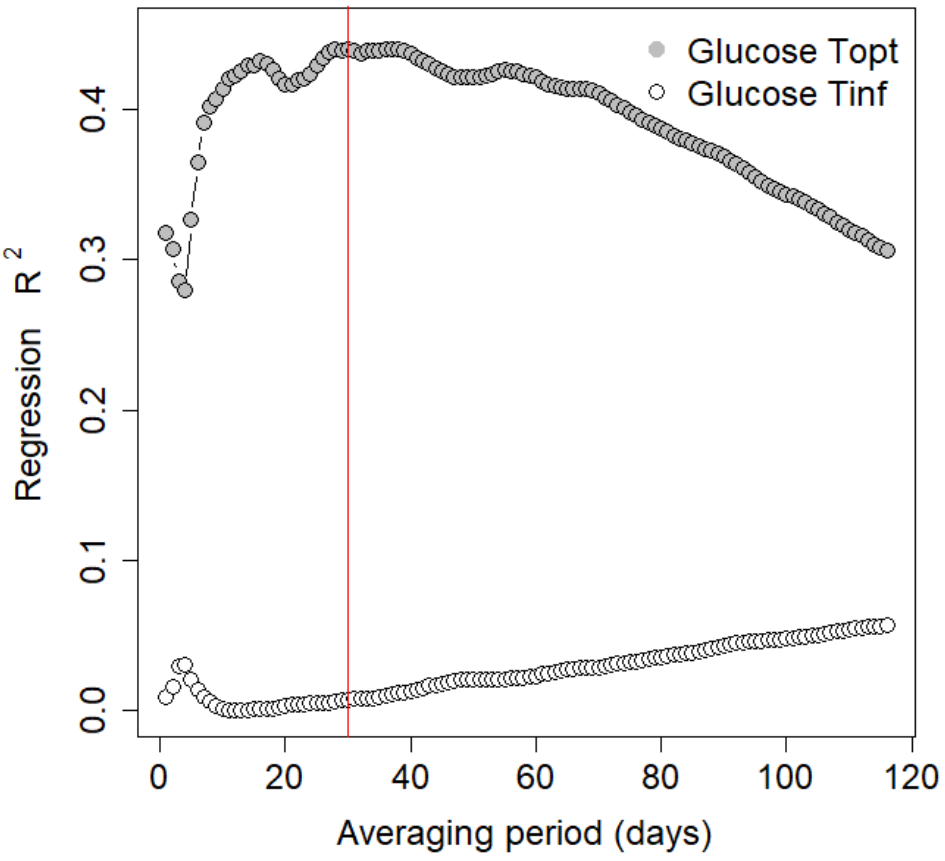

Figure 5.8 R^2 values for each regression fit between glucose T_{inf}/T_{opt} and environmental temperature over each averaging period of temperature (days). Analysis was completed using the glucose T_{opt} and T_{inf} values from the 20 glucose experiments. Temperature for the averaging periods extrapolated from the long-term iButton data. The red vertical line shows the 30-day averaging period.

The curve fits for SOM-R_S and Glucose-R_S can be found in Appendix C, here, the relationship between T_{opt} and T_{inf} with environmental temperature is the focus (e.g. **Figure 5.9**). There was little evidence for a relationship between T_{opt} of SOM-R_S with environmental temperature (R^2 = 0.021; **Figure 5.9**). The slope of the trendline was 0.068 ^oC increase in T_{opt} per ^oC increase in environmental temperature (units ^oC $^oC^{-1}$; Standard error (SE) ± 0.108; n = 20) and was non-significant (*P* = 0.539). The T_{opt} values for SOM-R_S were 48.0 ^oC on average (SEM ± 0.607; n = 20).

The Glucose-R_S T_{opt} values showed a moderately positive relationship with increasing temperature (R^2 = 0.446). The slope of the trendline was 0.157 ^oC $^oC^{-1}$ (SE ± 0.041; n = 20) and was significant with a p-value of 0.001. The average T_{opt} value for Glucose-R_S was 34.5 ^oC (SEM ± 0.304; n = 20) and was ~13.5 ^oC less than the average T_{opt} value for SOM-R_S.

The range of glucose T_{opt} values calculated here was 32.2-37.5 ^oC (**Figure 5.9**). For comparison, the Glucose-R_S T_{opt} values from Numa *et al.* (2021), who used the same method, ranged from 32.4-39.2 ^oC. In Numa *et al.* (2021) the average environmental temperatures at the field site were much lower at 9.5-13.8 ^oC than the average temperatures found here (18.0-36.5 ^oC). The t-test found that the average Glucose-R_S T_{opt} of this work (34.5 ^oC) was not significantly different (*P* = 0.320) from the mean Glucose-R_S T_{opt} found in Numa *et al.* (2021) (35.1 ^oC).

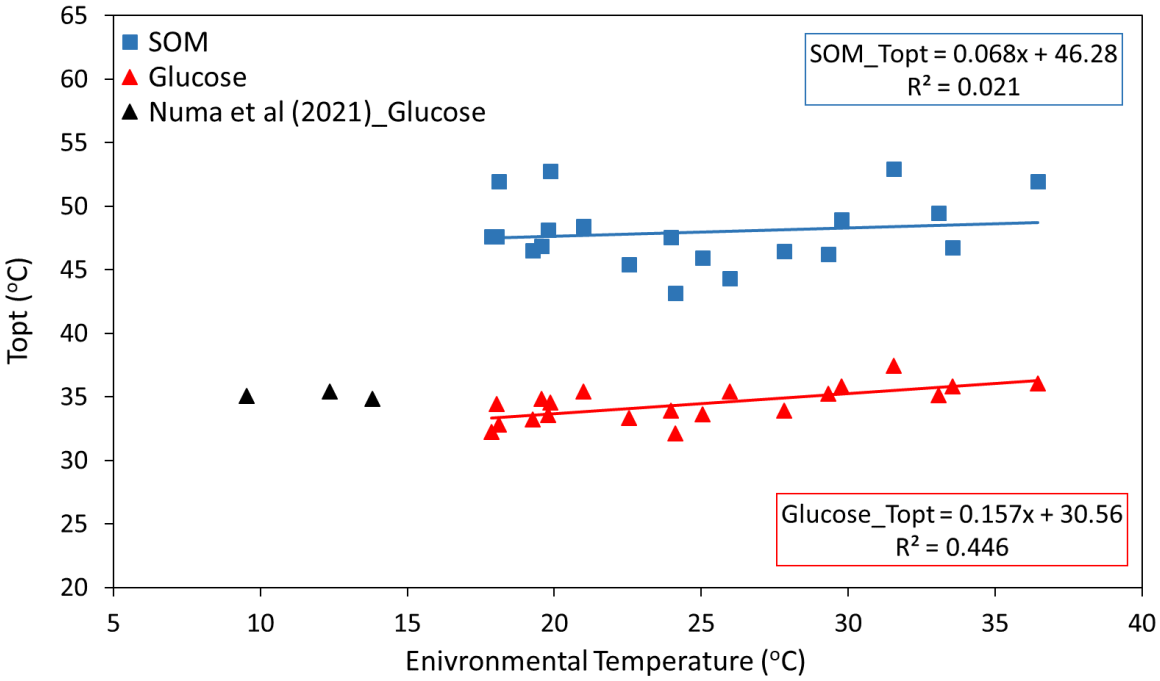

Figure 5.9 The T_{opt} values plotted against environmental temperature (°C) for SOM and glucose respiration for the 20 labile C runs completed (n=20 for each). Note axes do not start at zero. The environmental temperature used was the 30-day averaging period temperature prior to the day of sampling. The glucose data in black was taken from Numa *et al.* (2021) and environmental temperature for these values were averaged over 30 days from DairyNZ soil temperature data for Scott Farm NZ, prior to the day of sampling (DairyNZ, 2021).

The SOM-R_S T_{inf} values with environmental temperature showed a weak positive relationship with an R^2 value of 0.223 (**Figure 5.10**). The slope of the trendline was 0.183 °C °C^{-1} (SE ± 0.08; n = 20) and was marginally significant (*P* = 0.035). The average T_{inf} value for SOM-R_S was 25.2 °C (SEM ± 0.505; n = 20).

There was little evidence of a relationship between the T_{inf} values of Glucose-R_S with environmental temperature (R^2 = 0.005). The slope of the trendline was -0.032 °C °C^{-1} (SE ± 0.102; n = 20) and was non-significant (*P* = 0.758). The T_{inf} values for Glucose-R_S were 14.9 °C on average (SEM ± 0.562; n = 20) and were about 10.2 °C lower on than the average T_{inf} value for SOM-R_S. The MMRT 1.5 output parameters for SOM and glucose respiration are presented in Appendix F.

The T_{inf} values from here ranged between 11.6-20.1 °C and were on the lower end of the range observed in Numa *et al.* (2021) (17.3-21.0 °C). The T_{inf} values from Numa *et al.* (2021) tended to sit between the T_{inf} values found for SOM-R_S and Glucose-R_S measured in this work (**Figure 5.10**). The Glucose-R_S T_{inf} average in this work (14.9 °C) was significantly different (*P* = <0.001) from the average found in Numa *et al.* (2021) (19.2 °C).

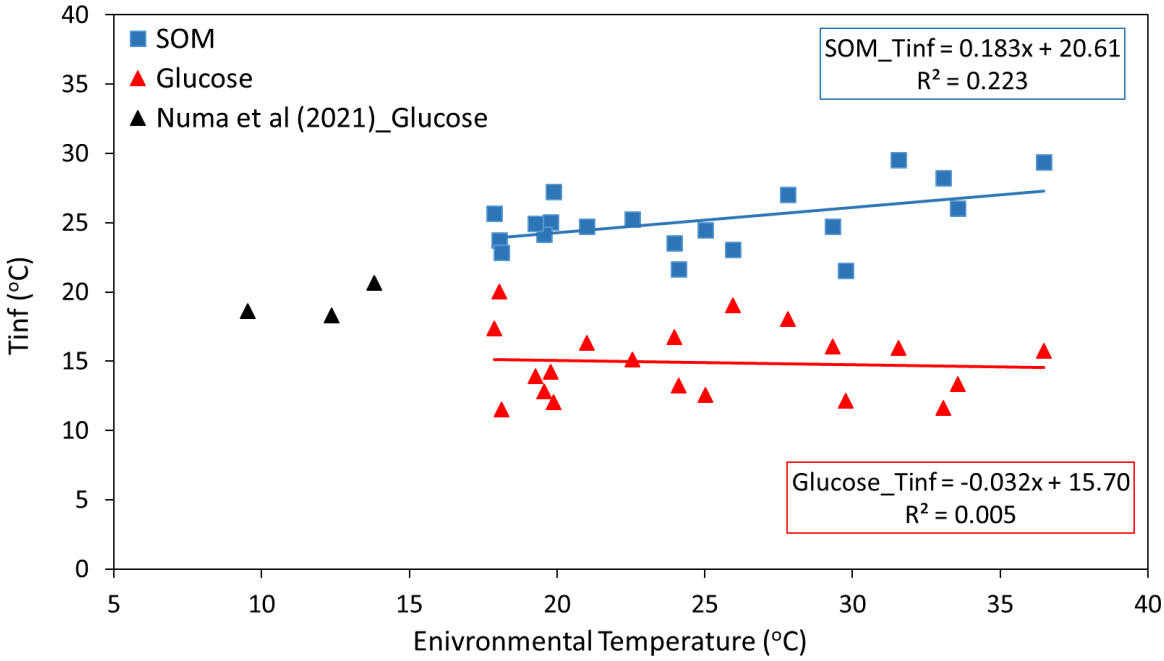

Figure 5.10 The T_{inf} values plotted against environmental temperature (°C) for SOM and glucose respiration for the 20 labile C runs completed (n=20 for each). Note x-axis does not start at zero. The environmental temperature used was the 30-day averaging period temperature prior to the day of sampling. The glucose data in black was taken from Numa *et al.* (2021) and environmental temperature for these values were averaged over 30 days from DairyNZ soil temperature data for Scott Farm NZ, prior to the day of sampling (DairyNZ, 2021).

5.4.3 Labile C experiment - Yeast extract

The yeast extract runs followed similar trends to the glucose data with similar curve shapes and T_{opt} values (**Figure 5.11**; **Table 5.1**). The average T_{opt} of the Yeast Extract-R_S was 34.2 °C (SEM ± 1.02; n = 3). This was only 0.30 °C less than the T_{opt} average for Glucose-R_S (34.5 °C) and was not significantly different (P = 0.766). The average T_{inf} of the Yeast Extract-R_S was 15.3 °C (SEM ± 2.45; n = 3) which was 0.40 °C less than the T_{inf} average for Glucose-R_S (14.9 °C). This difference between means was also not statistically significant (P = 0.818).

The yeast SOM-R_S had an average T_{opt} of 47.2 °C (SEM ± 1.66; n = 3) and an average T_{inf} of 22.8 °C (SEM ± 2.21; n = 3). The SOM-R_S T_{opt} value had a 0.8 °C difference from the average glucose SOM-R_S T_{opt} (48.0 °C) but this difference was not statistically significant (P = 0.658). SOM-R_S T_{inf} had a 2.4 °C difference from the average glucose SOM-R_S T_{inf} value (25.2 °C) but was also non-significant (P = 0.137).

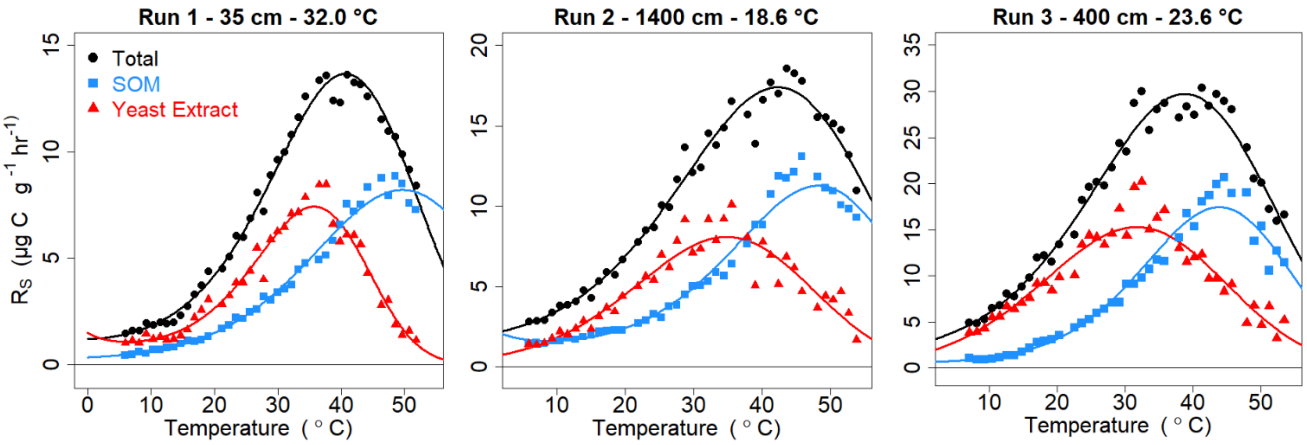

Figure 5.11 The Total, SOM and Yeast Extract respiration (µg C g^{-1} hr^{-1}) at different incubation temperatures (°C) after five hours of incubating for the three yeast extract experiments completed (n=3). Sampled at different distances along the temperature gradient which are noted above the graph along with the average environmental temperature.

Table 5.1 Yeast Extract-R_S, Total-R_S and SOM-R_S MMRT 1.5 parameters from the three yeast extract runs completed. The environmental temperature (30 day average) was 32.0 °C, 18.6 °C and 23.6 °C for 35 cm, 1400 cm and 400 cm, respectively. The number given (1-3) was the run order (n=3).

Sample Rs type	Distance (cm)	Topt (°C)	Tinf (°C)	A	B	$\Delta H^{\ddagger}_{T_0}$ (J mol^{-1} K^{-1})	$\Delta S^{\ddagger}_{T_0}$ (J mol^{-1} K^{-1})
Yeast 1	35	35.8	20.2	-221	-9718	-3718	-241
Yeast 2	1400	34.5	12.9	-104	-6544	-11566	-265
Yeast 3	400	32.3	12.8	-110	-7046	-25629	-305
Total 1	35	40.8	19.2	-106	-4787	24591	-106
Total 2	1400	42.4	16.8	-59.2	-2994	20511	-59.2
Total 3	400	38.7	12.0	-64.1	-4097	9654	-64.1
SOM 1	35	49.2	21.5	-66.2	-2394	46759	-66.2
SOM 2	1400	48.5	27.1	-91.7	-2035	45089	-91.7
SOM 3	400	43.9	19.8	-107	-4522	44138	-107

5.4.4 Priming experiment

For all three priming runs completed, the respiration magnitudes varied, however, the shape of the curves were very similar (**Figure 5.12**). The Priming-R_S for each of the three runs was relatively small, compared to the SOM and ^{13}C glucose respiration, and became negative at ~ 40 ^oC incubation temperature. The T_{opt} for the Priming-R_S was variable ranging between 27.6 and 48.5 ^oC (**Table 5.2**). The third priming run (20 cm) Priming-R_S results were highly variable and did not show a clear response. The average T_{opt} with the addition of priming run 3 was 35.5 ^oC, however, this produced a large standard error of ± 6.55 (n = 3). This large standard error likely demonstrates the difficulty of this technique in obtaining precise curves. The average T_{opt} for Priming-R_S without priming run 3 was 29.0 ^oC (SEM ± 1.14; n = 2). This average was 9.1 ^oC lower than the T_{opt} average found for the ^{13}C-Glucose-R_S (38.1 ^oC; SEM ± 1.31; n = 3).

The average T_{inf} for Priming-R_S including priming run 3, was 18.2 ^oC with a large standard error of ± 5.97 (n = 3). In contrast, the average T_{inf} for Priming-R_S not including priming run 3, was 12.3 ^oC (SEM ± 0.245; n = 2). This T_{inf} value had a 1.55 ^oC difference from the average T_{inf} found for the ^{13}C-Glucose-R_S (13.8 ^oC; SEM ± 2.46; n = 3). This result agrees more closely with the findings of the other incubation experiments. The average T_{opt} and T_{inf} values for SOM-R_S for all the runs were 47.9 ^oC (SEM ± 1.47; n = 3) and 26.4 ^oC (SEM ± 1.47; n = 3), respectively.

The average contribution of SOM, glucose and priming decomposition to total respiration rates was 36 %, 52 % and 12 %, respectfully (**Figure 5.13**). At lower temperatures, SOM contributed more to the respiration rates but above 10 ^oC the labile glucose contributed more. The graph (**Figure 5.13**) shows the upturn of SOM contribution and the declining contribution of ^{13}C-Glucose-R_S as the incubation temperature raised past the average T_{opt} of ^{13}C-Glucose-R_S. The highest contribution percentage for SOM was reached at 53 ^oC at 80.7 % contribution.

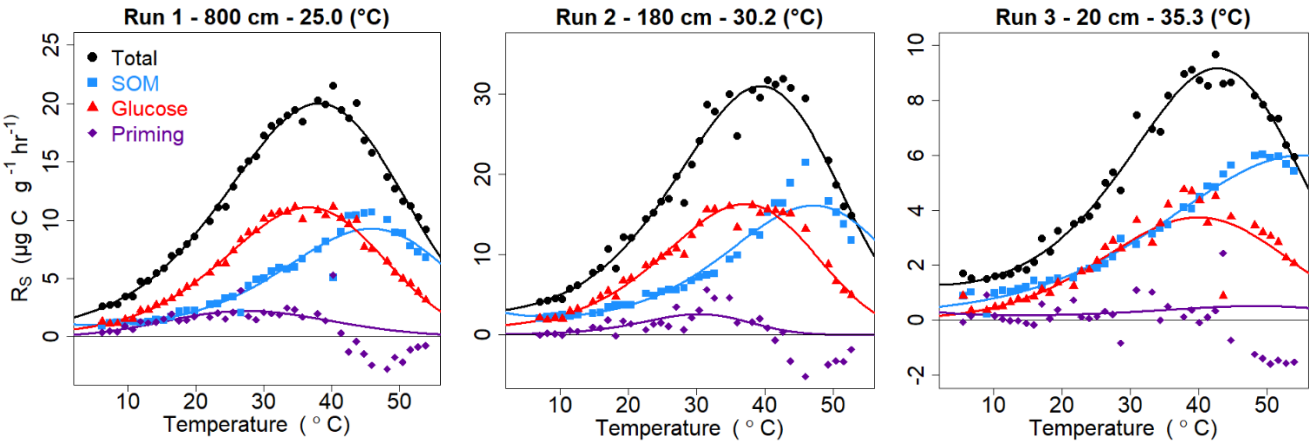

Figure 5.12 The Total, SOM, ^{13}C Glucose and Priming respiration (µg C g^{-1} hr^{-1}) at different incubation temperatures (ºC) after five hours of incubating for the three priming experiments completed (n=3). Sampled at different distances along the temperature gradient which are noted above the graph along with the average environmental temperature.

Table 5.2 ^{13}C glucose-R_S, Total-R_S, SOM-R_S and Priming-R_S MMRT 1.5 parameters from the three priming runs completed. The number given (1-3) was the run order (n=3). The environmental temperature (30 day average) was 25.0 ºC, 30.2 ºC and 35.3 ºC for 800 cm, 180 cm and 20 cm, respectively.

Sample R_S type	Distance (cm)	T_{opt} (ºC)	T_{inf} (ºC)	A	B	$\Delta H^{\ddagger}_{T_0}$ (J mol^{-1} K^{-1})	$\Delta S^{\ddagger}_{T_0}$ (J mol^{-1} K^{-1})
^{13}C Glucose 1	800	36.5	9.4	-84.6	-6011	1006	-222
^{13}C Glucose 2	180	37.1	14.2	-105	-6184	4920	-206
^{13}C Glucose 3	20	40.7	17.9	-92.9	-4493	22409	-162
Total 1	800	38.4	12.6	-70.3	-4391	9057	-191
Total 2	180	39.5	17.0	-93.2	-4773	16248	-164
Total 3	20	42.8	22.5	-98.0	-3527	28833	-135
SOM 1	800	45.9	23.8	-91.4	-2900	40147	-99.2
SOM 2	180	47.1	26.5	-101	-2432	43881	-83.1
SOM 3	20	50.8	28.9	-72.2	-1211	39545	-106
Priming 1	800	27.6	12.0	-193	-13067	-90926	-536
Priming 2	180	30.4	12.6	-258	-16862	-83689	-510
Priming 3	20	48.5*	30.2*	-76.8*	-1076*	29480*	-158*

*Results potentially unreliable due to the large variation in the temperature response.

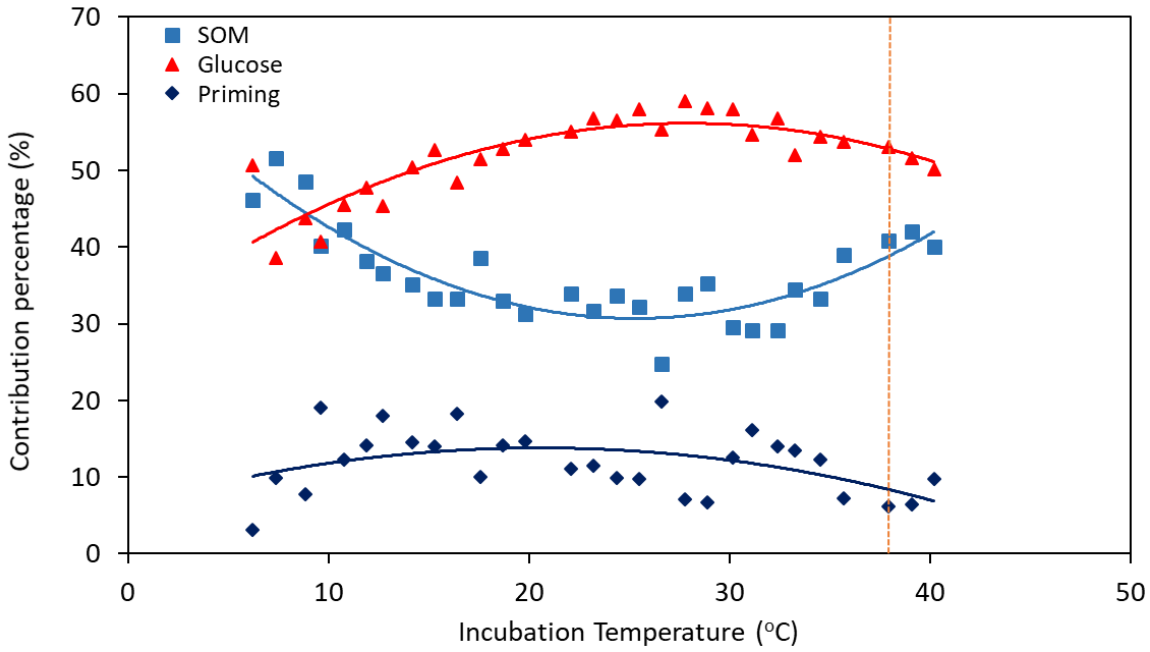

Figure 5.13 The contribution of priming, glucose and SOM to respiration (%) at different incubation temperatures (°C). The averages of all three priming runs were used to calculate these percentages. The fitted curves are polynomial trendlines. Data cut off at 40 °C due to negative values of priming above this temperature. The orange dotted line shows the ^{13}C-Glucose-R_S T_{opt}.

5.5 Discussion

5.5.1 Respiration rates from labile C and SOM

5.5.1.1 *Labile C*

The T_{opt} of labile C respiration increased slightly with increasing environmental temperature, suggesting potential thermal adaptation (**Figure 5.9**). The T_{opt} was estimated to have an average increase of 0.157 °C per °C increase in environmental temperature (°C °C^{-1}) (SE ± 0.041; n = 20). Additionally, even if the average was an underestimate of the true rate adding the SE resulted in an upper rate of 0.198 °C °C^{-1} (0.157 + 0.041).

Overall, our results suggest that respiration of labile C in soil may be relatively conserved with temperature increases, despite the significant correlation with environmental temperature. If applied to a projected global warming of 2.0 °C, the T_{opt} of labile C respiration would only increase by ~0.30 °C (see fuller discussion later in section 5.1.1.3). The range of T_{opt} values for labile C respiration was 32.2-37.5 °C and not significantly different from those reported by Numa *et al.* (2021) for glucose metabolism. Many organisms, including some microbes, humans and other endotherms have their T_{opt} at

~37 ^{o}C, likely due to homeostasis. Why microorganisms outside the human body (i.e. in soil) also have a T_{opt} in this small range is unknown, potentially by coincidence or some underlying biological limit. However, it is likely that other factors interacting with temperature also determine this T_{opt} range (Haaf *et al.*, 2021). Therefore, it is possible that this temperature range might be linked to protein or DNA sequences, as increasing temperatures can negatively affect DNA coding and protein structure (Zeldovich *et al.*, 2007). The T_{opt} of an organism could also be determined by substrate availability, substrate translocation rate within the cell or even oxygen availability (lack of, presence of) (Blackman, 1905). Water dynamics in the soil and interactions with temperature may also play a role in determining the temperature response of labile C respiration (Lellei-Kovács *et al.*, 2011). Oxidative stress may also occur in organisms as temperatures rise (>40 ^{o}C) and promote the formation of oxygen radicals (Watanabe *et al.*, 1997; Kashmiri, 2014; Olczyk *et al.*, 2016). Any of these factors could limit the temperature range of soil microorganisms, however, a full understanding of the reasons for this T_{opt} range was beyond the scope of this research.

Although the significant positive increase of T_{opt} with increasing environmental temperature was small, it suggests quite modest thermal adaptation. It is possible that changes in the microbial respiration of labile C could support the enzyme rigidity or optimum-driven hypotheses proposed by Alster *et al.* (2020). Enzyme rigidity is linked to the stability of enzymes at different temperatures, at higher temperatures enzyme rigidity increases. The enzyme rigidity hypothesis suggests that microorganisms increase their T_{opt} to warming environments based on these changes in enzyme rigidity. The optimum-driven hypothesis suggests that microorganisms adapt their T_{opt} to match the environmental temperature more closely. It is hard with the MMRT 1.5 model to assess and compare $\Delta C_P^{\ddagger}$ across the samples since in this model $\Delta C_P^{\ddagger}$ changes with temperature (unlike MMRT 1.0). Therefore, it is difficult to effectively link Alster *et al.* (2020) hypotheses, which makes predictions about both $\Delta C_P^{\ddagger}$ and T_{opt}. However, it is still possible that at least one of these two hypotheses could help explain the modest increase in T_{opt} with increasing temperature along the geothermal gradient.

The observed response of thermal adaptation was unlikely to be the result of substrate depletion, which is commonly proposed as a contributor to changes in observed responses (Hartley *et al.*, 2007; Bradford *et al.*, 2008; Walker *et al.*, 2018). In these cases, indirect warming effects, such as increased substrate depletion at warmer temperatures, can help to partly explain thermal adaptation to prolonged warming (Bradford, 2013). However,

here, the soil was flooded with glucose at ratios previously proven to prevent substrate depletion (Numa *et al.*, 2021), additionally, the incubation times were short (Numa, 2020; Numa *et al.*, 2021). However, some authors have argued that the distribution of glucose in the soil was an important factor affecting substrate availability (Knorr *et al.*, 2005). Here, the wetter soil samples sometimes formed clumps when mixed which may have affected substrate availability and distribution in the system. Although, the results suggest that there was no strong influence or limitation on labile C respiration for the different MCs and substrate quantity. The independence of respiration responses at different MCs suggests that the respiration responses observed were more likely related to other environmental factors or biological thermal adaptation (Alster *et al.*, 2016; Alster *et al.*, 2018). Future studies should look at the interacting factors with soil temperature to help explain the temperature response observed (Haaf *et al.*, 2021).

Changes in C content or elemental compositions along the gradient may have also influenced the observed changes in T_{opt}. Lower substrate availability and the presence of heavy metals can influence respiration rates (Laskowski *et al.*, 1994; Bradford *et al.*, 2008). The total C content varied along the length of the gradient, with typically lower total C % closer to the geothermal source and the highest total C % in the middle of the gradient. This varying C content along the geothermal gradient seemed to change the magnitude of respiration rates but not the overall shape of the temperature response curve (see Appendix C for examples). The geothermal gradient used in this study may have also differed in metal composition along its length. Highly mineralised waters found in geothermal areas can carry harmful heavy metals and trace elements (Given, 1980; Boothroyd, 2009) which could alter microbial activity. Future work should determine the elemental and ion compositions along the gradient to determine if there were any significant differences that could contribute to microbial responses. The determination of the biological communities along the gradient would also be valuable to understand if the community composition changes or remains the same along the gradient's length. This information would inform whether the same organisms were adapting to the warming environments or if specific thermophilic organisms were present closer to the geothermal source.

Thermal adaptation responses can also be dependent on the length of warming experienced, with short term and long term warming displaying different effects (Bradford *et al.*, 2008). Plots with sustained warming for long periods are more likely to produce results consistent with thermal adaptation (Bradford *et al.*, 2008; Bradford, 2013;

Carey *et al.*, 2016). The geothermal source in this study was at minimum ~ 17 years old (based on aerial photographs (Appendix A) and greenkeepers knowledge) and likely more than 40 years old. This is more than sufficient warming for soil microbial communities to adjust their metabolic rates and select for most competitive organisms. It was surprising to see such a small change along the gradient in both SOM-R_S and labile C respiration after many years of prolonged warming.

In contrast to the small changes in T_{opt}, the T_{inf} of labile C respiration expressed a negative but non-significant relationship with increasing environmental temperature ($P = 0.758$). The T_{inf} values calculated here were statistically lower ($P < 0.05$) than Numa *et al.* (2021) by about 4.3 ^{o}C on average. We hypothesised that the environmental temperature of soil was positively related to the T_{inf} measured (Prentice *et al.*, 2020), therefore, we expected to measure higher T_{inf} values than Numa *et al.* (2021) since the mean environmental temperatures were higher. Potentially, geothermal stress and soil properties influenced T_{inf} at an ecosystem scale resulting in a non-significant negative relationship between T_{inf} and environmental temperature. Alternatively, the T_{inf} hypothesis proposed by Prentice *et al.* (2020) for enzymes aligning with environmental temperature may not scalable be to an ecosystem response.

This research has assumed that the Glucose-R_S results for T_{opt} and T_{inf} were applicable for a wide range of labile C responses. This assumption was supported by the results of the yeast extract experiment, as the mean T_{opt} and T_{inf} values for yeast extract and glucose runs were not statistically different from one another. This suggests that the results here were likely applicable to responses of labile C for other geothermal areas, although this would need further research. The CO_2 production from yeast extract was lower in magnitude than most glucose runs suggesting glucose was a better labile C source for investigating soil respiration. The results of the yeast extract experiment overall supported the use of glucose as a reasonable proxy for labile C respiration (c.f. Numa *et al.* (2021)).

When combining the work presented here with results from Numa *et al.* (2021) the relationships between T_{opt} and T_{inf} with environmental temperature changed. The relationship between the T_{inf} of labile C respiration and environmental temperature steepened negatively although remained non-significant (slope $P = 0.063$; $R^2 = 0.155$). Whereas the relationship between the T_{opt} of labile C respiration and environmental temperature flattened, becoming non-significant (slope $P = 0.080$; $R^2 = 0.139$). Care with interpreting this result is needed because changes in slope could also be due to differences in the models used (MMRT 1.0 vs MMRT 1.5) for finding T_{inf} or T_{opt} or differences in

soil types (Numa *et al.* (2021) soil types: Horotiu, Te Rapa & Te Kowhai). The mean annual temperature (MAT) of the soil measured by Numa *et al.* (2021) was <14 ^{o}C. Lower environmental soil temperatures (MAT <18 ^{o}C) were underrepresented in this work. Future work including lower soil temperatures further from the geothermal source would be beneficial to capture a wider range of environmental temperatures.

5.5.1.2 ***SOM***

The temperature response of glucose represents the activity of microbes when they are not substrate limited, whereas SOM-R_S is derived from a complex of C sources. The T_{inf} of SOM-R_S showed a slight increase with increasing environmental temperature and this relationship was significant (**Figure 5.10**). The average change in SOM-R_S T_{inf} with increasing environmental temperature was 0.183 ^{o}C $^{o}C^{-1}$ (SE ± 0.08; n = 20). Additionally, adding the SE to the calculated average slope suggested a change no greater than 0.263 ^{o}C $^{o}C^{-1}$. Because this increase was small any changes would likely remain within the range of measured T_{inf} values (21.6-29.6 ^{o}C).

The T_{inf} of SOM-R_S was closer to the average environmental temperature than the T_{inf} of labile C respiration. It was expected that the T_{inf} of both processes would be around the environmental temperature of the corresponding sample site (Prentice *et al.*, 2020). However, it seems that only the T_{inf} of SOM-R_S was close to the average environmental temperature. Setting T_{inf} (the steepest change in reaction rate) to the environmental temperature allows organisms to maintain intrinsic homeostasis across a range of fluctuating environmental temperatures (Prentice *et al.*, 2020). Considering it is of evolutionary advantage to have the T_{inf} set to the environmental temperature, this result for SOM-R_S T_{inf} was not surprising.

However, it was interesting that the T_{inf} of SOM-R_S and the T_{opt} of labile C both changed with increasing environmental temperature, suggesting these two parameters might be linked. Potentially, together these T_{inf} and T_{opt} responses reflect the ecosystem temperature response as a whole and that both have thermally adapted to warmer temperatures along the gradient. However, this potential linkage between the two parameters could be related to many environmental or genetic factors (Alster *et al.*, 2016; Alster *et al.*, 2018). If these results are related the relationship would be of some evolutionally adaptive advantage to warming environments (Bradford *et al.*, 2019).

In contrast to the changes in SOM-R_S T_{inf}, the T_{opt} of SOM-R_S had a positive but non-significant relationship with increasing environmental temperature (P = 0.539). The results suggested that the T_{opt} of SOM-R_S did not change with increasing temperatures. It was expected that the T_{opt} of SOM-R_S may have adapted to warming temperatures following the optimum-driven hypothesis (Alster *et al.*, 2020). Potentially the thermal adaptation of SOM-R_S T_{opt} was not detectable at ecosystem scales or potentially the response was highly dependent on other factors such as availability of SOM for decomposition (**Figure 5.14**).

It is worth noting that in this work T_{opt} and T_{inf} values were obtained for SOM-R_S, in contrast to other studies that were unable to fit MMRT to SOM-R_S (e.g. Numa *et al.* (2021), Robinson *et al.* (2020)). These studies also found that SOM-R_S showed a generally Arrhenius-like response (exponential) with increasing temperature which they suggested was due to the dominance of chemical-physical processes controlling substrate supply to microbes in the soil (**Figure 5.14**) (Robinson *et al.*, 2020). Unlike these studies, the SOM temperature response here displayed a clear MMRT response (e.g. **Figure 5.11** & **Figure 5.12**). The T_{opt} and T_{inf} values obtained for SOM-R_S were similar to those measured for enzymes (Arcus *et al.*, 2016; Prentice *et al.*, 2020). This suggested that potentially the soil along this geothermal gradient was more biologically active than the soil used in the other studies. This higher activity could be due to the higher temperatures at the site, the presence of more labile C or a wider range of nutrients provided by the geothermal activity (Boothroyd, 2009).

Methodological limitations of these previous studies may also have precluded identifying T_{opt} and T_{inf}. Numa *et al.* (2021) was unable to measure an MMRT response when utilising 18 different incubation temperatures. Using only 18 temperatures likely limited the ability to determine the curvature of the SOM-R_S response (Robinson *et al.*, 2017). Related studies by Numa (2020) using >25 different temperatures also found no MMRT response with increasing temperature. However, the maximum incubation in these studies was 40 ^oC which was below the T_{opt} range calculated here (range 43.2-53.0 ^oC), making it difficult to fit the MMRT curve (**Figure 5.14**). A study by Robinson *et al.* (2017) used 40 different incubation temperatures (~2.0-50.0 ^oC) and measured an Arrhenius SOM-R_S response with higher T_{opt} values than found here (60-81 ^oC). These high T_{opt} values could be a result of higher SOM temperature sensitivity in that soil (Davidson & Janssens, 2006; Robinson *et al.*, 2020). However, it would be expected that geothermal areas would have

higher T_{opt} values for SOM-R_S than areas of more temperate soil temperatures, following the optimum-driven hypothesis (Alster *et al.*, 2020).

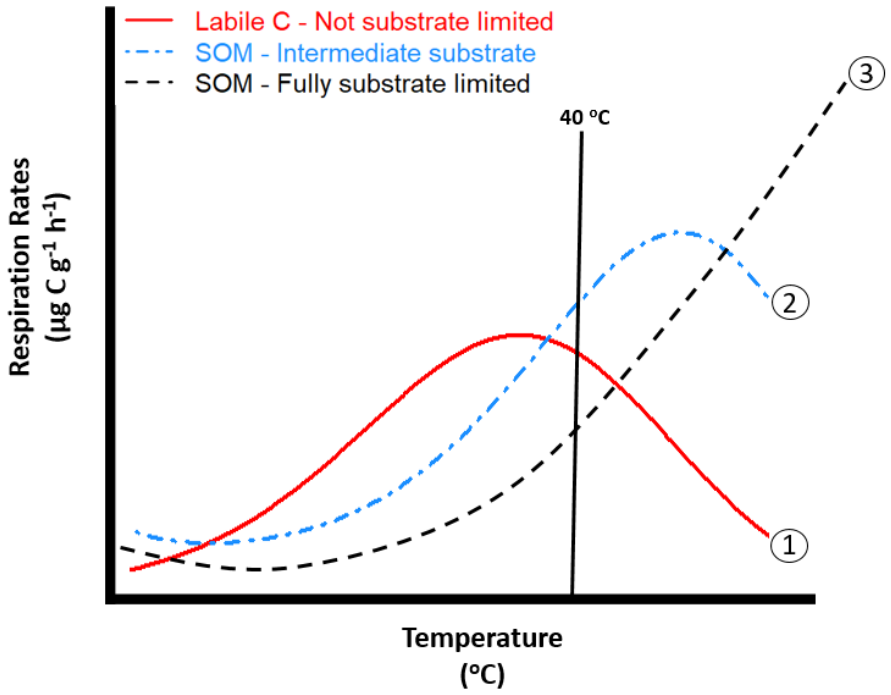

Figure 5.14 A schematic diagram illustrating the likely temperature response curves produced with varying substrate availability. The graph illustrates respiration rates (µg C g^{-1} h^{-1}) with temperature (°C) for three curves, 1) Labile C – the addition of labile substrate to soil (e.g. glucose; red), 2) SOM – at intermediate substrate availability (blue) and 3) SOM – with full substrate limitation (black; physical-chemical dominated). The black vertical line identifies 40 °C and demonstrates that if respiration rates are not measured >40 °C it can be difficult to correctly distinguish curves 2 and 3.

The results from here and from previous studies suggest that differences in ecosystem properties or incubation method play a part in the temperature response of SOM-R_S, particularly determining T_{opt} and T_{inf}. However, the model type used (MMRT 1.0 or MMRT 1.5) may also play a part in these discrepancies. The studies mentioned previously were unable to adequately fit an MMRT response for SOM-R_S with increasing temperature when using MMRT 1.0. Here, the MMRT 1.5 model visually fitted the data better and produced reasonable T_{opt} and T_{inf} values that were in visual agreement with the fitted curve and raw data. When the MMRT 1.0 model was used, the result was similar to those values determined by Robinson *et al.* (2017). Numa *et al.* (2021) and Robinson *et al.* (2020) could not find any T_{opt} or T_{inf} values for SOM-R_S suggesting that MMRT 1.0 is not always able to accurately model the response of SOM-R_S with temperature.

However, if the temperature response for the SOM-R_S in these soils is chemically or physically based (truly Arrhenius) then this inability to model the response would make sense since MMRT was not designed to model these processes (Hobbs *et al.*, 2013). Possibly, the new assumptions of the MMRT 1.5 model (i.e. that $\Delta C_P^{\ddagger}$ changes with temperature) may just be better at finding SOM-R_S parameter values than MMRT 1.0. The SOM-R_S responses Arrhenius-like curve response may be true for some soils (e.g. Horotiu, Te Rapa, Te Kowhai soils used in Numa *et al.* (2021) & Robinson *et al.* (2017)) but here for a geothermal soil, the response of SOM-R_S was MMRT-like with distinct T_{opt} and T_{inf} values (**Figure 5.15**).

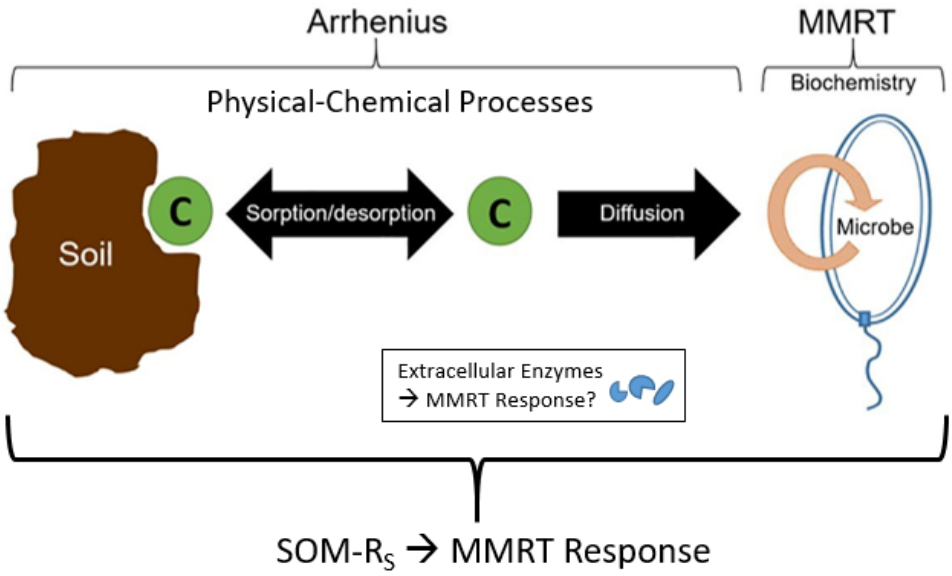

Figure 5.15 A schematic diagram of the processes occurring in soil. Microbial communities show an MMRT response, whereas physical-chemical processes show an Arrhenius response. In combination, the dominating mechanism in the soil is the response observed by SOM-R_S. In most cases, it would be expected for SOM-R_S to show an MMRT response. Adapted from Numa *et al.* (2021).

5.5.1.3 *Implications for responses to climate change*

It is important to note that although the relationship of environmental temperature with labile C respiration T_{opt} and SOM-R_S T_{inf} were statistically significant ($P < 0.05$), the extent of change in both T_{opt} and T_{inf} was small. Here, the potential response of microbial respiration with climate change predictions will be discussed based on data collected along the geothermal gradient. This section will briefly discuss a scenario where the average global temperature increases by 4.8 ^{o}C, an extreme warming scenario predicted by the 2014 IPCC highest emission pathway (RCP8.5; 2.6-4.8 ^{o}C (Friedlingstein *et al.*, 2014; Abramoff *et al.*, 2019)).

With a 4.8 ^{o}C warming of environmental temperature, the average change in labile C respiration T_{opt} would be 0.754 ^{o}C $^{o}C^{-1}$ (SE ± 0.197; n = 20). Including the ±SE, this change would be no smaller than 0.557 ^{o}C (–SE) and no larger than 0.951 ^{o}C (+SE). These temperature increases are small in terms of potential global temperature changes, however, with large soil C pools, any sized change could be important. Although, considering the range of glucose T_{opt} values was between 32.2-37.5 ^{o}C it is likely that this change would remain within this small biological range. It seems that this range of T_{opt} values was highly conserved at a range of environmental temperatures, at least at our study site. This narrow biological range is illustrated in **Figure 5.16** which shows the MMRT 1.5 temperature response of three different environmental temperatures. Each curve was scaled by the total C% of the soil in an attempt to partially reduce the between-site supply of substrate to microbes. Here, we were less concerned with the magnitude of the response and more so the shape of the temperature response itself. Future work should investigate the magnitude of these responses and their interactions with C content. The graphs show visually how small the actual difference of the T_{opt} values are for the environmental temperatures more than 10 ^{o}C apart (**Figure 5.16**).

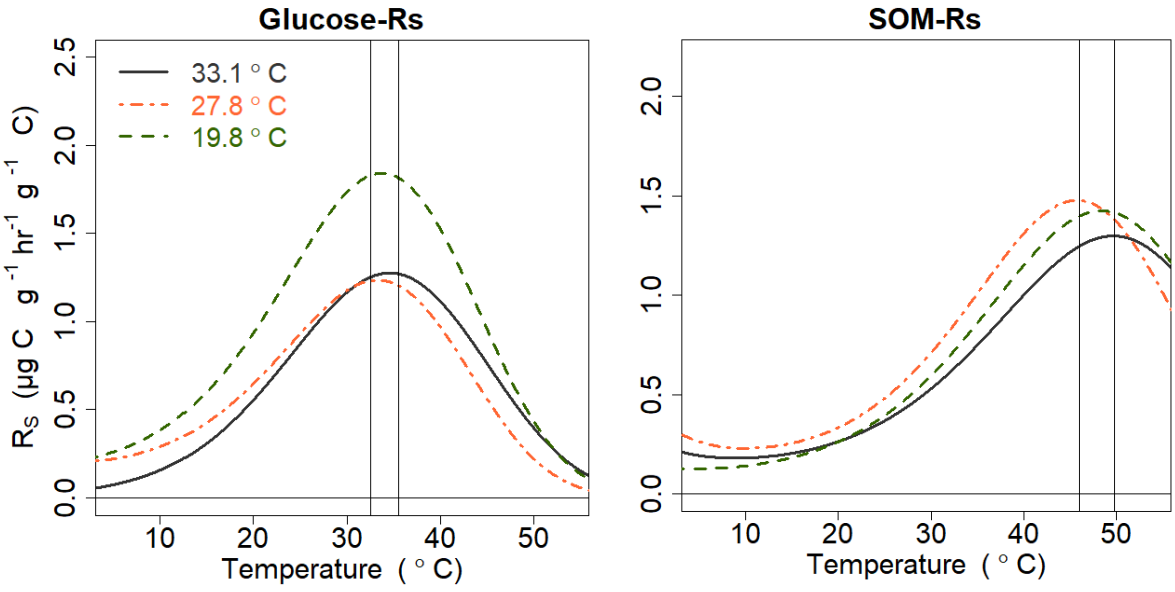

Figure 5.16 The SOM and Glucose respiration rates (µg C g^{-1} hr^{-1} g^{-1} C) with incubation temperature (^{o}C) from three distances, 25 cm, 150 cm and 1505 cm, along the geothermal gradient. These distances were at three different environmental temperatures, 33.1 ^{o}C, 27.8 ^{o}C and 19.8 ^{o}C, respectfully. The vertical lines identify the T_{opt} ranges on the Glucose graph between 32.5-35.5 ^{o}C and on the SOM graph between 46.0-49.8 ^{o}C. Each curve was scaled by the total C content (%) at the corresponding distance.

When applying the same climate change extreme of 4.8 ^{o}C average global temperature increase, we predict very small changes in the T_{inf} of SOM-R_S. The average change in

SOM-R_S T_{inf} with environmental temperature would be 0.878 ^oC $^oC^{-1}$ (SE ± 0.384; n = 20). Applying the ±SE to this increase in T_{inf} would result in a change no smaller than 0.494 ^oC (I–SE) and no larger than 1.26 ^oC (+SE). Again, this range is small and suggests that the changes are relatively conserved even when assuming extreme global warming (**Figure 5.17**). The changes in T_{inf} may even remain within the large range of values calculated here (21.6-29.6 ^oC).

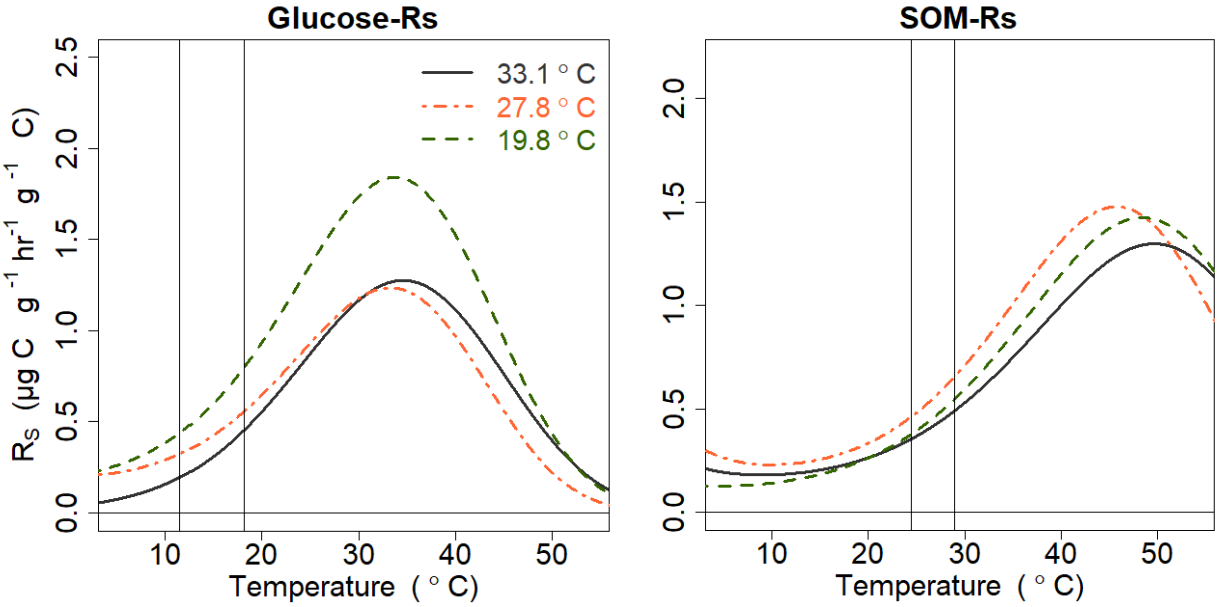

Figure 5.17 The SOM and Glucose respiration rates (µg C g^{-1} hr^{-1} g^{-1} C) with incubation temperature (^oC) from three distances, 25 cm, 150 cm and 1505 cm, along the geothermal gradient. These distances were at three different environmental temperatures, 33.1 ^oC, 27.8 ^oC and 19.8 ^oC, respectfully. The vertical lines identifying the T_{inf} range on the Glucose graph between 11.5-18.2 ^oC and on the SOM graph between 24.5-29 ^oC. Each curve was scaled by the C content (%) at the corresponding distance.

If T_{opt} of labile C respiration and the T_{inf} of SOM-R_S do adapt to global warming then soil feedback loops may be dampened in response to climate change (Luo *et al.*, 2001). However, despite the need for further work, it is clear that the temperature response of microbial respiration utilising labile C or SOM does not change dramatically with soil warming. These very small changes may mean that thermal adaptation does not occur or is quite modest in response to global warming. However, the lack of change in temperature response shape does not equate to the changes potentially observed in the overall magnitude of the respiration rate. If thermal adaptation does not occur in response to global warming, then stricter mitigation strategies may be needed to offset positive soil feedbacks. These results are useful because they give insight into the response of soil microorganisms to warming temperature. Ultimately, if thermal adaptation does occur, it

appears to be minimal, and this may mean that feedback loops to climate change may not be buffered.

These conclusions need further research to gain more knowledge around how these changes scale to whole ecosystems. It is important to note that some studies find spatial gradients insufficient to study the temperature sensitivity of SOM in response to climate change (Abramoff *et al.*, 2019), however, most of these studies have not looked at geothermal gradients. Geothermal gradients do have their downfalls, but also possess many advantages over other types of spatial gradients (O'Gorman *et al.*, 2014; Sigurdsson *et al.*, 2016). Future work comparing a range of spatial gradient results would be beneficial to document some of these potential discrepancies, along with national scale surveys where climate (particularly soil temperature) naturally varies.

It is important to note that here, only the effect of temperature on microbial responses was measured. The environmental effects produced by climate change (e.g. increased rainfall or longer dry periods) may interact with one another and may alter these findings. Future work should look at these interacting factors in more depth (Haaf *et al.*, 2021). It is also important to note that the rises in global atmospheric temperature may not reflect equally in soil environments. If the air temperature rises by 4.8 ^{o}C globally on average, the soil temperature may not necessarily reflect these changes.

5.5.2 Priming experiment

The temperature response of priming appeared to follow an MMRT response curve. The temperature response of soil priming following MMRT was expected because it is a biologically driven process (Kuzyakov *et al.*, 2000; Bastida *et al.*, 2013; Numa, 2020). Nevertheless, the complexity of the measurement approach meant that variability was high and the MMRT fits were not always strong. The first two priming runs were better fitted by MMRT than the final priming run (20 cm). The Priming-R_S results measured here (average without run 3: T_{inf} = 12.3 ^{o}C, T_{opt} = 29.0 ^{o}C) were similar to that measured by Numa (2020), who measured Priming-R_S with an average T_{inf} of 14.5 ^{o}C and a T_{opt} average of 30 ^{o}C. These values align well, suggesting that the Priming-R_S temperature response may be similar across a range of environmental temperatures. The priming response was similar to that of labile C respiration from both the ^{13}C experiments and the labile C experiments. This was also unsurprising considering soil priming is induced by labile C additions, meaning the same organisms are likely to be involved. The first two

priming runs that worked had T_{inf} values within the range of T_{inf} values found for Glucose-R_S in the labile C experiments (11.6-20.1 ^oC). The T_{opt} values were slightly lower than the range found for the Glucose-R_S T_{opt} values (32.2-37.5 ^oC).

Priming run three had higher than expected variability that may have been due to technical issues, as not long after this run the machine needed a part replaced. Conversely, the position of the sample (20 cm from the geothermal source) along the geothermal gradient may have also affected its ability to produce PEs. For example, the sample closer to the geothermal source had lower soil total C% compared to the other two runs and soils with lower C contents often have lower PEs (Sun *et al.*, 2019). Another possible reason related to the spatial distribution of the samples is the potential for higher concentrations of metals and trace elements (e.g. titanium, arsenic) closer to the geothermal source (Given, 1980; Boothroyd, 2009). These metals/trace elements have the potential to negatively impact the ability of the microbes to produce $^{13}CO_2$ as they can be toxic (Nwachukwu & Pulford, 2011). Although, the composition of these metals still needs to be determined along the gradient. The magnitude of the CO_2 fluxes from the third priming run was much lower than the other two runs which may also have made it harder to capture the priming response. The other responses for SOM, ^{13}C-Glucose and Total were consistent throughout the three runs and so it is possible that the response of priming was close to the lower detection limit of the machine. This low output may have made it hard to accurately measure the PE temperature response.

The average contribution of SOM, glucose and priming decomposition to respiration rates were 36 %, 52 % and 12 %, respectfully (**Figure 5.13**). This contribution of priming to respiration was much lower than found for Horotiu soil by Numa (2020) who measured a 30 % average contribution from priming. This soil likely had lower PEs due to the different composition of the soil, such as a lower pH which has been found to produce negative priming effects (Zhang *et al.*, 2019). The different structures of the soil and variable moisture contents may have also contributed to variation in observed priming (Kuzyakov, 2010; Sun *et al.*, 2019). These results suggest that soil within the same climatic zone can have different priming responses. This suggestion is supported by Bastida *et al.* (2019), who showed that the priming response was highly dependent on the nutrient and moisture contents of the soil. The Priming-R_S contribution here was much lower than the range found in a meta-analysis completed by Sun *et al.* (2019) (26.2-60.9 %). However, our findings agree with a meta-analysis by Luo *et al.* (2015) who showed average PEs of 14.2 % with a range of 9.9-31.2 % across ecosystems. Low PE

contributions measured here could also be due to the amount of ^{13}C added or the glucose solution used, as the quantity and quality of substrate can influence how it is utilised and the PEs produced (Kuzyakov *et al.*, 2000; Kuzyakov, 2010; Sun *et al.*, 2019).

Here, negative Priming-R_S values were observed above 40 ^oC incubation temperature for all three runs completed. Potentially, above 40 ^oC the lower detection limits of the machine were met in terms of $\delta\,^{13}C$. It is also possible that above 40 ^oC the temperature response changes as the system collapses or active microbial communities shift. Since the Priming-R_S decline occurred after the T_{opt}, the decline could be due to enzyme or organism failure (Hobbs *et al.*, 2013; Arcus *et al.*, 2016). Many priming studies have not measured the temperature response of priming over a wide range of temperatures or at higher temperatures (>40 ^oC). However, from the few studies that have, PEs decreased with increasing incubation temperature, which may be due to N immobilisation or the natural increase in SOM decomposition at higher temperatures (Thiessen *et al.*, 2013; Wang *et al.*, 2016; Sun *et al.*, 2019). These potential reasons may be why negative priming values were observed after 40 ^oC. A negative relationship between temperature and the degree of priming may partly compensate for the acceleration of soil C decomposition due to climate change (Sun *et al.*, 2019).

Soil priming can be 'apparent', where there is an acceleration of microbial metabolism and biomass turnover in response to an added substrate, or 'real', where the microbial activity enhances the decomposition of SOM in response to an added substrate (Blagodatskaya & Kuzyakov, 2008). Apparent priming occurs shortly after the addition of available substrates (hours to days), whereas real priming may start weeks to months after addition (Blagodatskaya & Kuzyakov, 2008; Kuzyakov, 2010; Luo *et al.*, 2016; Bastida *et al.*, 2019). Here, it is likely that the apparent priming was measured since the incubation time was only five hours. In future studies, it would be valuable to see if the same response was seen over a few days to months to get at the 'real' priming response. In the priming mechanism sequence proposed by Blagodatskaya and Kuzyakov (2008), it is likely that here, the triggering effect, pool substitution and preferential substrate utilization occurred in the soil. These mechanisms happen early in the sequence and are linked to apparent priming (Blagodatskaya & Kuzyakov, 2008). It seems as though positive apparent priming occurred in this system, suggesting either pool substitution or the triggering effect (both produce positive PEs) were occurring (Blagodatskaya & Kuzyakov, 2008). Preferential substrate utilization (negative PEs) may have occurred above 40 ^oC and may be the cause of negative respiration output values observed

(Blagodatskaya & Kuzyakov, 2008). However, it is also possible that the experiment was such a short incubation time that the response captured was only one of many responses occurring. The negative respiration response observed may be indicative of the switch between priming mechanisms occurring in the soil (Blagodatskaya & Kuzyakov, 2008).

5.5.2.1 *Priming implications for climate change*

Soil PEs are important because they may be incredibly sensitive to climate change (Ghee *et al.*, 2013). Only recently has the importance of soil PEs been identified in the modelling of potential feedback loops (Ghee *et al.*, 2013; Luo *et al.*, 2016). Here, if the negative relationship between PEs and higher temperatures is accurate then it may partly compensate for the acceleration of soil C decomposition due to climate change (Sun *et al.*, 2019). However, rising temperatures and higher atmospheric CO_2 concentrations are likely to increase plant productivity (Scurlock & Hall, 1998). Therefore, there is more likely to be higher plant inputs into soil and alterations to the microbial community structure (Ghee *et al.*, 2013; Zhang *et al.*, 2019). Both of these factors influence soil PEs and both have the potential to accelerate feedback loops to climate change (Ghee *et al.*, 2013). Overall, the response of SOM decomposition to climate change is partially dependent on the temperature response of PEs with warming temperature (Wang *et al.*, 2016). Therefore, to make better predictions and to develop mitigation strategies more research is required in this space (Luo *et al.*, 2016).

5.6 Conclusion

The results of the labile C experiments showed that the T_{inf} of labile C respiration and the T_{opt} of SOM-R_S were conserved with increasing environmental temperature. The results also showed that the T_{opt} of labile C respiration and the T_{inf} of SOM-R_S increased with increasing environmental temperature but only at average rates of 0.157 ^oC $^oC^{-1}$ and 0.183 ^oC $^oC^{-1}$, respectively. These results suggested minimal thermal adaptation in response to soil warming with climate change. This outcome might be considered beneficial as small thermal adaptation may partially offset the acceleratory feedback loops produced by global warming. However, the findings suggested that even with extreme increases in average global temperature, the changes to T_{opt} and T_{inf} values would be small. If that is the case, then for climate change this could mean that feedback loops may not be alleviated. Further research to determine how applicable these results are at a broader scale and how they can be considered with likely climate change impacts. In future studies, more sites, more soil types and more diverse climate ranges should be investigated. Further work is also required to understand why the T_{opt} of labile C respiration is relativity conserved in soil around 37 ^oC and what this means from an evolutionary standpoint.

The priming results showed that the temperature response of priming followed MMRT, which supports findings from other studies. The overall temperature response of priming was relatively conserved, however, the magnitude/contribution of priming to the total soil respiration changed dramatically with soil type and soil characteristics when compared with other studies. The results also suggested that the magnitude of priming decreased with rising temperatures and so may dampen feedbacks to climate change. Future studies should complete more priming runs to confirm these findings and to investigate further trends in the priming temperature responses. Improvements to the method used here would also be useful in future studies to obtained higher quality data.

Overall, the response of microbial respiration and priming to a warming climate is dependent on a multitude of factors. The results presented here suggest potential responses to rising temperatures and their potential mechanisms. However, this study has highlighted the need for further research in this space to fully understand the underlying processes affecting microbial responses to a changing climate.

Chapter 6
Conclusions

6.1 Conclusions

The main aim of this research thesis was to determine if the temperature response of SOM and labile C respiration in soil changed along a geothermal gradient that ranged from average temperatures of 18-36 ^{o}C. T_{opt} and T_{inf} were the main parameters used to test for changes in temperature response and were calculated using MMRT. Firstly, the results of this study found that the T_{opt} of labile C respiration and the T_{inf} of SOM-R_S increased with increasing environmental temperature, suggesting the potential for thermal adaptation. However, while changes may have been observed, these changes were modest with average slopes of 0.157 ^{o}C ^{o}C^{-1} and 0.183 ^{o}C ^{o}C^{-1}, for the T_{opt} of labile C respiration and the T_{inf} of SOM-R_S, respectively. Even adding SE to the mean rate of change resulted in a rate of change no greater than 0.198 ^{o}C ^{o}C^{-1} and 0.263 ^{o}C ^{o}C^{-1}, respectively. These changes in T_{opt} and T_{inf} with environmental temperature were also calculated to be small when extrapolating for extreme climate warming scenarios (4.8 ^{o}C). These small changes may indicate these parameters are relatively constrained across a wide range of environmental temperatures.

The use of glucose T_{opt} findings as a proxy for labile C sources was supported by an experiment using yeast extract instead of glucose (see also Numa *et al.* (2021)). Based on the results here and from previous studies the T_{opt} for labile C respiration has consistently been ~37 ^{o}C, however, the reasons for this temperature are unknown. Potential reasons for a T_{opt} ~37 ^{o}C, could be related to substrate properties or uptake, DNA or protein related, water or stress related. However, there are many other environmental and genetic factors that could be influencing the temperature response of microbes.

The temperature response of SOM-R_S also demonstrated an MMRT response that contrasted results from previous studies (Robinson *et al.*, 2017; Robinson *et al.*, 2020; Numa *et al.*, 2021). Discrepancies between methods and model types used (MMRT 1.0 vs MMRT 1.5) may have contributed to this result. Perhaps differences in substrate availability and soil properties influenced the temperature response of SOM-R_S. Overall, the SOM-R_S here showed minor thermal adaptation in response to increasing temperature.

The observed modest thermal adaptation for both SOM-R_S and labile C respiration might partially offset the positive acceleration of C cycling with warming climate (Luo *et al.*, 2001). However, the results suggested that the T_{inf} of labile C respiration and the T_{opt} of SOM-R_S were relatively conserved with increasing environmental temperature. For climate change, this could mean that feedback loops may not be alleviated.

The second aim was to characterise the temperature response of priming (T_{opt} & T_{inf}) along the geothermal gradient. The temperature response of priming followed an MMRT curve as observed in previous work (Numa, 2020). As with previous efforts to measure priming data, quality was not always high and there is a need to improve the measurement approach. This work found that soil characteristics are possibly key determinants of priming magnitude/contribution to soil respiration and that priming became negative at >40 ^{o}C. Qualitatively, the priming response was similar to that of labile C perhaps not surprisingly as priming is induced by labile C additions (Kuzyakov *et al.*, 2000). This study measured apparent priming (a short-term response; Blagodatskaya and Kuzyakov (2008)); it would be interesting to see if the real priming (a long-term response) of the system follows the same/similar pattern. Only a few priming runs could be completed due to the complexity of the method and equipment limitations, therefore, these findings need further investigation. If confirmed, these results suggest that as temperatures increase with global warming, the priming responses may weaken and so may partially offset accelerations due to feedbacks (Sun *et al.*, 2019).

Overall, the results suggested minimal thermal adaptation in response to soil warming. There is further work that needs to be done to understand what this means for future climate change management, which may be best explored by incorporating this data in C cycling models. In terms of priming, it is likely that the degree of priming will decrease with higher warming temperatures and so feedback loops could be dampened. These findings provide some insight into the potential responses of microbial communities to soil warming.

6.2 Future Work

Despite a large amount of research done on the temperature dependence of C cycling, there remains a need for further work to deepen our knowledge and understanding of microbial processes at ecosystem scales. This thesis has identified gaps in the literature and new areas for further investigation. Many factors can constrain the temperature

response of an organism, what is actually happening in the cells or at an ecosystem scale requires further research.

Below is a partial list of future research needs:

- The results of this study were derived from a single geothermal site. Future work should examine additional geothermal sites to determine if these results are applicable more broadly. This could be either in the same Arikikapakapa area or another geothermal area. Equally valuable would be a national (or international) scale study looking at latitudinal effects on the temperature response or microbes. More sites at colder soil temperatures may also strengthen the environmental temperature relationship with microbial responses. Overall, more sites are needed to support the findings of this research.
- Future studies should consider other factors potentially interacting with soil temperature to help explain the observed temperature response along this geothermal gradient (Haaf *et al.*, 2021). This may include a full characterisation of the elemental, trace metal and nutritional compositions, and an investigation into the biological community composition at each site. Such information would also be valuable if these factors differ along other geothermal gradients and could help explain variation in temperature responses.
- The results here showed small changes to the temperature response of microbial respiration with increasing environmental temperature. We focused on the T_{opt} and T_{inf} of microbes with temperature rather than the magnitude of respiration. However, the magnitude of the CO_2 flux may be more important in terms of climate change responses. Future studies should look at how the magnitude of the response changes with warming temperatures. Such investigations should take into account C supply and potentially the effects of different land-uses and management.
- Future work should look at increasing the number of soil priming replicates. The small amount of work completed here was not enough to form solid conclusions around the temperature response of priming even when combined with previous work.

- Future work should investigate the temperature response of priming over a longer incubation period (days-months) to capture the 'real' priming response of the system. This would be interesting to see how the response changes over different incubation times.
- The methods used for priming in this thesis requires adaptation to increase the throughput of runs. Therefore, future work should further attempt to automate the measurement process or find ways of simplifying this challenging method.
- Further work could also investigate *in situ* temperature responses in the field, either in a temperate regime or along a geothermal or elevational gradient. This work would be good to validate laboratory findings and relate to real *in situ* ecosystem responses.

Geothermal gradients may provide a useful approach to explore many of these questions. Geothermal soils make a great proxy for soil warming because they are naturally warmed, can be studied *in situ* as a whole ecosystem, and are confined in space which reduces other confounding environmental factors (O'Gorman *et al.*, 2014; Sigurdsson *et al.*, 2016). Along with this, geothermal gradients are often decades old and so the microbial communities have had time to adapt to the wide range of temperatures. Geothermal gradients pose a range of warming scenarios projected by the IPCC which make them important tools for investigating the effects of climate change (Marañón-Jiménez *et al.*, 2018). Therefore, these future work endeavours should consider and may benefit from using geothermal gradients.

References

Abramoff, R. Z., Torn, M. S., Georgiou, K., Tang, J., & Riley, W. J. (2019). Soil Organic Matter Temperature Sensitivity Cannot be Directly Inferred From Spatial Gradients. *Global Biogeochemical Cycles, 33*(6), 761-776.

Aciego Pietri, J. C., & Brookes, P. C. (2008). Relationships between soil pH and microbial properties in a UK arable soil. *Soil Biology and Biochemistry, 40*(7), 1856-1861.

Allison, S. D., & Vitousek, P. M. (2005). Responses of extracellular enzymes to simple and complex nutrient inputs. *Soil Biology and Biochemistry, 37*(5), 937-944.

Alster, C. J. (2019). Microbes adjust to heat. *Nature Ecology & Evolution, 3*(2), 155-156.

Alster, C. J., Koyama, A., Johnson, N. G., Wallenstein, M. D., & von Fischer, J. C. (2016). Temperature sensitivity of soil microbial communities: An application of macromolecular rate theory to microbial respiration. *Journal of Geophysical Research: Biogeosciences, 121*(6), 1420-1433.

Alster, C. J., von Fischer, J. C., Allison, S. D., & Treseder, K. K. (2020). Embracing a new paradigm for temperature sensitivity of soil microbes. *Global Change Biology, 26*(6), 3221-3229.

Alster, C. J., Weller, Z. D., & von Fischer, J. C. (2018). A meta-analysis of temperature sensitivity as a microbial trait. *Global Change Biology, 24*(9), 4211-4224.

Arcus, V. L., Prentice, E. J., Hobbs, J. K., Mulholland, A. J., Van der Kamp, M. W., Pudney, C. R., Parker, E. J., & Schipper, L. A. (2016). On the Temperature Dependence of Enzyme-Catalyzed Rates. *Biochemistry, 55*(12), 1681-1688.

Arcus, V. L., & Pudney, C. R. (2015). Change in heat capacity accurately predicts vibrational coupling in enzyme catalyzed reactions. *FEBS Letters, 589*(17), 2200-2206.

Atkin, O. K., & Tjoelker, M. G. (2003). Thermal acclimation and the dynamic response of plant respiration to temperature. *Trends in plant science, 8*(7), 343-351.

Barker, S. L. L., Dipple, G. M., Dong, F., & Baer, D. S. (2011). Use of Laser Spectroscopy To Measure the 13C/12C and 18O/16O Compositions of Carbonate Minerals. *Analytical Chemistry, 83*(6), 2220-2226.

Bastida, F., García, C., Fierer, N., Eldridge, D. J., Bowker, M. A., Abades, S., Alfaro, F. D., Asefaw Berhe, A., Cutler, N. A., Gallardo, A., et al. (2019). Global ecological predictors of the soil priming effect. *Nature Communications, 10*(1), 3481.

Bastida, F., Torres, I. F., Hernández, T., Bombach, P., Richnow, H. H., & García, C. (2013). Can the labile carbon contribute to carbon immobilization in semiarid soils? Priming effects and microbial community dynamics. *Soil Biology and Biochemistry, 57*, 892-902.

Beinlich, A., Barker, S. L. L., Dipple, G. M., Gupta, M., & Baer, D. S. (2017). Stable isotope (δ13C, δ18O) analysis of sulfide-bearing carbonate samples using laser absorption spectrometry. *Economic geology and the bulletin of the Society of Economic Geologists, 112*(3), 693-700.

Blackman, F. F. (1905). Optima and Limiting Factors. *Annals of Botany*, 281-296.

Blagodatskaya, E., & Kuzyakov, Y. (2008). Mechanisms of real and apparent priming effects and their dependence on soil microbial biomass and community structure: critical review. *Biology and Fertility of Soils, 45*(2), 115-131.

Boothroyd, I. K. G. (2009). Ecological characteristics and management of geothermal systems of the Taupo Volcanic Zone, New Zealand. *Geothermics, 38*(1), 200-209.

Boscutti, F., Casolo, V., Beraldo, P., Braidot, E., Zancani, M., & Rixen, C. (2018). Shrub growth and plant diversity along an elevation gradient: Evidence of indirect effects of climate on alpine ecosystems. *PloS one, 13*(4), e0196653-e0196653.

Bradford, M. (2013). Thermal adaptation of decomposer communities in warming soils. *Frontiers in Microbiology, 4*(333).

Bradford, M., Davies, C., Frey, S., Maddox, T., Melillo, J., Mohan, J., Reynolds, J., Treseder, K., & Wallenstein, M. (2008). Thermal adaptation of soil microbial respiration to elevated temperature. *Ecology Letters, 11*(12), 1316-1327.

Bradford, M., McCulley, R., Crowther, T., Oldfield, E., Wood, S., & Fierer, N. (2019). Cross-biome patterns in soil microbial respiration predictable from evolutionary theory on thermal adaptation. *Nature Ecology & Evolution, 3*(2), 223-231.

Carey, J. C., Tang, J., Templer, P. H., Kroeger, K. D., Crowther, T. W., Burton, A. J., Dukes, J. S., Emmett, B., Frey, S. D., Heskel, M. A., et al. (2016). Temperature response of soil respiration largely unaltered with experimental warming. *Proceedings of the National Academy of Sciences, 113*(48), 13797.

Condalab. (2021). *Yeast Extract Data Sheet*. Retrieved March, 2021, from https://www.condalab.com/int/en/peptones-and-extracts/1256-11747-yeast-extract.html.

Cooper, A. (2005). Heat capacity effects in protein folding and ligand binding: a re-evaluation of the role of water in biomolecular thermodynamics. *Biophysical Chemistry, 115*(2), 89-97.

Craine, J. M., Fierer, N., & McLauchlan, K. K. (2010). Widespread coupling between the rate and temperature sensitivity of organic matter decay. *Nature Geoscience, 3*(12), 854-857.

Crowther, T. W., & Bradford, M. A. (2013). Thermal acclimation in widespread heterotrophic soil microbes. *Ecology Letters, 16*(4), 469-477.

Dacal, M., Bradford, M. A., Plaza, C., Maestre, F. T., & García-Palacios, P. (2019). Soil microbial respiration adapts to ambient temperature in global drylands. *Nature Ecology & Evolution, 3*(2), 232-238.

DairyNZ. (2021). *Scott Farm Hamilton*. Retrieved June, 2021, from https://www.dairynz.co.nz/feed/farmwatch/scott-farm-hamilton/.

Dalenberg, J. W., & Jager, G. (1989). Priming effect of some organic additions to 14C-labelled soil. *Soil Biology and Biochemistry, 21*(3), 443-448.

Darros‐Barbosa, R., Balaban, M. O., & Teixeira, A. A. (2003). Temperature and Concentration Dependence of Heat Capacity of Model Aqueous Solutions. *International Journal of Food Properties, 6*(2), 239-258.

Dash, P. K., Bhattacharyya, P., Roy, K. S., Neogi, S., & Nayak, A. K. (2019). Environmental constraints' sensitivity of soil organic carbon decomposition to temperature, management practices and climate change. *Ecological Indicators, 107*, 105644.

Davidson, E. A., & Janssens, I. A. (2006). Temperature sensitivity of soil carbon decomposition and feedbacks to climate change. *Nature, 440*(7081), 165-173.

Davidson, E. A., Janssens, I. A., & Luo, Y. (2006). On the variability of respiration in terrestrial ecosystems: moving beyond Q10. *Global Change Biology, 12*(2), 154-164.

De Frenne, P., Graae, B. J., Rodríguez-Sánchez, F., Kolb, A., Chabrerie, O., Decocq, G., De Kort, H., De Schrijver, A., Diekmann, M., Eriksson, O., et al. (2013). Latitudinal gradients as natural laboratories to infer species' responses to temperature. *Journal of Ecology, 101*(3), 784-795.

Degens, B. P., Schipper, L. A., Sparling, G. P., & Duncan, L. C. (2001). Is the microbial community in a soil with reduced catabolic diversity less resistant to stress or disturbance? *Soil Biology and Biochemistry, 33*(9), 1143-1153.

Fabian, C., Reimann, C., Fabian, K., Birke, M., Baritz, R., & Haslinger, E. (2014). GEMAS: Spatial distribution of the pH of European agricultural and grazing land soil. *Applied Geochemistry, 48*, 207-216.

Fang, C., & Moncrieff, J. B. (2001). The dependence of soil CO2 efflux on temperature. *Soil Biology and Biochemistry, 33*(2), 155-165.

Field, C. B., Lobell, D. B., Peters, H. A., & Chiariello, N. R. (2007). Feedbacks of Terrestrial Ecosystems to Climate Change. *Annual Review of Environment and Resources, 32*(1), 1-29.

Fierer, N., Craine, J. M., McLauchlan, K., & Schimel, J. P. (2005). Litter Quality and the Temperature Sensitivity of Decomposition. *Ecology, 86*(2), 320-326.

Finzi, A. C., Abramoff, R. Z., Spiller, K. S., Brzostek, E. R., Darby, B. A., Kramer, M. A., & Phillips, R. P. (2015). Rhizosphere processes are quantitatively important components of terrestrial carbon and nutrient cycles. *Global Change Biology, 21*(5), 2082-2094.

Fontaine, S., Bardoux, G., Abbadie, L., & Mariotti, A. (2004). Carbon input to soil may decrease soil carbon content. *Ecology Letters, 7*(4), 314-320.

Friedlingstein, P., Meinshausen, M., Arora, V., Jones, C., Anav, A., Liddicoat, S., And, & Knutti, R. (2014). Uncertainties in CMIP5 Climate Projections due to Carbon Cycle Feedbacks. *Journal of Climate, 27*.

Garcia-Pausas, J., & Paterson, E. (2011). Microbial community abundance and structure are determinants of soil organic matter mineralisation in the presence of labile carbon. *Soil Biology and Biochemistry, 43*(8), 1705-1713.

German, D. P., Chacon, S. S., & Allison, S. D. (2011). Substrate concentration and enzyme allocation can affect rates of microbial decomposition. *Ecology, 92*(7), 1471-1480.

Ghee, C., Neilson, R., Hallett, P. D., Robinson, D., & Paterson, E. (2013). Priming of soil organic matter mineralisation is intrinsically insensitive to temperature. *Soil Biology and Biochemistry, 66*, 20-28.

Ghosh, A., & McSween Jr, H. Y. (1999). Temperature dependence of specific heat capacity and its effect on asteroid thermal models. *Meteoritics & planetary science, 34*(1), 121-127.

Given, D. R. (1980). Vegetation on heated soils at Karapiti, central North Island, New Zealand, and its relation to ground. *New Zealand Journal of Botany, 18*(1), 1-13.

Guenet, B., Leloup, J., Raynaud, X., Bardoux, G., & Abbadie, L. (2010). Negative priming effect on mineralization in a soil free of vegetation for 80 years. *Eur J Soil Sci, 61*, 384-391.

Gunina, A., & Kuzyakov, Y. (2015). Sugars in soil and sweets for microorganisms: Review of origin, content, composition and fate. *Soil Biology and Biochemistry, 90*, 87-100.

Haaf, D., Six, J., & Doetterl, S. (2021). Global patterns of geo-ecological controls on the response of soil respiration to warming. *Nature Climate Change*.

Hamdi, S., Moyano, F., Sall, S., Bernoux, M., & Chevallier, T. (2013). Synthesis analysis of the temperature sensitivity of soil respiration from laboratory studies in relation to incubation methods and soil conditions. *Soil Biology and Biochemistry, 58*, 115-126.

Hanrahan, G. (2012). *Key concepts in environmental chemistry*. Waltham, MA: Waltham, MA : Academic Press.

Harding, D. E., & Ross, D. J. (1964). Some factors in low-temperature storage influencing the mineralisable-nitrogen of soils. *Journal of the Science of Food and Agriculture, 15*(12), 829-834.

Hartley, I. P., Heinemeyer, A., & Ineson, P. (2007). Effects of three years of soil warming and shading on the rate of soil respiration: substrate availability and not thermal acclimation mediates observed response. *Global Change Biology, 13*(8), 1761-1770.

Hartley, I. P., Hopkins, D. W., Garnett, M. H., Sommerkorn, M., & Wookey, P. A. (2008). Soil microbial respiration in arctic soil does not acclimate to temperature. *Ecology Letters, 11*(10), 1092-1100.

Hobbs, J. K., Jiao, W., Easter, A. D., Parker, E. J., Schipper, L. A., & Arcus, V. L. (2013). Change in Heat Capacity for Enzyme Catalysis Determines Temperature Dependence of Enzyme Catalyzed Rates. *ACS Chemical Biology, 8*(11), 2388-2393.

Hochachka, P., & Somero, G. (2002). *Bio-Chemical Adaptation: Mechanism and Process in Physiological Evolution*. (Vol. 30).

Hong, S., Gan, P., & Chen, A. (2019). Environmental controls on soil pH in planted forest and its response to nitrogen deposition. *Environmental Research, 172*, 159-165.

IPCC. (2007). *Climate Change 2007: Synthesis Report. Contribution of Working Groups I, II and III to the Fourth Assessment Report of the Intergovernmental Panel on Climate Change.* Geneva, Switzerland.

IPCC. (2014). *Climate Change 2014: Impacts, Adaptation, and Vulnerability*. Cambridge, UK.

Janzen, H. H. (2004). Carbon cycling in earth systems—a soil science perspective. *Agriculture, Ecosystems & Environment, 104*(3), 399-417.

Jenkinson, D. S., Adams, D. E., & Wild, A. (1991). Model estimates of CO2 emissions from soil in response to global warming. *Nature, 351*(6324), 304-306.

Jenkinson, D. S., Fox, R. H., & Rayner, J. H. (1985). Interactions between fertilizer nitrogen and soil nitrogen—the so-called 'priming' effect. *Journal of Soil Science, 36*(3), 425-444.

Jobbágy, E. G., & Jackson, R. B. (2000). The vertical distribution of soil organic carbon and its relation to climate and vegetation. *Ecological Applications, 10*(2), 423-436.

Jones, D. L., Cooledge, E. C., Hoyle, F. C., Griffiths, R. I., & Murphy, D. V. (2019). pH and exchangeable aluminum are major regulators of microbial energy flow and carbon use efficiency in soil microbial communities. *Soil Biology and Biochemistry, 138*, 107584.

Kashmiri, Z. (2014). Free radicals and oxidative stress in bacteria.

Keiluweit, M., Bougoure, J. J., Nico, P. S., Pett-Ridge, J., Weber, P. K., & Kleber, M. (2015). Mineral protection of soil carbon counteracted by root exudates. *Nature Climate Change, 5*(6), 588-595.

Kirschbaum, M. U. F. (2004). Soil respiration under prolonged soil warming: are rate reductions caused by acclimation or substrate loss? *Global Change Biology, 10*(11), 1870-1877.

Kleber, M. (2010). What is recalcitrant soil organic matter? *Environmental Chemistry - ENVIRON CHEM, 7*.

Knorr, W., Prentice, I. C., House, J. I., & Holland, E. A. (2005). Long-term sensitivity of soil carbon turnover to warming. *Nature, 433*(7023), 298-301.

Kohn, M. J. (2010). Carbon isotope compositions of terrestrial C3 plants as indicators of (paleo)ecology and (paleo)climate. *Proceedings of the National Academy of Sciences, 107*(46), 19691.

Kuzyakov, Y. (2010). Priming effects: Interactions between living and dead organic matter. *Soil Biology and Biochemistry, 42*(9), 1363-1371.

Kuzyakov, Y., Friedel, J., & Stahr, K. (2000). Review of mechanisms and quantification of priming effects. *Soil Biology and Biochemistry, 32*(11), 1485-1498.

Laskowski, R., Maryański, M., & Niklińska, M. (1994). Effect of heavy metals and mineral nutrients on forest litter respiration rate. *Environmental Pollution, 84*(1), 97-102.

Lavallee, J. M., Soong, J. L., & Cotrufo, M. F. (2020). Conceptualizing soil organic matter into particulate and mineral-associated forms to address global change in the 21st century. *Global Change Biology, 26*(1), 261-273.

Lellei-Kovács, E., Botta-Dukát, Z., de Dato, G., Estiarte, M., Guidolotti, G., Kopittke, G. R., Kovács-Láng, E., Kröel-Dulay, G., Larsen, K. S., Peñuelas, J., et al. (2016). Temperature Dependence of Soil Respiration Modulated by Thresholds in Soil Water Availability Across European Shrubland Ecosystems. *Ecosystems, 19*(8), 1460-1477.

Lellei-Kovács, E., Kovács-Láng, E., Botta-Dukát, Z., Kalapos, T., Emmett, B., & Beier, C. (2011). Thresholds and interactive effects of soil moisture on the temperature response of soil respiration. *European Journal of Soil Biology, 47*(4), 247-255.

Liang, L. L., Arcus, V. L., Heskel, M. A., O'Sullivan, O. S., Weerasinghe, L. K., Creek, D., Egerton, J. J. G., Tjoelker, M. G., Atkin, O. K., & Schipper, L. A. (2017). Macromolecular rate theory (MMRT) provides a thermodynamics rationale to underpin the convergent temperature response in plant leaf respiration. *Global Change Biology, 24*(4), 1538-1547.

Lindsey, R. (2021). *Climate Change: Atmospheric Carbon Dioxide*. Retrieved March, 2021, from https://www.climate.gov/news-features/understanding-climate/climate-change-atmospheric-carbon-dioxide.

Lloyd, J., & Taylor, J. A. (1994). On the Temperature Dependence of Soil Respiration. *Functional Ecology, 8*(3), 315-323.

Lohnis, F. (1926). Nitrogen availability of green manures. *Soil Science, 22*(4), 253-290.

Lugato, E., Lavallee, J. M., Haddix, M. L., Panagos, P., & Cotrufo, M. F. (2021). Different climate sensitivity of particulate and mineral-associated soil organic matter. *Nature Geoscience, 14*(5), 295-300.

Luo, Y., Wan, S., Hui, D., & Wallace, L. (2001). Acclimatization of soil respiration to warming in a tall grass prairie. *Nature, 413*(6856), 622-625.

Luo, Z., Wang, E., & Smith, C. (2015). Fresh carbon input differentially impacts soil carbon decomposition across natural and managed systems. *Ecology, 96*(10), 2806-2813.

Luo, Z., Wang, E., & Sun, O. (2016). A meta-analysis of the temporal dynamics of priming soil carbon decomposition by fresh carbon inputs across ecosystems. *Soil Biology and Biochemistry, 101*, 96-103.

Mackelprang, R., Waldrop, M. P., DeAngelis, K. M., David, M. M., Chavarria, K. L., Blazewicz, S. J., Rubin, E. M., & Jansson, J. K. (2011). Metagenomic analysis of a permafrost microbial community reveals a rapid response to thaw. *Nature, 480*(7377), 368-371.

Maljanen, M., Yli-Moijala, H., Sigurdsson, B. D., & Biasi, C. (2019). Abiotic CO2 sources confound interpretation of temperature responses of in situ respiration in geothermally warmed forest soils of Iceland. *Biogeosciences Discuss., 2019*, 1-22.

Marañón-Jiménez, S., Soong, J. L., Leblans, N. I. W., Sigurdsson, B. D., Peñuelas, J., Richter, A., Asensio, D., Fransen, E., & Janssens, I. A. (2018). Geothermally warmed soils reveal persistent increases in the respiratory costs of soil microbes contributing to substantial C losses. *Biogeochemistry, 138*(3), 245-260.

Meyer, J. (2013). Sugarcane Nutrition and Fertilization. In (pp. 117 to 168).

Mudge, P. L., Schipper, L. A., Baisden, W. T., Ghani, A., & Lewis, R. W. (2014). Changes in soil C, N and δ15N along three forest–pasture chronosequences in New Zealand. *Soil Research, 52*(1), 27-37.

Nottingham, A. T., Griffiths, H., Chamberlain, P. M., Stott, A. W., & Tanner, E. V. J. (2009). Soil priming by sugar and leaf-litter substrates: A link to microbial groups. *Applied Soil Ecology, 42*(3), 183-190.

Nottingham, A. T., Meir, P., Velasquez, E., & Turner, B. L. (2020). Soil carbon loss by experimental warming in a tropical forest. *Nature, 584*(7820), 234-237.

Numa, K. (2020). *The Temperature Response of Soil Respiration from Labile and Stable Carbon.* University of Waikato., University of Waikato, New Zealand.

Numa, K., Robinson, J., Arcus, V., & Schipper, L. (2021). Separating the temperature response of soil respiration derived from soil organic matter and added labile carbon compounds. *Geoderma, 400*, 115128.

Nwachukwu, O. I., & Pulford, I. D. (2011). Microbial respiration as an indication of metal toxicity in contaminated organic materials and soil. *Journal of Hazardous Materials, 185*(2), 1140-1147.

O'Gorman, E. J., Benstead, J. P., Cross, W. F., Friberg, N., Hood, J. M., Johnson, P. W., Sigurdsson, B. D., & Woodward, G. (2014). Climate change and geothermal ecosystems: natural laboratories, sentinel systems, and future refugia. *Global Change Biology, 20*(11), 3291-3299.

Olczyk, P., Ramos, P., Komosinska-Vassev, K., Mencner, L., Olczyk, K., & Pilawa, B. (2016). Influence of Temperature on Free Radical Generation in Propolis-Containing Ointments. *Evidence-Based Complementary and Alternative Medicine, 2016*, 7292379.

Oliveberg, M., Tan, Y. J., & Fersht, A. R. (1995). Negative activation enthalpies in the kinetics of protein folding. *Proceedings of the National Academy of Sciences of the United States of America, 92*(19), 8926-8929.

Parts, K., Tedersoo, L., Schindlbacher, A., Sigurdsson, B. D., Leblans, N. I. W., Oddsdóttir, E. S., Borken, W., & Ostonen, I. (2019). Acclimation of Fine Root Systems to Soil Warming: Comparison of an Experimental Setup and a Natural Soil Temperature Gradient. *Ecosystems, 22*(3), 457-472.

Peterse, F., Schouten, S., van der Meer, J., van der Meer, M. T. J., & Sinninghe Damsté, J. S. (2009). Distribution of branched tetraether lipids in geothermally heated soils: Implications for the MBT/CBT temperature proxy. *Organic Geochemistry, 40*(2), 201-205.

Prentice, E. J., Hicks, J., Ballerstedt, H., Blank, L. M., Liáng, L. n. L., Schipper, L. A., & Arcus, V. L. (2020). The Inflection Point Hypothesis: The Relationship between the Temperature Dependence of Enzyme-Catalyzed Reaction Rates and Microbial Growth Rates. *Biochemistry, 59*(38), 3562-3569.

Reeves, R., & Rae, L. (2016). Changes in aerial thermal infrared signature over the Rotorua Geothermal Field, New Zealand: 1990–2014. *Geothermics, 64*, 262-270.

Reynolds, S. G. (1970). The gravimetric method of soil moisture determination Part III An examination of factors influencing soil moisture variability. *Journal of Hydrology, 11*(3), 288-300.

Robinson, J. M. (2016). *Temperature Sensitivity of Soil Respiration.* University of Waikato, University of Waikato.

Robinson, J. M., Barker, S. L. L., Arcus, V. L., McNally, S. R., & Schipper, L. A. (2020). Contrasting temperature responses of soil respiration derived from soil organic matter and added plant litter. *Biogeochemistry*.

Robinson, J. M., O'Neill, T. A., Ryburn, J., Liang, L. L., Arcus, V. L., & Schipper, L. A. (2017). Rapid laboratory measurement of the temperature dependence of soil respiration and application to changes in three diverse soils through the year. *Biogeochemistry, 133*(1), 101-112.

Roznik, E. A., & Alford, R. A. (2012). Does waterproofing Thermochron iButton dataloggers influence temperature readings? *Journal of Thermal Biology, 37*(4), 260-264.

Satyanarayana, T., Raghukumar, C., & Shivaji, S. (2005). Extremophilic microbes: Diversity and perspectives. *Current Science, 89*(1), 78-90.

Scharlemann, J. P. W., Tanner, E. V. J., Hiederer, R., & Kapos, V. (2014). Global soil carbon: understanding and managing the largest terrestrial carbon pool. *Carbon Management, 5*(1), 81-91.

Schindlbacher, A., de Gonzalo, C., Díaz-Pinés, E., Gorría, P., Matthews, B., Inclán, R., Zechmeister-Boltenstern, S., Rubio, A., & Jandl, R. (2010). Temperature sensitivity of forest soil organic matter decomposition along two elevation gradients. *Journal of Geophysical Research: Biogeosciences, 115*(G3).

Schipper, L. A., Hobbs, J. K., Rutledge, S., & Arcus, V. L. (2014). Thermodynamic theory explains the temperature optima of soil microbial processes and high Q10 values at low temperatures. *Global Change Biology, 20*(11), 3578-3586.

Schipper, L. A., Petrie, O. J., O'Neill, T. A., Mudge, P. L., Liáng, L. L., Robinson, J. M., & Arcus, V. L. (2019). Shifts in temperature response of soil respiration between adjacent irrigated and non-irrigated grazed pastures. *Agriculture, Ecosystems & Environment, 285*, 106620.

Schlesinger, W. H. (1977). Carbon Balance in Terrestrial Detritus. *Annual Review of Ecology and Systematics, 8*(1), 51-81.

Scurlock, J. M. O., & Hall, D. O. (1998). The global carbon sink: a grassland perspective. *Global Change Biology, 4*(2), 229-233.

Seward, A., Reeves, R., Pearson, S., Macdonald, N., Rae, L., & Scott, B. (2015). *Geothermal Feature Resurvay of Kuirau Park and Arikikapakapa Areas, Rotorua.* GNS. 18pp.

Shahbaz, M., Kumar, A., Kuzyakov, Y., Börjesson, G., & Blagodatskaya, E. (2018). Interactive priming effect of labile carbon and crop residues on SOM depends on residue decomposition stage: Three-source partitioning to evaluate mechanisms. *Soil Biology and Biochemistry, 126*, 179-190.

Sharp, C. E., Brady, A. L., Sharp, G. H., Grasby, S. E., Stott, M. B., & Dunfield, P. F. (2014). Humboldt's spa: microbial diversity is controlled by temperature in geothermal environments. *The ISME Journal, 8*(6), 1166-1174.

Sierra, C. A. (2012). Temperature sensitivity of organic matter decomposition in the Arrhenius equation: some theoretical considerations. *Biogeochemistry, 108*(1), 1-15.

Sierra, C. A., Trumbore, S. E., Davidson, E. A., Vicca, S., & Janssens, I. (2015). Sensitivity of decomposition rates of soil organic matter with respect to simultaneous changes in temperature and moisture. *Journal of Advances in Modeling Earth Systems, 7*(1), 335-356.

Sigurdsson, B. D., Leblans, N., Dauwe, S., Gudmundsdottir, E., Gundersen, P., Gunnarsdottir, G. E., Holmstrup, M., Ilieva-Makulec, K., Katterer, T., Marteinsdottir, B.-S., et al. (2016). Geothermal ecosystems as natural climate change experiments: The ForHot research site in Iceland as a case study.

Slessarev, E. W., Lin, Y., Bingham, N. L., Johnson, J. E., Dai, Y., Schimel, J. P., & Chadwick, O. A. (2016). Water balance creates a threshold in soil pH at the global scale. *Nature, 540*(7634), 567-569.

Sollins, P., Homann, P., & Caldwell, B. A. (1996). Stabilization and destabilization of soil organic matter: mechanisms and controls. *Geoderma, 74*(1), 65-105.

Stevenson, B. A., Parfitt, R. L., Schipper, L. A., Baisden, W. T., & Mudge, P. (2010). Relationship between soil δ15N, C/N and N losses across land uses in New Zealand. *Agriculture, Ecosystems & Environment, 139*(4), 736-741.

Sulman, B. N., Phillips, R. P., Oishi, A. C., Shevliakova, E., & Pacala, S. W. (2014). Microbe-driven turnover offsets mineral-mediated storage of soil carbon under elevated CO2. *Nature Climate Change, 4*(12), 1099-1102.

Sun, Z., Liu, S., Zhang, T., Zhao, X., Chen, S., & Wang, Q. (2019). Priming of soil organic carbon decomposition induced by exogenous organic carbon input: a meta-analysis. *Plant and Soil, 443*(1), 463-471.

Tarnocai, C., Canadell, J. G., Schuur, E. A. G., Kuhry, P., Mazhitova, G., & Zimov, S. (2009). Soil organic carbon pools in the northern circumpolar permafrost region. *Global Biogeochemical Cycles, 23*(2).

Thiessen, S., Gleixner, G., Wutzler, T., & Reichstein, M. (2013). Both priming and temperature sensitivity of soil organic matter decomposition depend on microbial biomass – An incubation study. *Soil Biology and Biochemistry, 57*, 739-748.

Tucker, C. L., Bell, J., Pendall, E., & Ogle, K. (2013). Does declining carbon-use efficiency explain thermal acclimation of soil respiration with warming? *Global Change Biology, 19*(1), 252-263.

von Lützow, M., Kögel-Knabner, I., Ekschmitt, K., Matzner, E., Guggenberger, G., Marschner, B., & Flessa, H. (2006). Stabilization of organic matter in temperate soils: mechanisms and their relevance under different soil conditions – a review. *European Journal of Soil Science, 57*(4), 426-445.

von Lützow, M., Kögel-Knabner, I., Ludwig, B., Matzner, E., Flessa, H., Ekschmitt, K., Guggenberger, G., Marschner, B., & Kalbitz, K. (2008). Stabilization mechanisms of organic matter in four temperate soils: Development and application of a conceptual model. *Journal of Plant Nutrition and Soil Science, 171*(1), 111-124.

Walker, T. W. N., Kaiser, C., Strasser, F., Herbold, C. W., Leblans, N. I. W., Woebken, D., Janssens, I. A., Sigurdsson, B. D., & Richter, A. (2018). Microbial temperature sensitivity and biomass change explain soil carbon loss with warming. *Nature Climate Change, 8*(10), 885-889.

Wang, Q., He, T., & Liu, J. (2016). Litter input decreased the response of soil organic matter decomposition to warming in two subtropical forest soils. *Scientific Reports, 6*(1), 33814.

Watanabe, Y., Ishigaki, H., Okada, H., & Suyama, S. (1997). Temperature Dependence of Initiation Reactions of Oxygen-Centered Radicals. *Polymer Journal, 29*(8), 693-696.

Woodwell, G. M., Mackenzie, F. T., Houghton, R. A., Apps, M., Gorham, E., & Davidson, E. (1998). Biotic Feedbacks in the Warming of the Earth. *Climatic Change, 40*(3), 495-518.

Wynn, J. G., & Bird, M. I. (2008). Environmental controls on the stable carbon isotopic composition of soil organic carbon: implications for modelling the distribution of C3 and C4 plants, Australia. *Tellus B, 60*(4), 604-621.

Xu, G., Jiang, H., Zhang, Y., Korpelainen, H., & Li, C. (2013). Effect of warming on extracted soil carbon pools of Abies faxoniana forest at two elevations. *Forest Ecology and Management, 310*, 357-365.

Xu, M., & Shang, H. (2016). Contribution of soil respiration to the global carbon equation. *Journal of Plant Physiology, 203*, 16-28.

Yang, C., Liu, N., & Zhang, Y. (2019). Soil aggregates regulate the impact of soil bacterial and fungal communities on soil respiration. *Geoderma, 337*, 444-452.

Zeldovich, K. B., Berezovsky, I. N., & Shakhnovich, E. I. (2007). Protein and DNA Sequence Determinants of Thermophilic Adaptation. *PLOS Computational Biology, 3*(1), e5.

Zhang, X., Johnston, E. R., Li, L., Konstantinidis, K. T., & Han, X. (2017). Experimental warming reveals positive feedbacks to climate change in the Eurasian Steppe. *The ISME journal, 11*(4), 885-895.

Zhang, Z., Wang, W., Qi, J., Zhang, H., Tao, F., & Zhang, R. (2019). Priming effects of soil organic matter decomposition with addition of different carbon substrates. *Journal of Soils and Sediments, 19*(3), 1171-1178.

Appendices

Appendix A: Site history

This Appendices shows aerial images from 1943 to 2018 using images from Retrolens (https://retrolens.co.nz/), Bay of Plenty Regional Council maps (https://boprc.maps.arcgis.com/) and Google Maps (® 2020).

1943

1945

1951

1959

1965

1966

1970

1971

1972

1976

1977

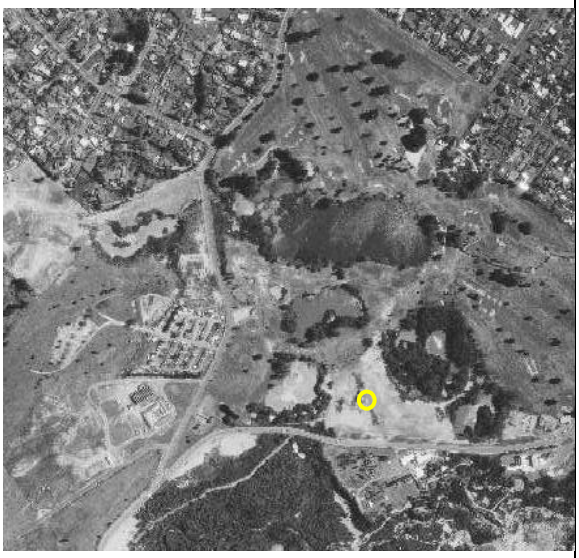

1980

1983

1988

1992

2003

2006

2011

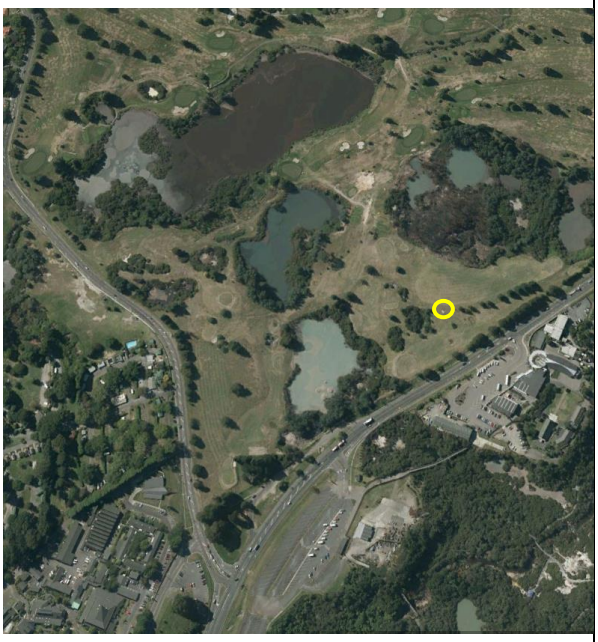

2016

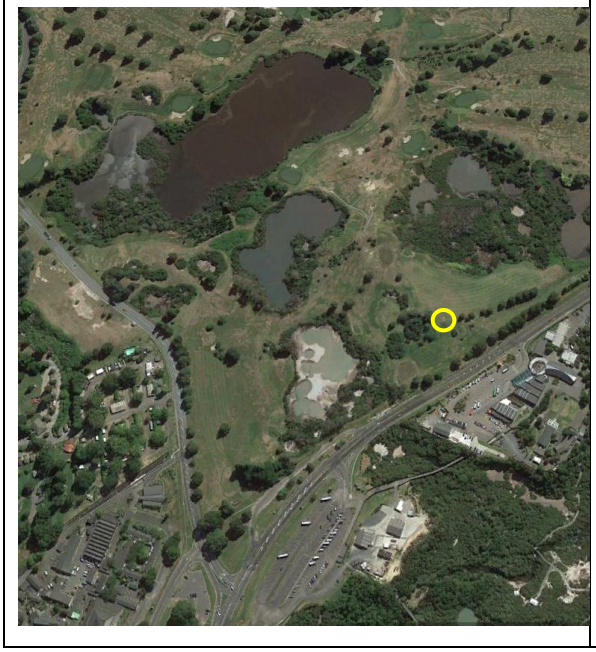

2018

Appendix B: Glucose Sample Details

Table B1 Summary of the 20 samples used in the glucose incubation experiments. The given temperature at each depth is the average environmental temperature across the width of the 3 m grid for the sampling distance on the day of sampling. The table order is the same as the run order.

Distance from Source (cm)	Moisture content (gg^{-1})	pH	Temperature 2 cm depth (°C)	Temperature 10 cm depth (°C)
30th Nov 2020 – 4th Dec 2020				
15	0.556	4.26	24.38	30.94
40	0.620	4.72	24.02	27.48
295	0.796	4.72	21.62	23.86
1495	0.602	5.32	18.80	19.56
7th – 11th Dec 2020				
25	0.539	5.09	29.80	35.40
50	0.525	5.38	27.42	31.50
305	0.647	4.93	23.82	25.30
1505	0.539	4.77	20.32	20.66
1st – 5th Feb 2021				
150	0.468	4.67	30.04	31.84
350	0.439	4.77	27.46	27.60
1595	0.354	5.19	20.64	22.08
23rd – 25th March 2021				
65	0.477	4.35	27.34	32.08
20th– 23rd April 2021				
1550	0.523	4.73	16.60	17.38
120	0.595	4.70	22.62	25.58
250	0.687	4.64	20.62	23.00
28th – 30th April 2021				
750	0.511	4.74	16.38	16.74
1250	0.537	4.83	15.40	16.44
4th – 7th May 2021				
45	0.543	4.31	24.38	28.76
500	0.621	4.81	17.84	17.38
1000	0.427	4.77	17.82	16.10

Appendix C: Glucose and Yeast Extract Temperature Response Curve Fits

These curve fits were fitted using MMRT 1.5 as described in section 4.3, Chapter 4.

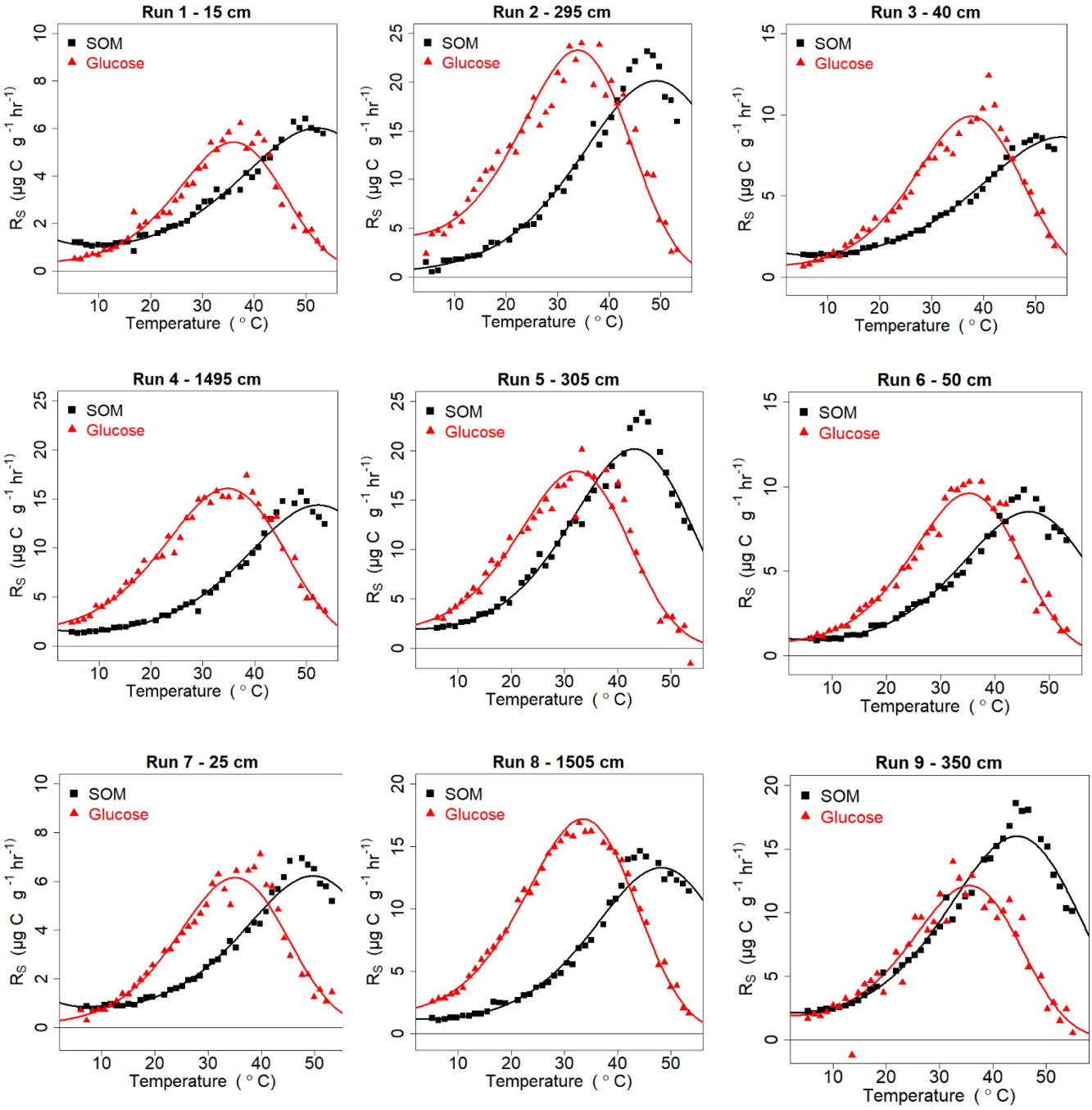

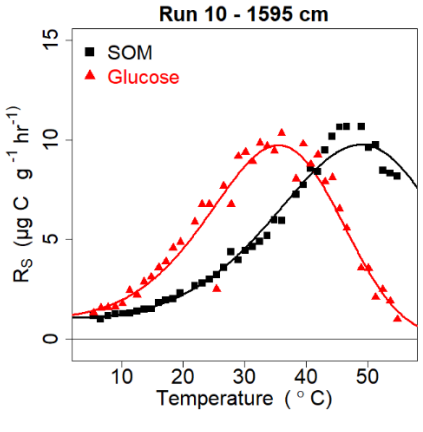
Run 10 - 1595 cm
SOM
Glucose
R_S (µg C g^{-1} hr^{-1})
Temperature (°C)

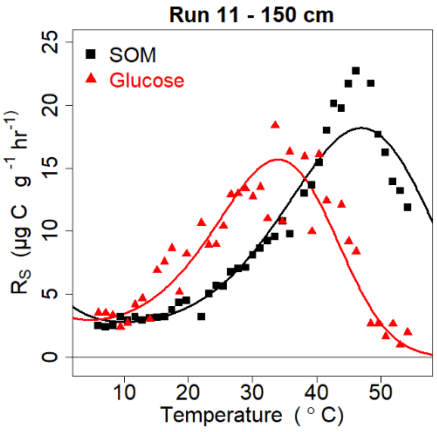
Run 11 - 150 cm
SOM
Glucose
R_S (µg C g^{-1} hr^{-1})
Temperature (°C)

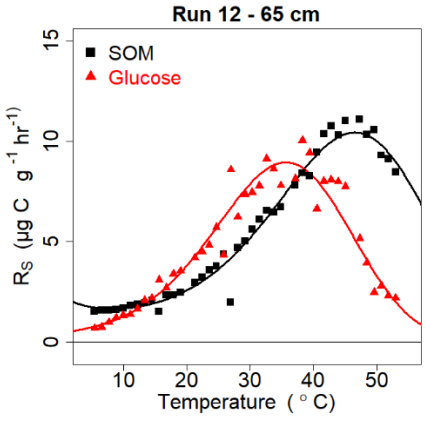
Run 12 - 65 cm
SOM
Glucose
R_S (µg C g^{-1} hr^{-1})
Temperature (°C)

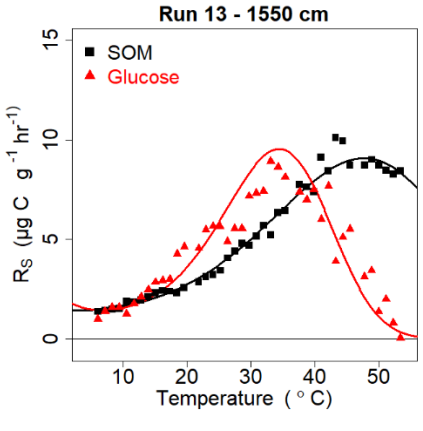
Run 13 - 1550 cm
SOM
Glucose
R_S (µg C g^{-1} hr^{-1})
Temperature (°C)

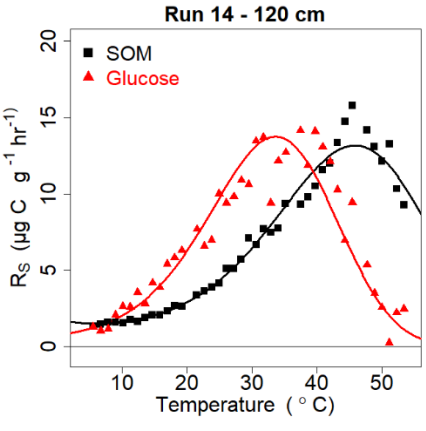
Run 14 - 120 cm
SOM
Glucose
R_S (µg C g^{-1} hr^{-1})
Temperature (°C)

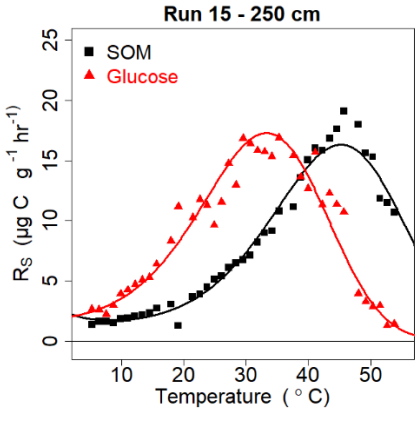
Run 15 - 250 cm
SOM
Glucose
R_S (µg C g^{-1} hr^{-1})
Temperature (°C)

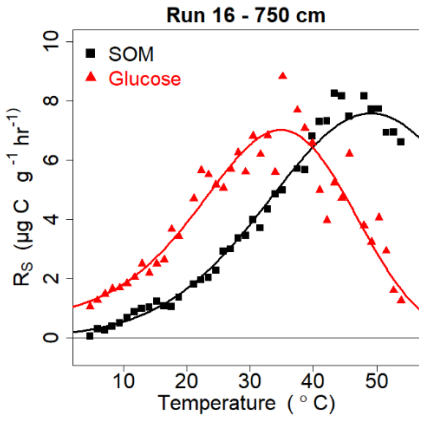
Run 16 - 750 cm
SOM
Glucose
R_S (µg C g^{-1} hr^{-1})
Temperature (°C)

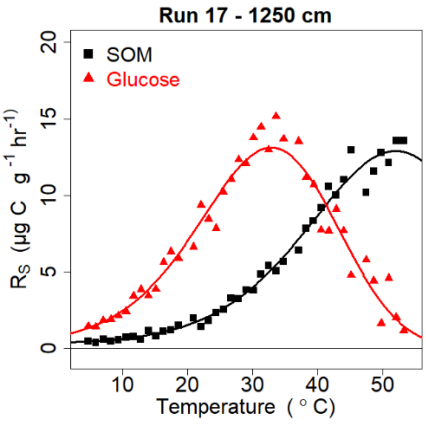
Run 17 - 1250 cm
SOM
Glucose
R_S (µg C g^{-1} hr^{-1})
Temperature (°C)

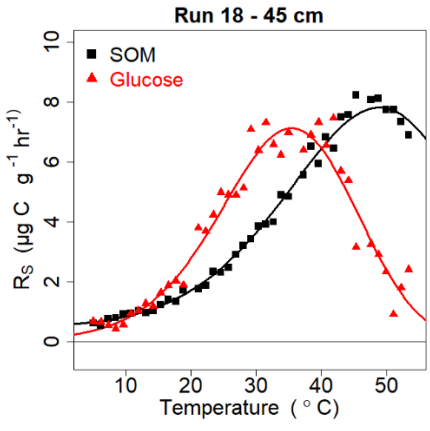
Run 18 - 45 cm
SOM
Glucose
R_S (µg C g^{-1} hr^{-1})
Temperature (°C)

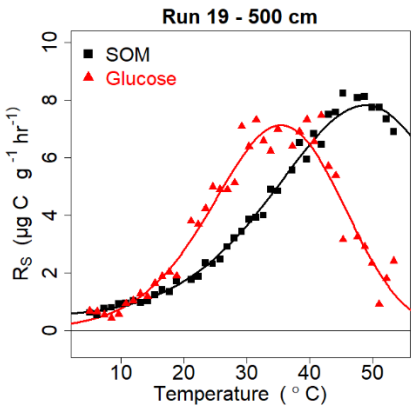
Run 19 - 500 cm
SOM
Glucose
R_S (µg C g^{-1} hr^{-1})
Temperature (°C)

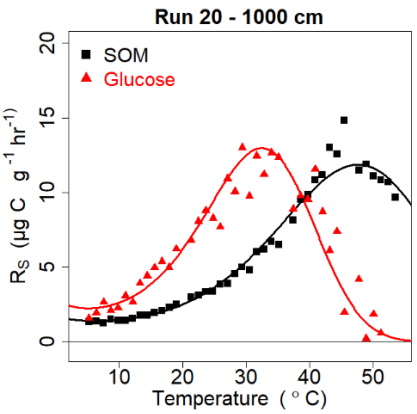
Run 20 - 1000 cm
SOM
Glucose
R_S (µg C g^{-1} hr^{-1})
Temperature (°C)

Appendix D: Priming Method Development

The priming method presented in section 4.2 was developed by Robinson *et al.* (2020) and first used for priming by Numa (2020). With the corporation of these two authors, attempts to automate the manual process were completed for serval months, the details of these attempts are presented below

The original method used by Robinson *et al.* (2020) and Numa (2020) is a manual, time consuming and technically challenging method. The aim of these small experiments were to find a way of automating the process. To automate the method, the gas product of incubation needs to be contained in a 4 mL exetainer to fit into the automation machine setup. Therefore, gas from the 24 mL hungate tubes used for the incubations required transferring into new exetainers to be measured. The following trails aimed to determine if the $\delta\ ^{13}C$ results from the hungate tubes and transferred exetainer were comparable.

For the first three trail experiments the internal standard WCS was used to mimic the $\delta\ ^{13}C$ labelled glucose used in the priming method. Following the method presented in section 4.2.1, the WCS standard was weighed into the corresponding hungate tubes and exetainers, acidified with 10 drops of orthophosphoric acid and left to acidify on 73 ^{o}C heating block for at least 45 minutes.

It was thought the first trial was unsuccessful due to transfer issues between the exetainers using a 1 mL insulin syringe. To try and minimise issues with gas leakages during transfers, a 1 mL gas tight syringe was obtained (Total Lab systems, Model 1001 SL) and used for the rest of the experiments.

The following two trials investigated the use of different WCS weights and its effect on the exetainer results. The results were inconsistent between vessels with no comparable pattern or trend. The results were unable to obtain any scaling factor nor a plausible error margin.

Due to issues with the trails using WCS only, the last two trails consisted of incubated Horotiu soil samples. The hungate tubes containing soil were incubated following methods form section 4.1.2.2. At the end of the incubation time the samples were placed one ice and then kept in the freezer overnight (-20 ^{o}C). The next day 1 mL of each tubes was transferred to the exetainers. These hungate tubes were analysed along with $\delta\ ^{13}C$ standards (**Table 4.7**, section 4.2.1) and transferred exetainers.

A summary of the experiments completed can be found in **Table 2** below. The relationship between the two vessels was weak so no scaling factor could be created to form a consistent result among the samples. The use of a gastight syringe had little effect on the results found in these experiments, suggesting the issue was something else. The developmental trails were stopped due to timing constraints. These timing restraints prevented further investigation into avenues such as, completing transfers in a vacuum box, changing $\delta\ ^{13}C$ concentrations in the soil solution, using different soil weights, flushing the exetainers or transferring greater gas concentrations.

Table D1 Summary table of priming method development experiments.

Attempt	Soil	Transfer amount	Tubes used	Transfer weights (mg)	Standard weights (mg)	Syringe used	Result
1	No	1 mL	25x Hungate tubes 3x standard hungate tubes 25x transfer exetainers 3x standard exetainers	WCS 5x hungate tubes for each weight: 0.1 mg, 0.3 mg, 0.6 mg, 1.0 mg, 2.5 mg.	WCS 3x hungate tubes at 1.0 mg 3x exetainers at 1.0 mg	1 mL insulin syringe (Becton-Dickinson and co)	No result. Hungate and exetainer results inconsistent, not comparable.
2	No	1 mL	25x Hungate tubes 3x standard hungate tubes 25x transfer exetainers 3x standard exetainers	WCS 25x hungate tubes with weight: 0.1 mg	WCS 3x hungate tubes at 1.0 mg 3x exetainers at 1.0 mg	1 mL gas tight syringe with locking valve (Total Lab systems, Model 1001 SL)	No result. Hungate and exetainer results inconsistent, not comparable.
3	No	1 mL	20x Hungate tubes 3x standard hungate tubes 20x transfer exetainers 3x standard exetainers	WCS 5x hungate tubes for each weight: 0.2 mg, 0.3 mg, 0.4 mg, 0.5 mg.	WCS 3x hungate tubes at 1.0 mg 3x exetainers at 1.0 mg	1 mL gas tight syringe with locking valve (Total Lab systems, Model 1001 SL)	No result. Hungate and exetainer results inconsistent, not comparable.
4	Yes	1 mL	40x Hungate soil tubes 15x standard hungate tubes 40x transfer exetainers	$\delta^{13}C$ labelled glucose at 29.9 **‰** (VPDB). Added to soil tubes at 0.125 g to 2 g of soil	Each at 0.1 mg: 3x WCS, 3x BDH, 3x NBS-19 Three drops: 3x bicarbonate standard 17A and 3x bicarbonate standard 68A	1 mL gas tight syringe with locking valve (Total Lab systems, Model 1001 SL)	No result. Hungate and exetainer results inconsistent, not comparable. Result: CO_2 lower than 2500 ppm maximum
5	Yes	1 mL	20x Hungate soil tubes 15x standard hungate tubes 20x transfer exetainers	$\delta^{13}C$ labelled glucose at 29.9 **‰** (VPDB). Added to soil tubes at 0.1875 g to 2 g of soil.	Each at 0.1 mg: 3x WCS, 3x BDH, 3x NBS-19 Three drops: 3x bicarbonate standard 17A and 3x bicarbonate standard 68A	1 mL gas tight syringe with locking valve (Total Lab systems, Model 1001 SL)	No result. Hungate and exetainer results inconsistent, not comparable. Result: CO_2 lower than 2500 ppm maximum

Appendix E: Example MMRT 1.0 and MMRT 1.5 Curve Fits

The example shows the different equations (MMRT 1.0 & MMRT 1.5) fitted to the same data set. The curve fits below are presented as the natural log of rate vs temperature in kelvins because the MMRT equation uses these as a default. The log fits of curves should look better than the un-logged plots, however, even in log form, the fit of MMRT 1.0 is not capturing the true curvature of the temperature responses.

MMRT 1.0: Matlab 2019b

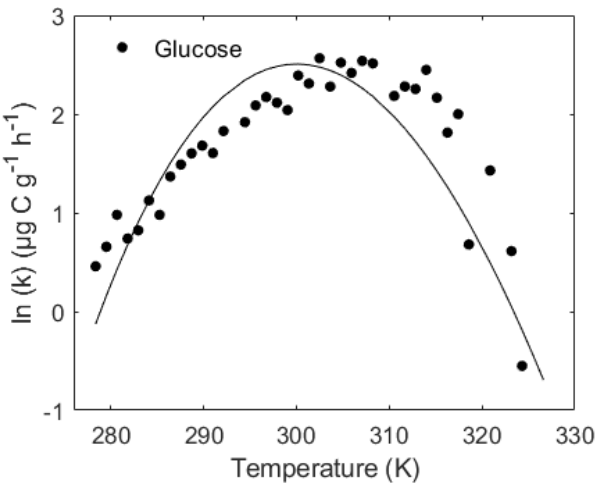

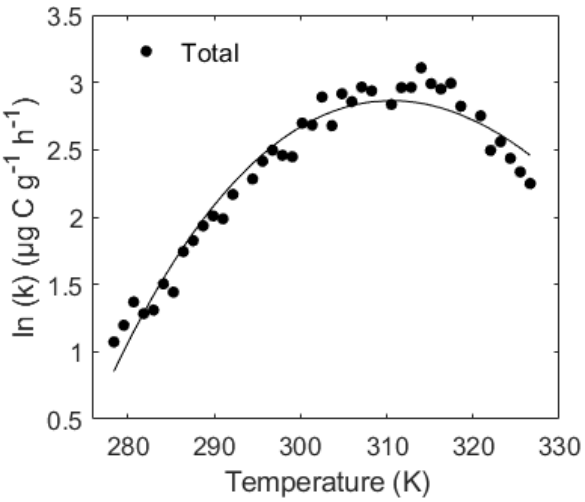

MMRT 1.5: R version 4.0.2

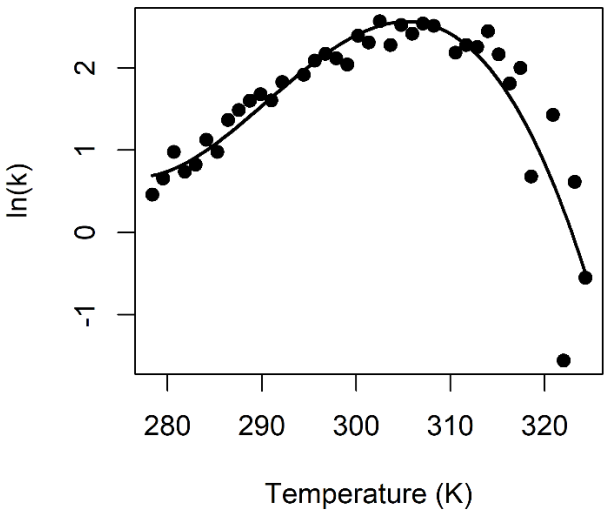

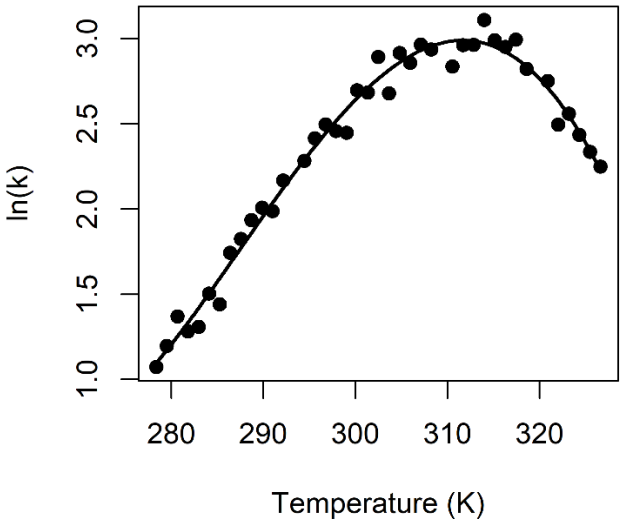

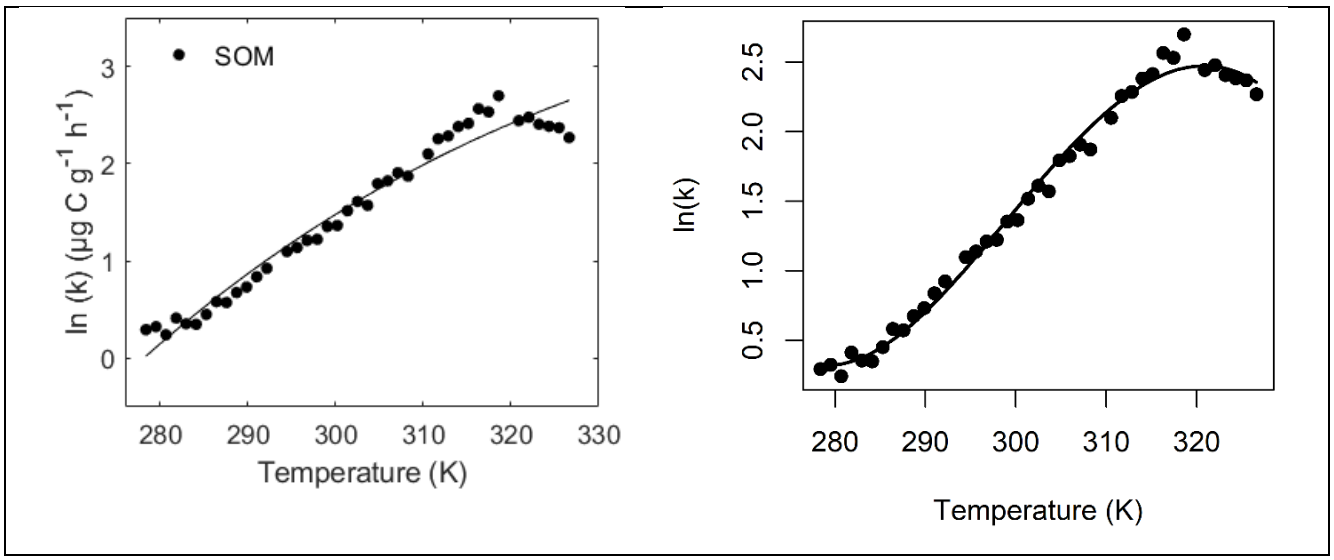
SOM
ln (k) (µg C g-1 h-1)
Temperature (K)
ln(k)
Temperature (K)

Appendix F: MMRT 1.5 Parameters

Glucose Experiments:

Table F1 Glucose-R_S MMRT 1.5 parameters from all 20 glucose experiments/distances along the geothermal gradient.

Sample R_S type	Distance (cm)	Environmental Temperature (^oC)	Topt (^oC)	Tinf (^oC)	A	B	$\Delta H^{\ddagger}_{T_0}$ (J mol^{-1} K^{-1})	$\Delta S^{\ddagger}_{T_0}$ (J mol^{-1} K^{-1})
Glucose 1	15	36.5	36.1	15.8	-136	-7541	-1041	-234
Glucose 2	295	24.0	34.0	16.8	-141	-7544	-16340	-272
Glucose 3	40	31.6	37.5	16.0	-125	-6835	8606	-198
Glucose 4	1495	19.9	34.6	12.1	-92	-6018	-9938	-254
Glucose 5	305	24.1	32.2	13.3	-136	-8547	-31198	-323
Glucose 6	50	29.3	35.3	16.1	-149	-8214	-7699	-251
Glucose 7	25	33.1	35.2	11.7	-118	-7800	-8016	-256
Glucose 8	1505	19.8	33.6	14.3	-133	-7952	-20001	-286
Glucose 9	350	26.0	35.5	19.1	-177	-8343	-5561	-242
Glucose 10	1595	21.0	35.5	16.4	-131	-7068	-5196	-243
Glucose 11	150	27.8	34.0	18.1	-172	-8605	-17694	-280
Glucose 12	65	33.6	35.9	13.4	-113	-6928	-2261	-234
Glucose 13	1550	18.1	34.5	20.1	-265	-11886	-18800	-287
Glucose 14	120	25.0	33.7	12.6	-141	-9037	-21288	-293
Glucose 15	250	22.6	33.4	15.2	-149	-8625	-22453	-294
Glucose 16	750	19.6	34.9	12.9	-87	-5496	-7737	-254
Glucose 17	1250	18.1	32.9	11.6	-130	-8711	-26827	-311
Glucose 18	45	29.8	35.9	12.2	-119	-7681	-2653	-237
Glucose 19	500	19.3	33.3	14.0	-157	-9548	-25502	-306
Glucose 20	1000	17.9	32.3	17.4	-238	-12457	-42749	-363

Table F2 Total-R_S MMRT 1.5 parameters from all 20 glucose experiments/distances along the geothermal gradient.

Sample R_S type	Distance (cm)	Environmental Temperature (°C)	Topt (°C)	Tinf (°C)	A	B	$\Delta H^{\ddagger}_{T_0}$ (J mol^{-1} K^{-1})	$\Delta S^{\ddagger}_{T_0}$ (J mol^{-1} K^{-1})
Total 1	15	36.5	41.9	20.4	-82.8	-3465	22849	-153
Total 2	295	24.0	39.7	17.2	-75.3	-3818	13362	-172
Total 3	40	31.6	42.3	19.5	-80.7	-3549	25065	-142
Total 4	1495	19.9	40.8	11.3	-48.1	-3102	14435	-172
Total 5	305	24.1	37.1	12.3	-76.0	-4835	3440	-205
Total 6	50	29.3	39.8	17.5	-96.8	-4815	18081	-164
Total 7	25	33.1	41.0	16.8	-79.3	-4061	21128	-158
Total 8	1505	19.8	38.7	11.5	-62.8	-4076	9485	-188
Total 9	350	26.0	40.5	20.7	-113.1	-4684	22394	-146
Total 10	1595	21.0	40.9	15.7	-67.2	-3620	17879	-164
Total 11	150	27.8	40.2	20.1	-90.5	-3914	16791	-164
Total 12	65	33.6	41.0	17.4	-79.2	-3935	20408	-156
Total 13	1550	18.1	39.6	14.1	-62.6	-3659	12306	-183
Total 14	120	25.0	39.3	12.5	-70.5	-4386	13751	-175
Total 15	250	22.6	38.8	15.1	-80.2	-4503	11410	-181
Total 16	750	19.6	40.6	na	-29.5	-3134	13025	-182
Total 17	1250	18.1	40.0	na	-20.0	-3258	11296	-184
Total 18	45	29.8	41.0	12.5	-67.6	-4164	21345	-155
Total 19	500	19.3	39.0	12.9	-72.6	-4463	12145	-180
Total 20	1000	17.9	38.6	14.2	-72.2	-4222	9439	-190

Table F3 SOM-R_S MMRT 1.5 parameters from all 20 glucose experiments/distances along the geothermal gradient.

Sample R_S type	Distance (cm)	Environmental Temperature (°C)	Topt (°C)	Tinf (°C)	A	B	$\Delta H^{\ddagger}_{T_0}$ (J mol^{-1} K^{-1})	$\Delta S^{\ddagger}_{T_0}$ (J mol^{-1} K^{-1})
SOM 1	15	36.5	52.0	29.4	-68.3	-1026	40626	-103
SOM 2	295	24.0	47.6	23.6	-86.9	-2747	47662	-69.3
SOM 3	40	31.6	53.0	29.6	-53.7	-728	40694	-101
SOM 4	1495	19.9	52.8	27.3	-65.9	-1321	48255	-72.0
SOM 5	305	24.1	43.2	21.7	-104.6	-3964	34840	-109
SOM 6	50	29.3	46.3	24.8	-99.3	-2882	43600	-89.0
SOM 7	25	33.1	49.5	28.3	-95.6	-1790	48280	-77.9
SOM 8	1505	19.8	48.2	25.1	-89.7	-2466	48019	-71.9
SOM 9	350	26.0	44.4	23.1	-91.8	-3119	33993	-114
SOM 10	1595	21.0	48.5	24.8	-74.3	-2098	41832	-94.2
SOM 11	150	27.8	46.5	27.1	-115.9	-2645	45255	-77.8
SOM 12	65	33.6	46.8	26.1	-95.6	-2422	40816	-96.4
SOM 13	1550	18.1	47.7	23.8	-61.9	-1920	33208	-122
SOM 14	120	25.0	46.0	24.5	-98.8	-2959	42617	-88.5
SOM 15	250	22.6	45.5	25.3	-125.1	-3501	48241	-68.7
SOM 16	750	19.6	46.9	24.2	-93.5	-2828	45626	-83.4
SOM 17	1250	18.1	52.0	22.9	-67.2	-2105	57893	-42.2
SOM 18	45	29.8	49.0	21.6	-59.6	-2148	41036	-98.6
SOM 19	500	19.3	46.6	25.0	-99.9	-2836	45276	-79.7
SOM 20	1000	17.9	47.7	25.7	-91.5	-2389	45061	-82.1